Hardin, R., Beckermann, C., Monroe, R., David, D., and Allyn, B., "Measurements and Predictions of Lower Bound Mechanical Properties of Cast Steels," in Proceedings of the 73rd SFSA Technical and Operating Conference, Paper No. 4.3, Steel Founders' Society of America, Chicago, IL, 2019.

Measurements and Predictions of Lower Bound Mechanical Properties of Cast Steels

Richard A. Hardin[1] and Christoph Beckermann[1]

Raymond Monroe[2], Diana David[2] and Barbara Allyn

[1]Department of Mechanical and Industrial Engineering
The University of Iowa, Iowa City, 52242

[2]Steel Founders' Society of America

Abstract

Statistical analyses are performed on tensile data collected by the Steel Founders' Society of America (SFSA) from its members to establish lower bound mechanical design properties. The data set contains measurements from over 7000 specimens. The results from this work are recommended lower bound mechanical properties for yield and ultimate strengths, elongation and reduction of area for use in designing cast components made from the steels analyzed. These are determined at the 1st and 10th percentiles of the data at the 95% confidence level using normal distributions. These levels are analogous to the *Metallic Material Properties Development and Standardization (MMPDS) Handbook* approach for the so-called "A" and "B" design allowables, respectively. The lower bound allowables are determined by grouping the data by grade, heat treatment and class according to two specifications; ASTM A958, and ASTM A487 for castings suitable for pressure service according to the ASME Boiler and Pressure Vessel Code (BPVC). For the data analyzed and grouped according to ASTM A487 and the ASME BPVC specification SA487, lower bound allowables for grades and classes 4A, 4B, and 4E are determined. Mechanical property predictions are presented using casting and heat treatment simulation results for cast 8630 quenched and tempered (Q&T) steel. In these predictions, specimens taken from a range of casting section sizes and casting geometries are used in these comparisons, in contrast to the SFSA datasets which is comprised mostly of keel block and other standard test coupon castings. Predicted results for cooling rate and thermal gradient are combined with software package predictions of mechanical properties to improve agreement with measurements. Best-fit models using predicted results are used to calculate yield strength, ultimate strength, elongation and reduction of area. Measured and predicted mechanical properties are compared. An approach to lower bound property predictions based on the 1st and 10th percentile levels are determined using the SFSA member data, and comparisons are made between lower bound strength property predictions at these level and measurements.

Introduction

Lower bound properties are minimum mechanical properties determined based on statistical analysis of mechanical test data for a given material. They provide engineers with a rational framework for selecting conservative, reliable design stresses, or design allowables, for use in the design of components and structures. In the United States the publishing of

statistically-based design allowables for metallic materials and fasteners began in the 1930s, and this became known in 1956 as the *Department of Defense Handbook: Metallic Materials and Elements for Aerospace Vehicle Structures* or MIL-HDBK-5. The Handbook was renamed the *Metallic Material Properties Development and Standardization (MMPDS) Handbook* in 2002 [1], and the Federal Aviation Administration's (FAA) assumed responsibility for the Handbook's supervision. The Handbook provides both lower bound design allowables and guidelines on the statistical analyses for determining them. The lower bound mechanical properties for cast steels presented here use two conservative levels in the statistical analysis described in the MMPDS Handbook guidelines for critical non-redundant (the more conservative level) and critical redundant designs (the less conservative level). While the MMPDS Handbook guidelines were not strictly followed here (on sampling method and sizes of samples for example), the analyses and results presented here use MMPDS Handbook statistical limits for determining the lower bound properties.

The two statistical levels used to establish the lower bound properties presented here, and based on the MMPDS approach [2], are demonstrated in Figure 1. In the figure a Normal (Gaussian) distribution of mechanical test data is shown represented by a relative frequency curve versus standard deviations from the mean. The statistical levels used for determining the lower bound properties are the 1st and 10th percentiles of the normal distribution at the lower 95% confidence level of each percentile. The more conservative property level (1st percentile) is termed in the "A" design allowable and the less conservative property level (10th percentile) is termed in the "B" design allowable. This terminology is followed here when referencing the two

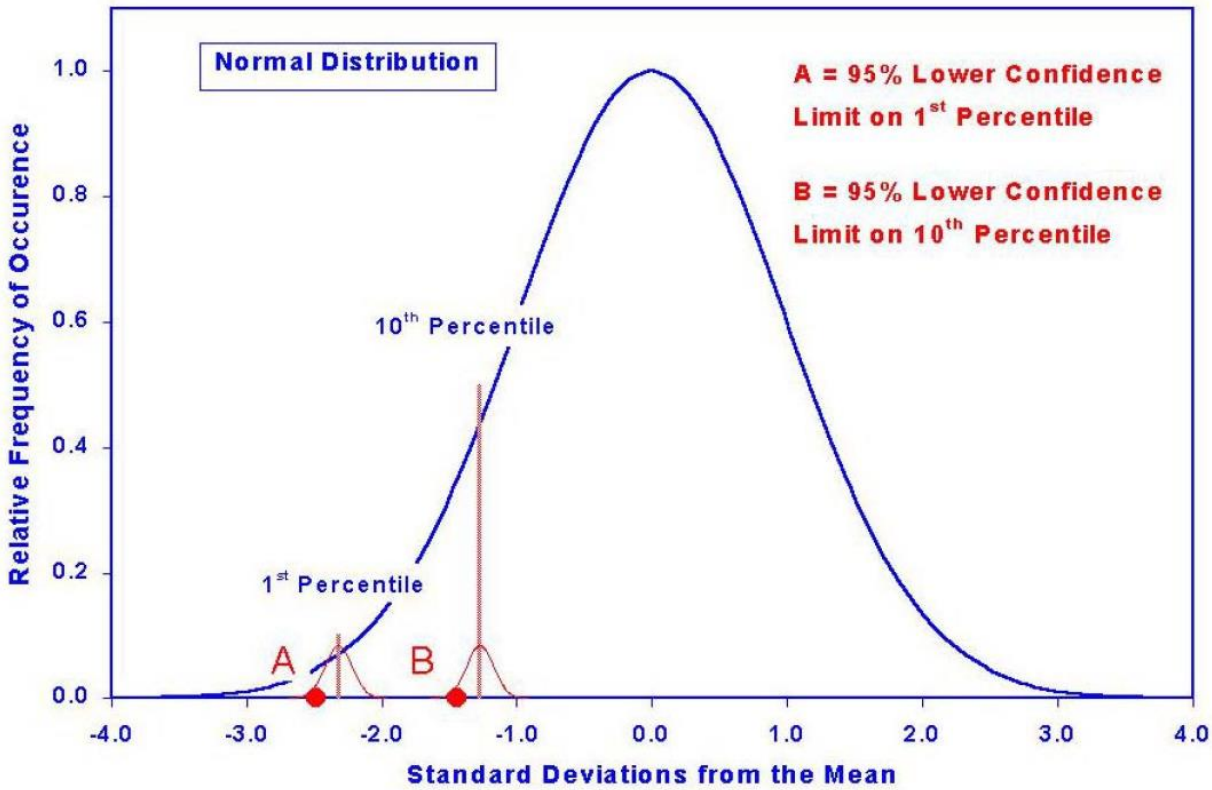

Figure 1 Demonstration of the two statistical levels used to establish the lower bound properties presented here, and based on the MMPDS approach (from [2]). Lower bound properties are determined at the 1st and 10th percentiles of a normal distribution at the 95% confidence level.

levels of lower bound property conservatism.

The lower bound mechanical properties of cast steels determined here at “A” and “B” design allowables result from the analysis of tensile data acquired from the Steel Founders’ Society of America (SFSA) membership. Mechanical property data for yield and ultimate strengths (YS and UTS), elongation (%El) and reduction of area (%RA) are analyzed and the resulting lower bound properties are presented. The results provide a basis for designing components made from the cast steels analyzed. The mechanical test data was grouped by the SFSA by grade, heat treatment, and class according to two specifications; ASTM A958 and ASTM A487 for castings suitable for pressure service according to the ASME Boiler and Pressure Vessel Code (BPVC). For the steels’ mechanical property data grouped by grade and heat treatment according to ASTM A958, the property data presented here are for; 8620, 8625, and 8630 in normalized and tempered condition (N&T), and 8620, 8625, 8630, and 8635 in quenched and tempered heat treatment condition (Q&T). For the data analyzed and grouped according to ASTM A487 and the ASME BPVC, lower bound allowables for grades and classes 4A, 4B, and 4E are determined.

Using the SFSA member test data, the statistical analysis was performed using *SAS* software [3] to determine the lower bound properties according to “A” and “B” design allowable levels. In determining the lower bound properties, outlier data was removed as described below. While performing the analysis, observations are noted from the data sets regarding the statistical distribution of the data and compliance bias apparent in the data in some cases. In the Appendices A and B, histogram and probability plots are given, respectively, for all steels and data analyzed with no outliers removed. The plots in these appendices were made using the *Minitab* software [4].

Analysis Procedures

In this paper, lower bound properties from tensile test results (yield and ultimate strengths, and elongation and reduction of area) are determined for ten cast steels. For each steel and tensile property, a histogram and normal distribution plot is determined along with descriptive statistics (the mean, standard deviation, and number of sample points). Note an example of such a plot given in Figure 2 for 8620 quenched and tempered steel. Descriptive statistics for all properties and steels are given in the results sections, and plots analogous to Figure 2 are given for all steels and properties in Appendix A. The legend in the plots show the average as “Mean”, standard deviations as “StDev” and number of data points as “N”. Plots like Figure 2 are a good snapshot and record of all the data analyzed.

Normal and three-parameter Weibull distributions were both considered as candidate distributions in best describing the data and determining the lower bound properties from the distribution. The Anderson-Darling statistic “AD” was used as to determine which distribution best described the data. The better the distribution fits the data, the lower the statistic will be. An example of the testing of the Normal and three-parameter Weibull distributions to the data is shown in Figures 3 and 4, respectively. The calculated distribution curves are the middle of the three lines plotted in the figures, and the 95% upper and lower bounds are plotted above and

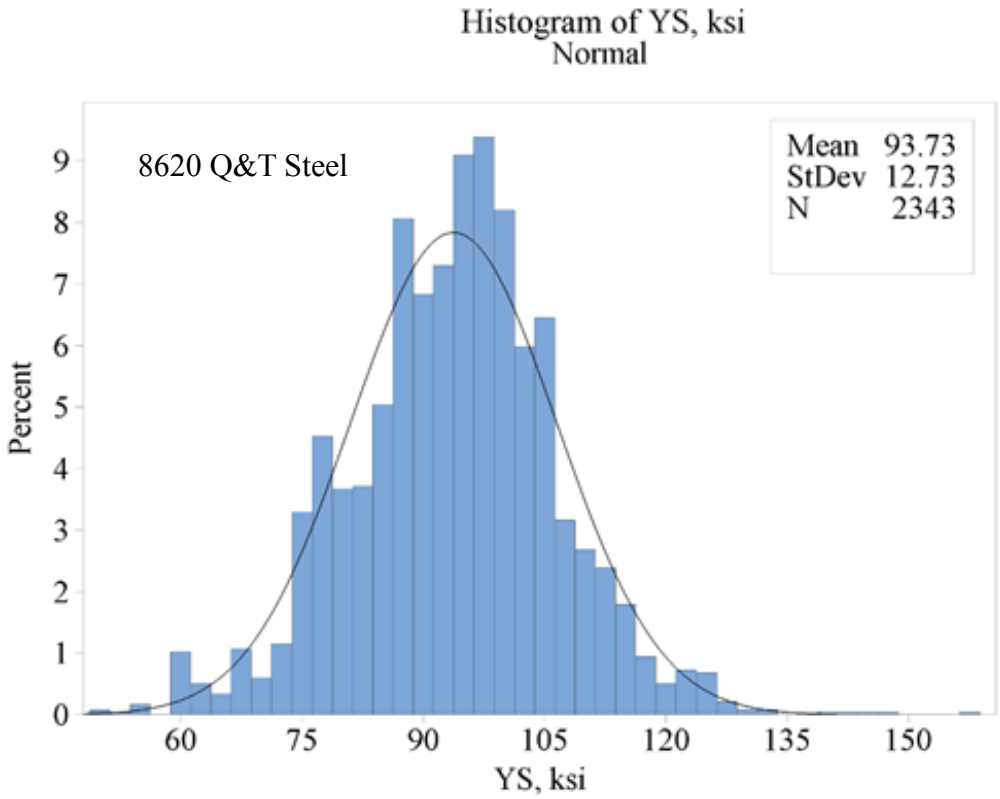

Figure 2 Histogram and normal distribution plot for yield strength of 8620 quenched and tempered steel. Legend gives the mean, standard deviation and number of sample points.

below it, respectively. Symbols in these curves denote the data points. Comparing the probability distribution plots and data in Figures 3 and 4, the Normal distribution appears to be the better fit. This is also supported by the Anderson-Darling statistic (given by the value "AD" in the plot legends) which is 3.7 for the Normal and 6.9 for the Weibull distribution. In general, the Normal distribution was shown to be the better fit for the data, and for cases where it was not, the difference between the two was not large. Therefore, the Normal distribution is used to determine all lower bound property data presented here. A comparison between the lower bound allowables determined from both Weibull and Normal distributions is presented later for the ASTM A487 steels (4A, 4B, and 4E). It is found that comparisons between the minimum requirements and code allowables under the ASME BPVC and the "A" and "B" allowables from both distributions are worth noting. Appendix B gives the Normal probability distribution plots and data for all steels and properties presented in this study, where lines and symbols are the calculated curves (with upper and lower 95% confidence bands) and data points, respectively.

Outlier data was identified in the data sets. The outliers appeared to be caused by data entry in some cases and by anomalous data well outside the range of probability distributions. Such outliers are shown by the data in Figure 3 for example well above and below the probability curves. The z-score of a data point was used as the basis for selecting it as an outlier. The z-score is a measure of a data points difference from the mean relative to the standard deviation of the data set. It is shown by example in Figure 5, where z-score values of -3 and -2 correspond to 0.1% and 2.3% of the Normal distribution, for example.

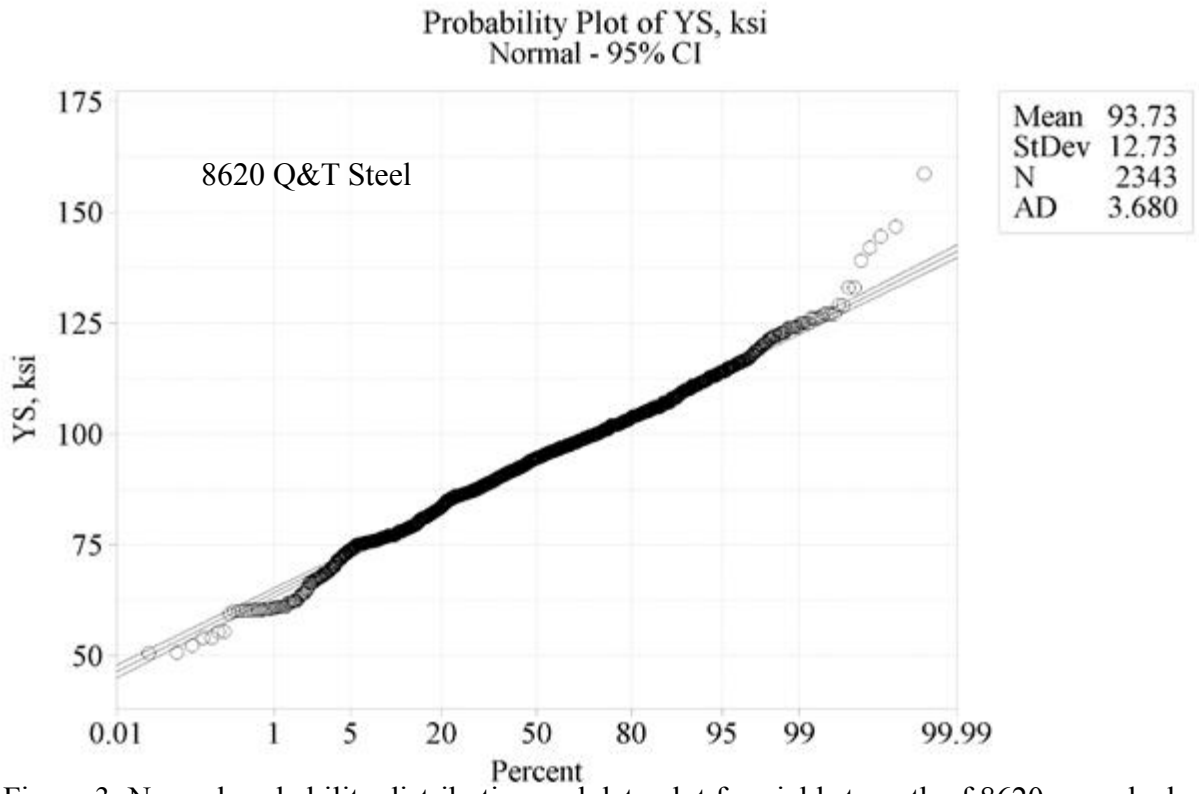

Figure 3 Normal probability distribution and data plot for yield strength of 8620 quenched and tempered steel. Legend gives the mean, standard deviation, number of sample points and Anderson-Darling statistic.

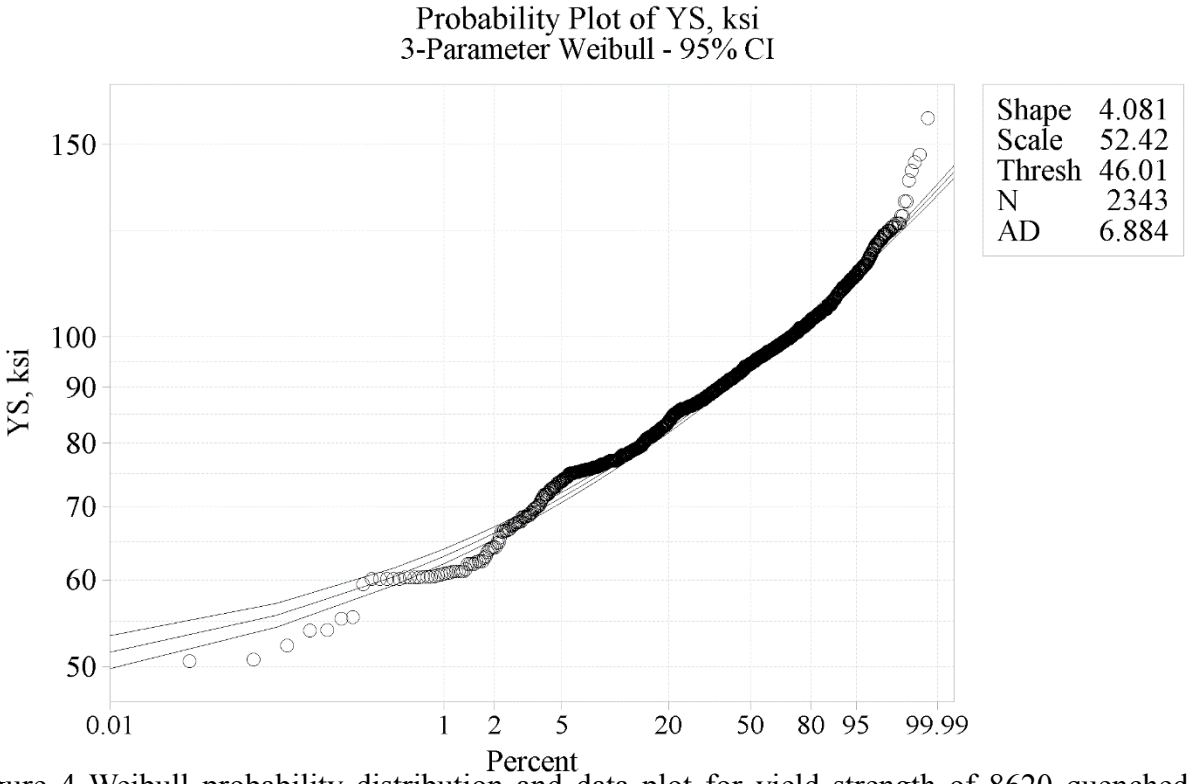

Figure 4 Weibull probability distribution and data plot for yield strength of 8620 quenched and tempered steel. Legend gives the three Weibull parameters, number of sample points and Anderson-Darling statistic.

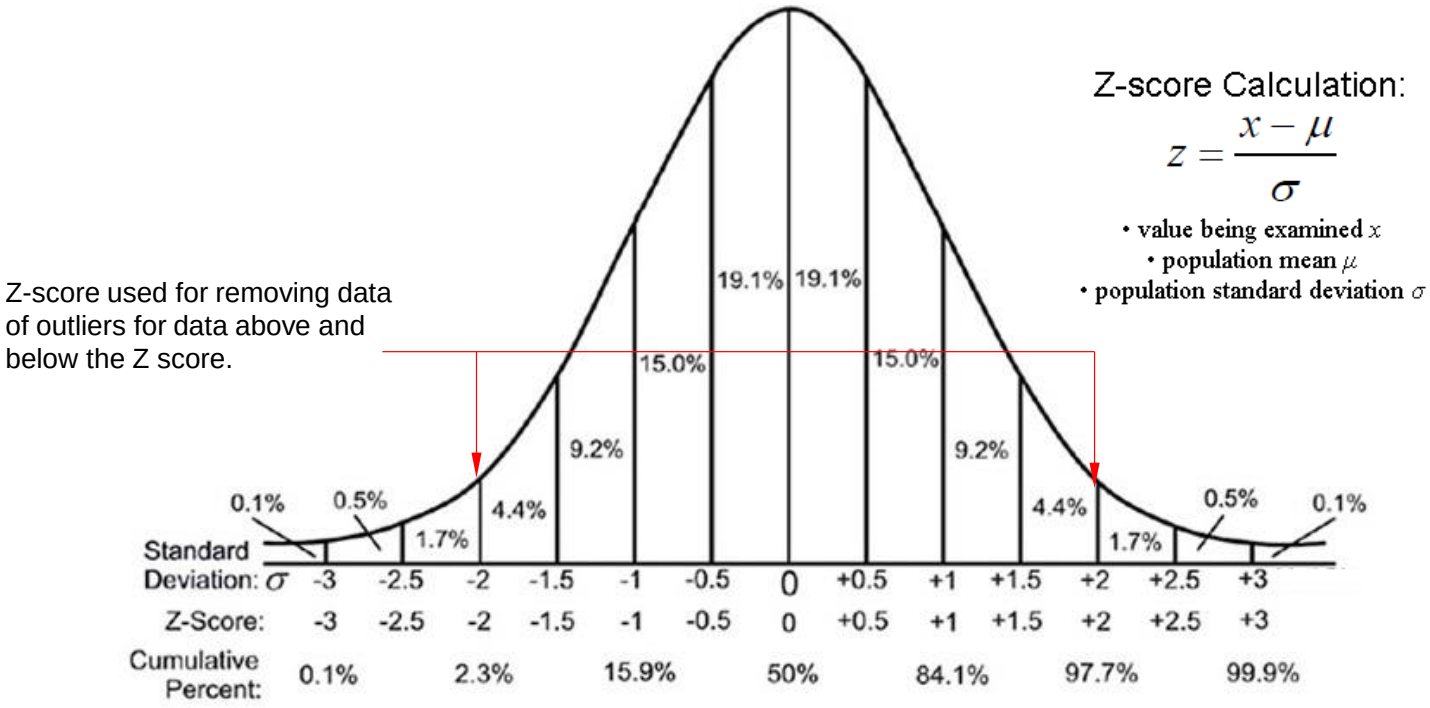

Figure 5 Locations of the z-score level (<-2 and >2) used to remove outliers from the datasets for a Normal distribution, where these levels correspond to 2.3% and 97.7% of the distribution.

Two cases were considered to compare the effect of outlier removal on the lower bound property calculations. In one case, the highest fidelity of the data was considered and in the other a dataset representing the cleanest data was considered. For the highest fidelity data set, data having z-scores below -3 and above +3 were removed (termed z-score level 3 removal). For the cleanest data set, data having z-scores below -2 and above +2 were removed (termed z-score level 2 removal here). An example of the application of the z-score level 2 outlier removal is given in Figure 6. In the figure, probability plots of ultimate tensile strength for 8620 quenched and tempered steel are presented with horizontal scales using the z-score (in Figure 6a) and percent probability (in Figure 6b). The z-score level 2 outlier removal is demonstrated in Figure 6a where data points having z-score values below -2 and above 2 are identified as outliers and are circled. Note that a z-score value of -2 corresponds to 2.3% of the calculated distribution in Figure 6b. The circled points are removed using the z-score level 2 outlier removal, and the lower bound property is calculated for the case. Though not shown here due to space limitations, the lower bound properties calculated after the z-score level 3 outlier removal were unchanged in a practical sense from using the entire data set. Hence the lower bound properties are presented in the results section below for the entire data sets (no outliers removed), and also after using the z-score level 2 outlier removal (for a “clean” data set).

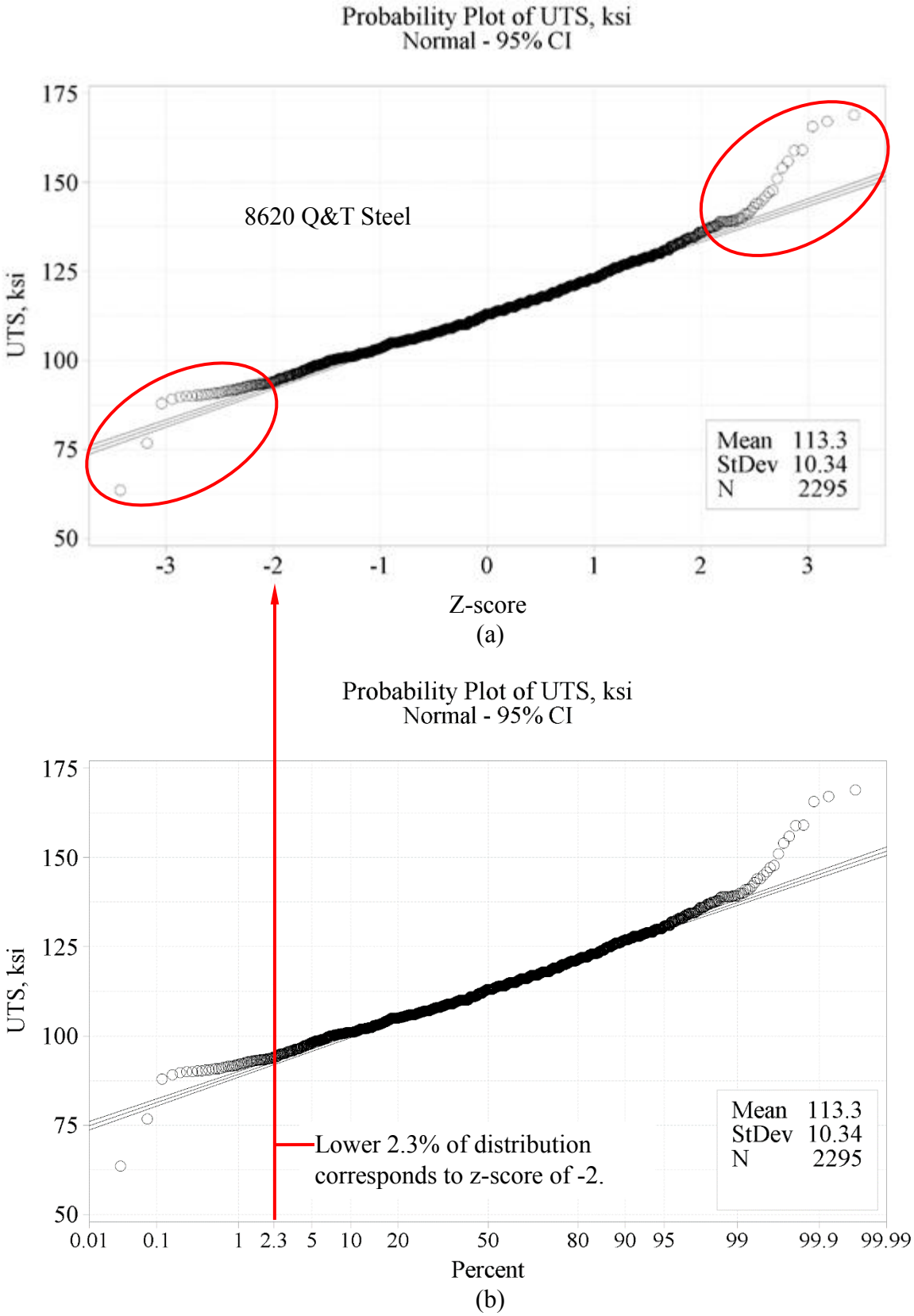

Figure 6 Probability plots of ultimate tensile strength for 8620 quenched and tempered steel presented using the (a) z-score and (b) percent probability scales. Using z-score values below -2 and above 2, the outliers are circled in (a).

Results for ASTM A958 86xx N&T and Q&T Grades

The property data used in the lower bound property calculations for the ASTM A958 steels are shown using histograms, Normal distributions, and statistical measures in Appendix A, Figures A1 to A28. Probability plots of the data and Normal distributions are given for these steel in Appendix B, Figures B1 to B28. In Table 1, the summary statistics are given for the mechanical property data for the 8620, 8625, and 8630 steels in normalized and tempered condition are given. Table 2 provides the summary statistics for the mechanical property data for the ASTM A958 standard grades 8620, 8625, 8630 and 8635 in quenched and tempered heat treatment condition. Note that very large data sets (about 1500 to 2600 data points) were available for the 8620, 8625, 8630 quenched and tempered steels, while much smaller sample sizes (60 to 230 data points) were available for the others. The tables provide the mean, standard deviation, minimum and maximum values, sample size, 1^{st} percentile data point and 10^{th} percentiles data point. The calculated lower bound mechanical property data at the 1% ("A level") and 10% ("B level") for the ASTM A958 standard steels are given in Table 3. Table 3a gives the data without any outliers removed and Table 3b provides lower bound properties with outliers removed using the z-score level 2 removal. Table 3b provides lower bound properties using the cleanest data set (outliers removed), and these properties are plotted by grade and heat treatment and percentage of lower bound in Figures 7 and 8. Figures 7a and 7b given the yield and ultimate strengths, and Figures 8a and 8b give the elongation and reduction of area.

With reference to Figures 7 and 8, it is not surprising that the lower bound strength data increase with Q&T heat treatment and with increasing carbon content. This trend is not born out by the 8630 and 8635 Q&T steels, but the 8635 Q&T steel has a relatively small data set. The minimum lower bound yield strength (at the "A" allowable level) for N&T steel is about 40 ksi and for the Q&T steels it is about 65 ksi. The minimum lower bound ultimate strength (at the "A" allowable level) for N&T steel is about 72 ksi and for the Q&T steels it is about 92 ksi. The ductility data show the 8635 Q&T steel has a low ductility relative to the others, but again this data set is small. The ductility decreases when using Q&T heat treatment and with increasing carbon content. Just looking at elongation as a ductility measure, the "A" allowable lower bound data range from 10% to 15%, and the "B" allowable lower bound data range from 13% to 19%. These remarks are made looking at the data with outliers removed, and excluding the 8635 Q&T data.

Table 1 Summary statistics for mechanical property data for steels grouped by grade and heat treatment according to the ASTM A958 standard; these are 8620, 8625, and 8630 in normalized and tempered condition.

8620 NT

Property	Mean	Standard Deviation	Minimum	Maximum	Number of Samples	1st Percentile	10th Percentile
Yield Strength (ksi)	85.8	16.4	57.6	153.5	208	60.0	63.0
Ultimate Strength (ksi)	108.1	11.7	86.8	168.0	208	89.4	93.5
Elongation (%)	22.0	3.3	18.0	43.0	208	18.0	18.6
Reduction of Area (%)	55.4	6.5	34.0	82.0	208	37.0	45.0

8625 NT

Property	Mean	Standard Deviation	Minimum	Maximum	Number of Samples	1st Percentile	10th Percentile
Yield Strength (ksi)	79.8	15.6	50.1	129.0	214	55.9	60.3
Ultimate Strength (ksi)	103.4	11.6	80.0	151.0	214	84.4	89.9
Elongation (%)	23.8	3.8	16.0	43.0	214	18.0	19.0
Reduction of Area (%)	51.3	7.4	25.4	69.0	214	33.0	42.0

8630 NT

Property	Mean	Standard Deviation	Minimum	Maximum	Number of Samples	1st Percentile	10th Percentile
Yield Strength (ksi)	79.5	16.1	41.3	126.0	230	54.3	59.6
Ultimate Strength (ksi)	105.7	14.1	52.8	150.4	230	85.0	89.7
Elongation (%)	21.7	4.4	11.0	33.0	230	11.5	16.0
Reduction of Area (%)	46.7	9.8	21.0	65.1	230	23.0	33.0

Table 2 Summary statistics for mechanical property data for steels grouped by grade and heat treatment according to the ASTM A958 standard; these are 8620, 8625, 8630 and 8635 in quenched and tempered heat treatment conditions.

8620 QT

Property	Mean	Standard Deviation	Minimum	Maximum	Number of Samples	1st Percentile	10th Percentile
Yield Strength (ksi)	93.7	12.7	50.5	158.6	2343	60.7	77.0
Ultimate Strength (ksi)	113.3	10.3	63.5	168.9	2295	92.0	101.0
Elongation (%)	20.9	3.5	8.0	62.5	2343	16.0	17.8
Reduction of Area (%)	53.0	7.7	24.1	78.8	2338	35.0	41.5

8625 QT

Property	Mean	Standard Deviation	Minimum	Maximum	Number of Samples	1st Percentile	10th Percentile
Yield Strength (ksi)	106.5	15.1	39.5	160.0	2703	71.0	87.6
Ultimate Strength (ksi)	125.5	13.6	52.3	174.0	2695	95.6	107.0
Elongation (%)	18.1	3.1	7.0	62.5	2698	12.0	14.0
Reduction of Area (%)	45.7	8.1	11.3	69.0	2696	30.0	35.9

8630 QT

Property	Mean	Standard Deviation	Minimum	Maximum	Number of Samples	1st Percentile	10th Percentile
Yield Strength (ksi)	108.8	13.7	49.3	160.0	1569	62.8	92.9
Ultimate Strength (ksi)	132.1	13.9	61.0	174.0	1569	97.3	116.0
Elongation (%)	16.7	3.2	7.0	49.0	1557	10.0	14.0
Reduction of Area (%)	40.7	8.0	11.3	75.0	1557	22.0	31.2

8635 QT

Property	Mean	Standard Deviation	Minimum	Maximum	Number of Samples	1st Percentile	10th Percentile
Yield Strength (ksi)	110.3	16.5	59.7	155.5	59	59.7	92.5
Ultimate Strength (ksi)	135.9	19.1	79.9	172.0	59	79.9	114.9
Elongation (%)	14.7	3.1	7.0	22.0	59	7.0	11.0
Reduction of Area (%)	33.4	7.9	15.4	57.0	59	15.4	24.0

Table 3 Lower bound mechanical property data for steels grouped by grade and heat treatment according to the ASTM A958 standard; these are 8620, 8625, 8630 and 8635 in normalized and tempered, and quenched and tempered heat treatment conditions.(a) No outliers are removed from data. (b) Outliers have been removed.

(a) Results with no outliers removed from data.

	Yield Strength (ksi)		Ultimate Strength (ksi)		Elongation (%)		Reduction of Area (%)	
Grade and Heat Treatment	10% Lower Bound	1% Lower Bound	10% Lower Bound	1% Lower Bound	10% Lower Bound	1% Lower Bound	10% Lower Bound	1% Lower Bound
8620 NT	62.1	43.8	91.2	78.1	17.3	13.6	46.0	38.8
8620 QT	76.8	63.3	99.6	88.6	16.3	12.6	42.8	34.6
8625 NT	57.3	39.8	86.7	73.8	18.3	14.0	40.5	32.2
8625 QT	86.5	70.4	107.4	92.9	13.9	10.6	35.1	26.5
8630 NT	56.3	38.4	85.5	69.8	15.3	10.4	32.6	21.7
8630 QT	90.4	75.7	113.5	98.6	12.4	9.0	30.1	21.5
8635 QT	83.6	63.8	105.1	82.2	9.6	5.9	20.7	11.3

(b) Results with outliers removed

	Yield Strength (ksi)		Ultimate Strength (ksi)		Elongation (%)		Reduction of Area (%)	
Grade and Heat Treatment	10% Lower Bound	1% Lower Bound	10% Lower Bound	1% Lower Bound	10% Lower Bound	1% Lower Bound	10% Lower Bound	1% Lower Bound
8620 NT	63.2	46.5	92.9	82.1	18.0	15.1	49.3	43.9
8620 QT	79.8	65.8	101.0	91.6	17.4	14.9	45.0	37.9
8625 NT	57.7	41.0	87.6	75.7	18.7	14.8	42.4	35.2
8625 QT	89.0	74.7	109.1	95.9	14.5	11.7	35.7	27.9
8630 NT	57.4	41.0	87.1	73.4	16.1	11.8	34.1	23.8
8630 QT	94.4	82.3	117.1	104.8	13.1	10.4	31.3	23.9
8635 QT	90.7	76.0	111.0	91.1	10.1	6.6	24.0	18.1

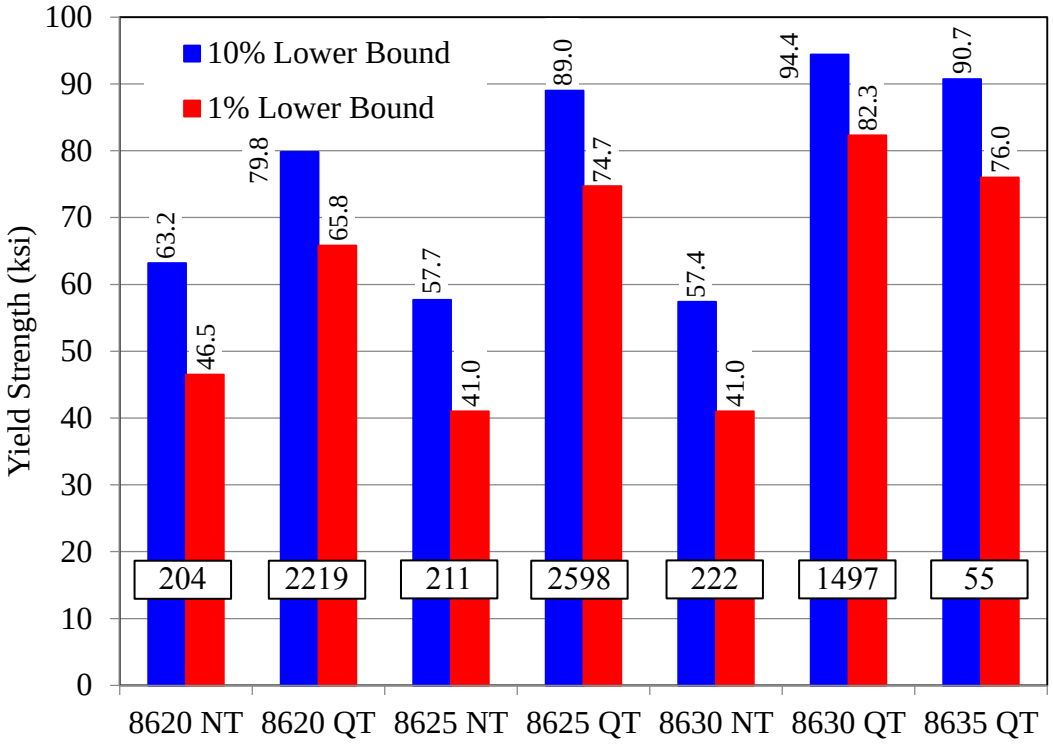

(a)

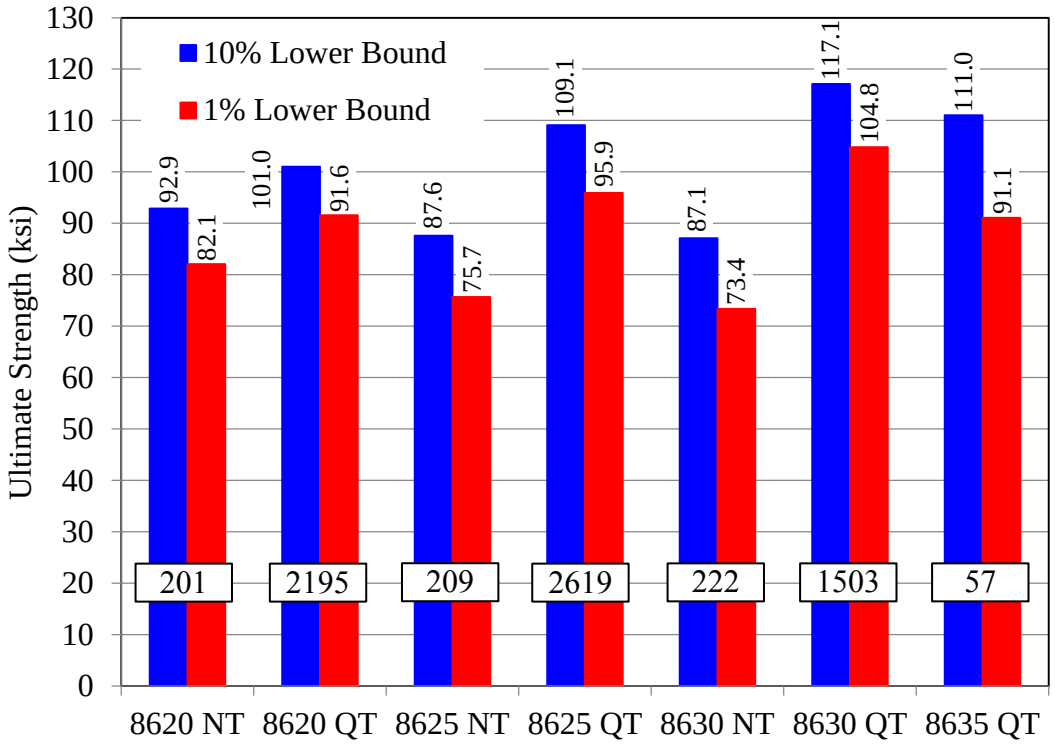

(b)

Figure 7 Lower bound (a) yield strength and (b) ultimate strength property data for steels grouped by grade and heat treatment according to the ASTM A958 standard. Outliers have been removed from the data set. Numbers of samples are given in the horizontal boxes, and property values are given at the tops of the bars.

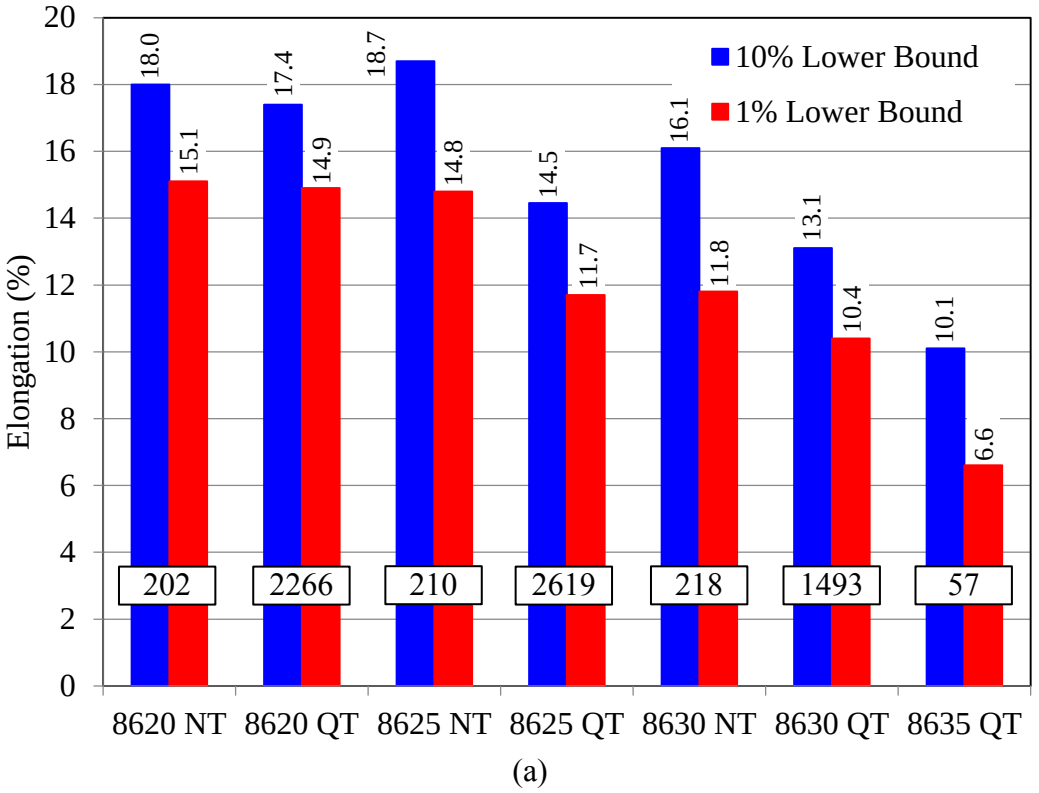

(a)

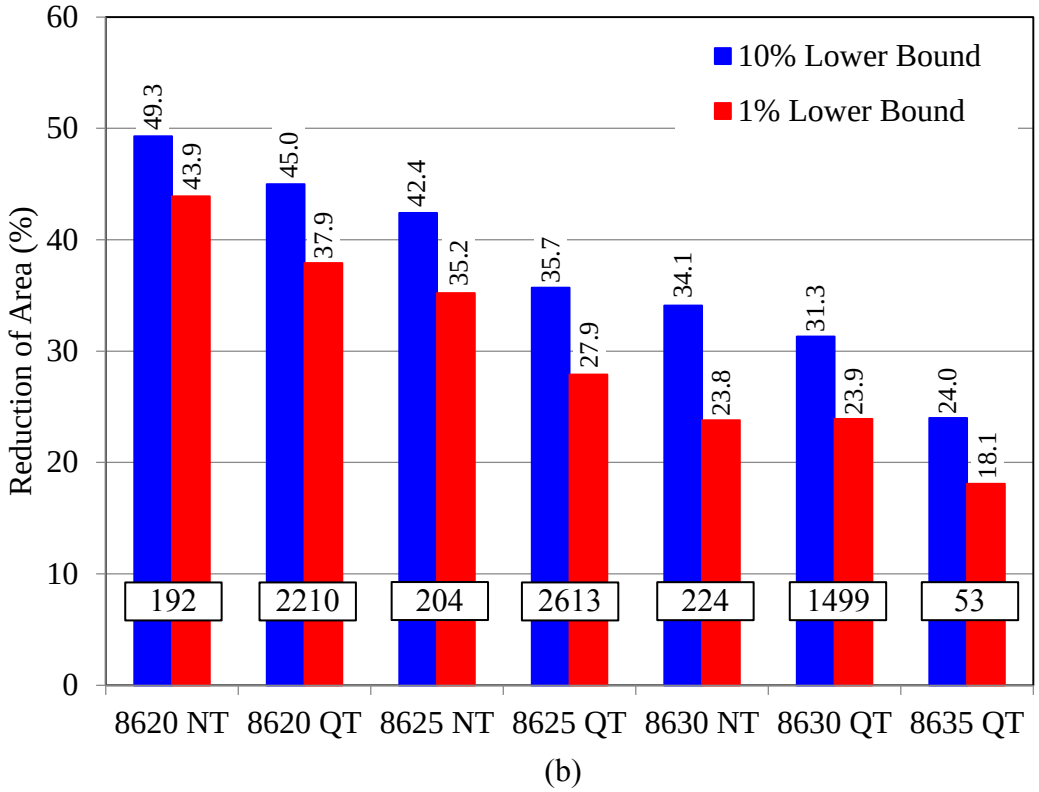

(b)

Figure 8 Lower bound (a) elongation and (b) reduction of area property data for steels grouped by grade and heat treatment according to the ASTM A958 standard. Outliers have been removed from the data set. Numbers of samples are given in the horizontal boxes, and property values are given at the tops of the bars.

Results for ASTM A487 Grades 4A, 4B, and 4E

The property data used in the lower bound property calculations for the ASTM A487 steels are shown using histograms, Normal distributions, and statistical measures in Appendix A, Figures A29 to A40. Probability plots of the data and Normal distributions are given for these steel in Appendix B, Figures B29 to B40. In Table 4 the summary statistics are given for the mechanical property data for the ASTM A487 Grades 4A, 4B and 4E. Note that consistently large data sets (about 1600 to 2100 data points) were available for the steels grouped by these classes. The table provides the mean, standard deviation, minimum and maximum values, sample size, 1^{st} percentile data point and 10^{th} percentiles data point for these steels. The calculated lower bound mechanical property data at the 1% ("A level") and 10% ("B level") for the ASTM A487 standard steels are given in Table 5. Table 5a gives the lower bound data without any outliers removed and Table 5b provides lower bound properties with outliers removed using the z-score level 2 removals. Note therefore that Table 5b provides lower bound properties using the cleanest data set (outliers removed), and the lower bound properties show only a small increase with the outliers removed. The properties from Table 5b are plotted by grade and class, and percentage of lower bound allowable level in Figures 9 and 10. Figures 9a and 9b given the yield and ultimate strengths, and Figures 10a and 10b give the elongation and reduction of area.

For the strength data in Figure 9, and the ductility data in Figure 10, it is not surprising that there is a trend for increasing strength and decreasing ductility, respectively, from steel 4A to 4B to 4E steels as the minimum requirements in Table 6 indicate there should be. It is interesting to note that for the "A" allowable data (at 1% lower bound) only grade 4A meets the minimum required strengths, and none of the elongation minimum requirements are met. For the "B" allowable data (at 10% lower bound) all the strength minimum requirements are met except for the 4E steel. It is interesting that the 4E steel has virtually no difference between the "A" and "B" lower bound allowables for yield strength.

There is evidence of compliance bias in the data for the steels grouped by the A487 grade 4 and classes A, B and E. This is made clear by the minimum requirements in Table 6, and the large number of samples observed at these requirements. The large numbers of samples at the requirements are clearly not stochastic, and do not follow the probability plots in Appendix B for the 4A, 4B and 4E steels. For example, in Figures 11 and 12, probability plots are shown from the *SAS* software of yield strength and elongation, respectively, for the 4A steel. The yield strength plot in Figure 11 shows a large number of samples at 60 ksi which is the minimum required yield strength (highlighted by a red box in Table 6). The elongation plot in Figure 12 shows an even larger number of samples at 18% which is the minimum required elongation (again called out by a red box in Table 6). If the reader observes the probability plots in Appendix B for the 4A, 4B and 4E steels, they will note: 1) For 4A steel not only is there bias at the yield strength (YS) and elongation, but also for the UTS at 90 ksi; 2) For 4B steel, there is a bias at 75 ksi for YS (not the requirement though), bias at 105 ksi for UTS and bias for elongation at 17%; 3) For the 4E steel, the is apparent bias at all the requirements, at 95 ksi for YS, at 115 ksi for UTS, and around 15% for elongation.

Table 4 Summary statistics for mechanical property data for steels grouped according to ASTM A487 for grades and classes 4A, 4B and 4E. No outliers have been removed.

ASTM A487 4A

Property	Mean	Standard Deviation	Minimum	Maximum	Number of Samples	1st Percentile	10th Percentile
Yield Strength (ksi)	85.1	10.4	50.1	118.1	1805	60.2	71.0
Ultimate Strength (ksi)	106.0	6.4	90.0	115.0	1810	90.8	96.3
Elongation (%)	21.6	3.7	9.3	62.5	1810	17.0	18.0
Reduction of Area (%)	51.8	8.4	21.5	82.0	1807	35.0	39.9

ASTM A487 4B

Property	Mean	Standard Deviation	Minimum	Maximum	Number of Samples	1st Percentile	10th Percentile
Yield Strength (ksi)	97.4	8.6	60.4	129.0	2120	75.8	86.5
Ultimate Strength (ksi)	116.9	7.3	105.0	130.0	2123	105.0	107.0
Elongation (%)	19.8	3.5	9.0	62.5	2123	12.0	17.0
Reduction of Area (%)	50.3	8.3	11.3	78.8	2120	31.0	38.0

ASTM A487 4E

Property	Mean	Standard Deviation	Minimum	Maximum	Number of Samples	1st Percentile	10th Percentile
Yield Strength (ksi)	104.7	8.1	60.4	148.0	1593	89.0	96.0
Ultimate Strength (ksi)	124.8	6.8	115.0	140.0	1594	115.0	116.0
Elongation (%)	18.5	3.2	9.0	50.5	1594	12.0	14.6
Reduction of Area (%)	47.2	8.0	11.3	78.8	1594	30.0	36.1

Table 5 Lower bound mechanical property data for steels grouped according to ASTM A487 for grades and classes 4A, 4B and 4E.

(a) Results with no outliers removed from data.

	Yield Strength (ksi)		Ultimate Strength (ksi)		Elongation (%)		Reduction of Area (%)	
Grade and Heat Treatment	10% Lower Bound	1% Lower Bound	10% Lower Bound	1% Lower Bound	10% Lower Bound	1% Lower Bound	10% Lower Bound	1% Lower Bound
A487 4A	71.8	61.0	97.8	91.2	16.8	12.9	41.0	32.3
A487 4B	86.3	77.3	107.6	100.0	15.3	11.6	39.6	30.9
A487 4E	94.3	85.9	116.1	109.1	14.4	11.8	36.9	28.5

(b) Results with outliers removed

	Yield Strength (ksi)		Ultimate Strength (ksi)		Elongation (%)		Reduction in Area (%)	
Grade and Heat Treatment	10% Lower Bound	1% Lower Bound	10% Lower Bound	1% Lower Bound	10% Lower Bound	1% Lower Bound	10% Lower Bound	1% Lower Bound
A487 4A	74.9	65.8	99.1	93.0	18.4	15.7	41.6	33.1
A487 4B	87.5	79.4	107.8	100.4	16.4	13.8	40.3	32.1
A487 4E	95.4	88.4	116.7	110.1	15.3	12.7	37.7	29.8

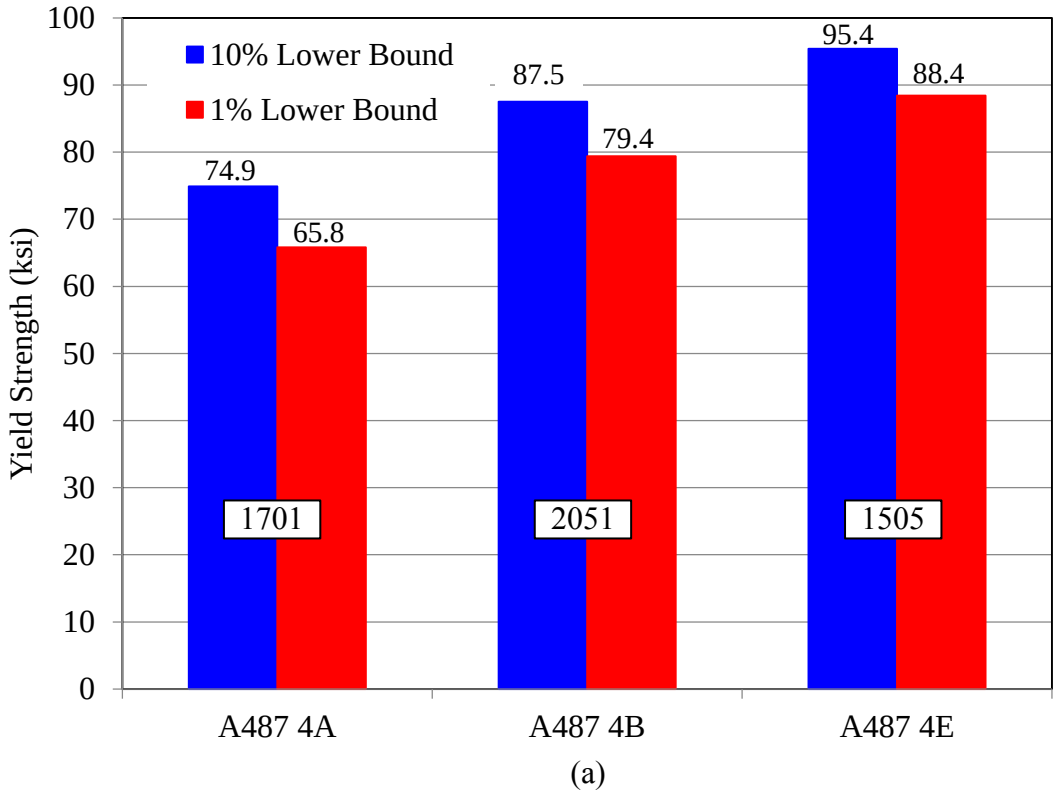

(a)

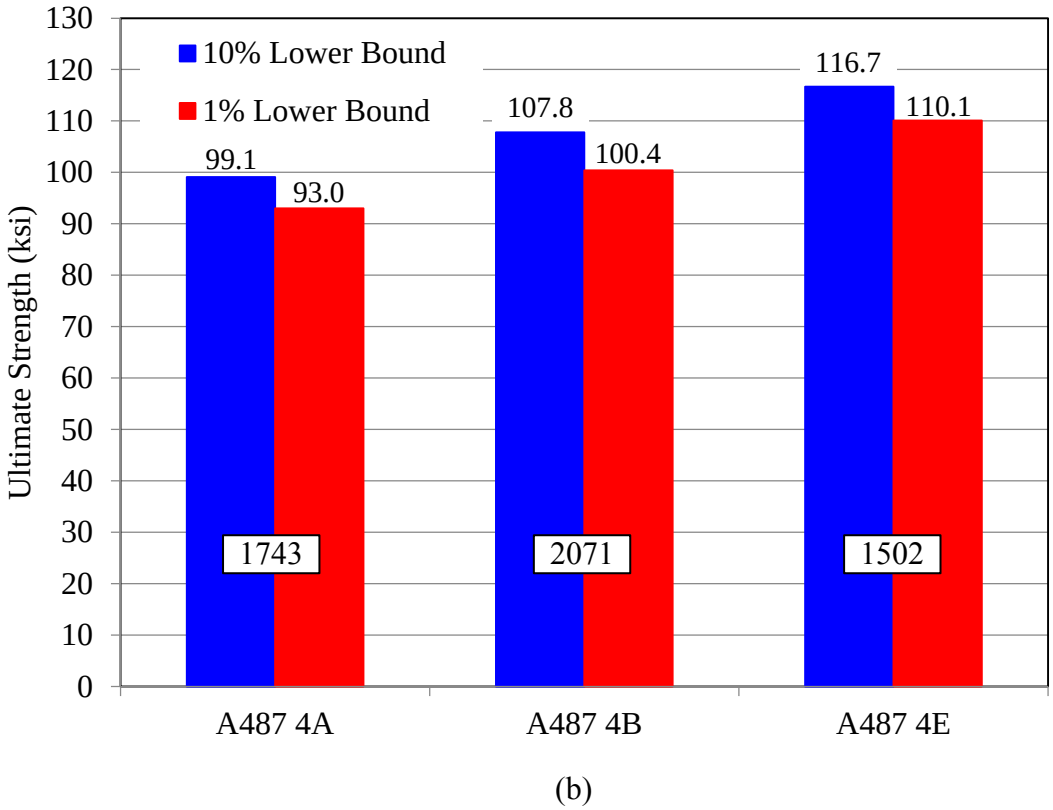

(b)

Figure 9 Lower bound (a) yield strength and (b) ultimate strength property data for steels grouped by grade and heat treatment according to the ASTM A487 standard. Outliers have been removed from the data set. Numbers of samples are given in the horizontal boxes, and property values are given at the tops of the bars.

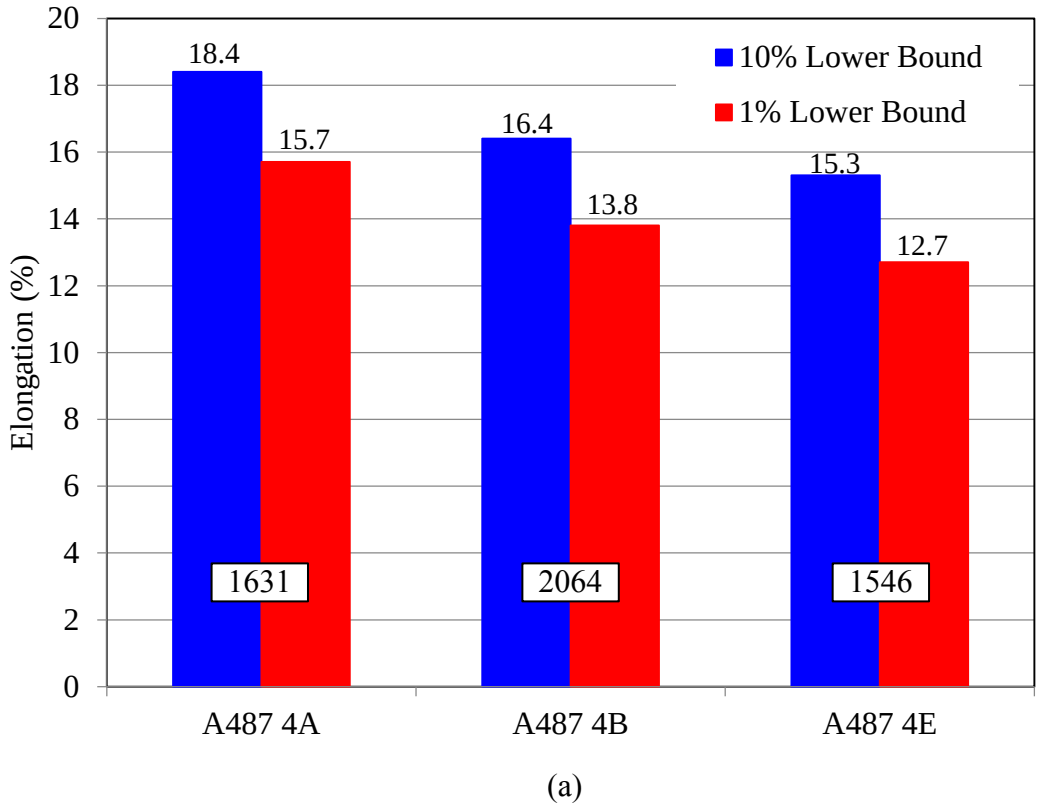

(a)

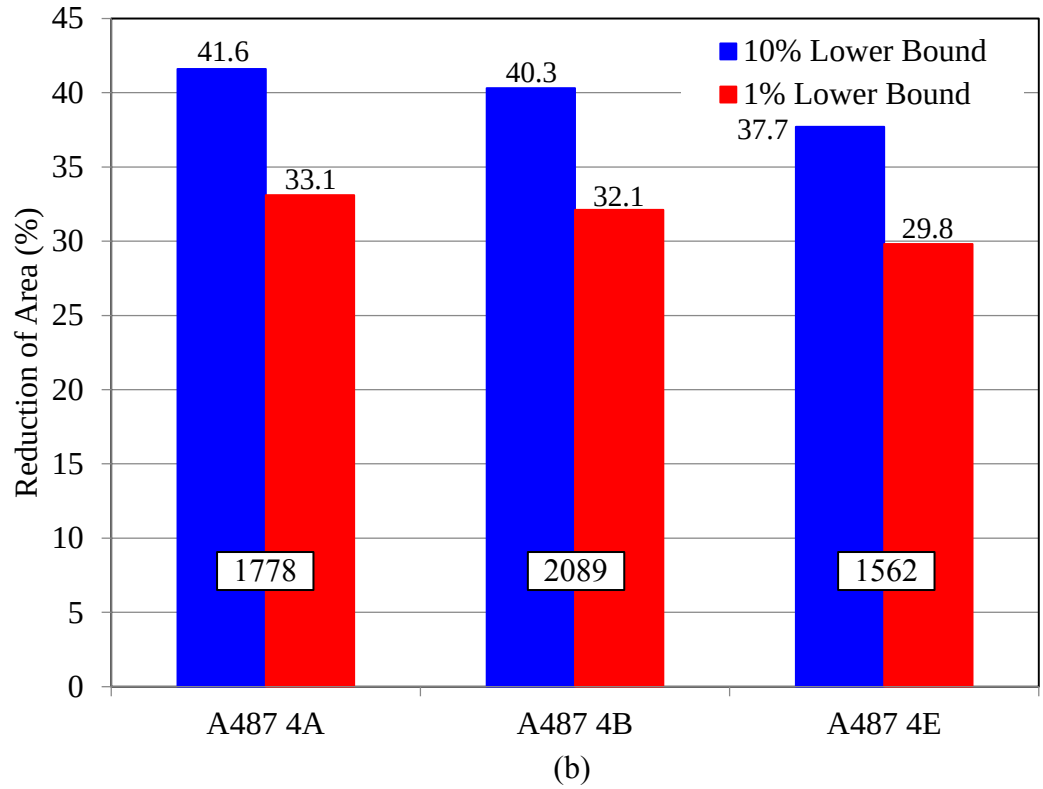

(b)

Figure 10 Lower bound (a) elongation and (b) reduction of area property data for steels grouped by grade and heat treatment according to the ASTM A487 standard. Outliers have been removed from the data set. Numbers of samples are given in the horizontal boxes, and property values are given at the tops of the bars.

Table 6 Minimum requirements and design code allowables for ASTM A487 grades and classes 4A, 4B and 4E steels.

		UTS (ksi)	YS (ksi)	Elongation (%)	Design Stress
Spec	Grade	Minimum Required	Minimum Required	Minimum Required	Code Allowable
SA487	4A	90	60	18	25.7
SA487	4B	105	85	17	30.0
SA487	4E	115	95	15	32.9

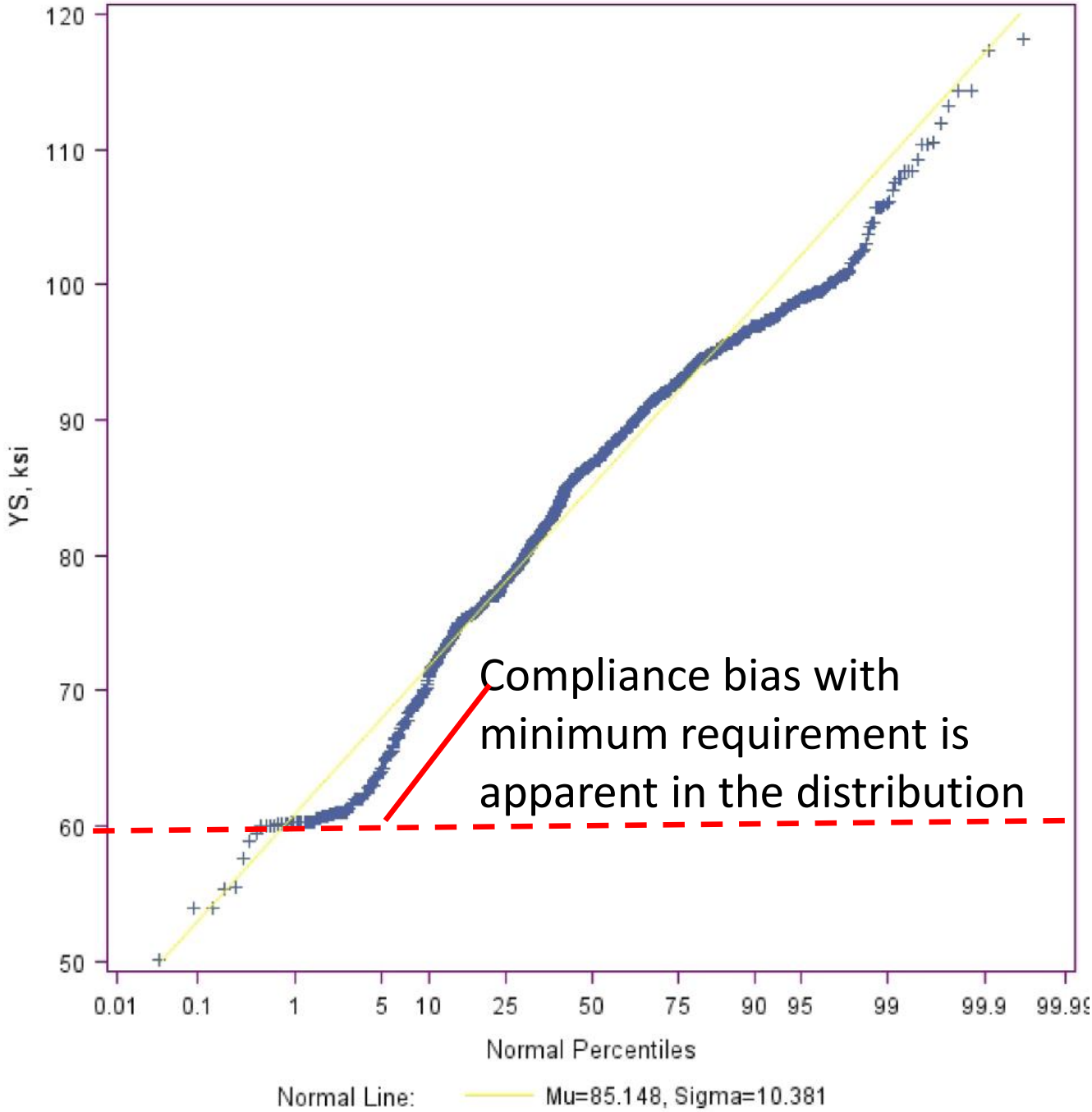

Figure 11 Probability plot from *SAS* software of yield strength for 4A steel. The plot gives a demonstration in the data of compliance bias at 60 ksi which is the minimum required yield strength.

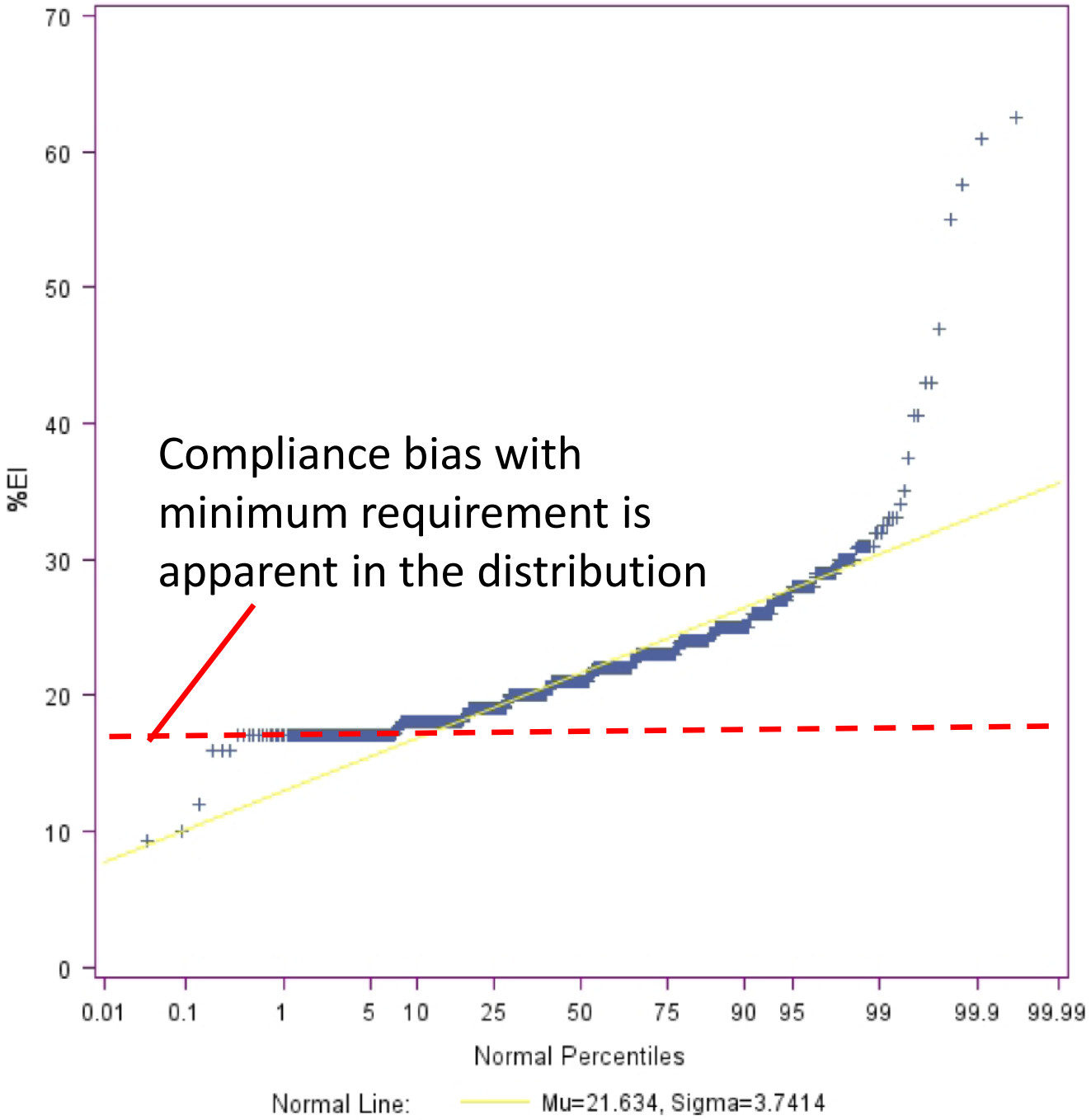

Figure 12 Probability plot from *SAS* software of elongation for 4A steel. The plot gives a demonstration in the data of compliance bias at 18% which is the minimum required elongation.

For the reduction of area, there appears to be no bias in the data related to minimum requirements. This data is very much smoother and evenly distributed in the probability plots than the elongation data (see plots B36 and B40). Although for the 4A steel the reduction in area data shown in Figure B32 demonstrate a strong bias at 35%.

Summarizing with some final observations, note the minimum requirements, design code allowables and lower bound mechanical property data calculated both Normal and Weibull

Table 7 Minimum requirements, design code allowables and lower bound mechanical property data for normal and Weibull distributions for steels grouped according to ASTM A487 for grades and classes 4A, 4B and 4E. No outliers have been removed.

	YS (ksi)						
Grade	Minimum Required	Code Allowable	"A" Allowable	"B" Allowable	Weibull "A"	Weibull "B"	3 Sigma
4A	60	25.7	61.0	71.8	55.5	70.9	54.0
4B	85	30.0	77.3	86.3	69.1	84.0	71.5
4E	95	32.9	85.9	94.3	73.9	90.0	80.1
	UTS (ksi)						
Grade	Minimum Required	Code Allowable	"A" Allowable	"B" Allowable	Weibull "A"	Weibull "B"	3 Sigma
4A	90	-	91.2	97.8	87.0	97.6	86.9
4B	105	-	100.0	107.6	92.8	105.9	95.1
4E	115	-	109.1	116.1	100.2	113.6	104.5
	Elongation (%)						
Grade	Minimum Required	Code Allowable	"A" Allowable	"B" Allowable	Weibull "A"	Weibull "B"	3 Sigma
4A	18	-	12.9	16.8	8.0	13.8	10.4
4B	17	-	11.6	15.3	6.9	12.3	9.2
4E	15	-	11.8	14.4	7.1	12.0	9.0
	Reduction of Area (%)						
Grade	Minimum Required	Code Allowable	"A" Allowable	"B" Allowable	Weibull "A"	Weibull "B"	3 Sigma
4A	-	-	32.3	41.0	29.4	40.5	26.7
4B	-	-	30.9	39.6	28.1	39.1	25.3
4E	-	-	28.5	36.9	25.5	36.1	23.1

distributions for steels grouped according to ASTM A487 for grades and classes 4A, 4B and 4E in Tables 7 and 8. In Table 7 the entire data set is used for each steel, and in Table 8 the outliers have been removed. Note that the Weibull distribution “A” and “B” allowables have been added in addition to the 3-Sigma lower bound allowables. The 3-Sigma lower bound is added for comparison as it is a very conservative level, at 0.1% of the distribution. In some cases this corresponds with the Weibull “A” allowable, which is seen to be always more conservative than the Normal distribution “A” allowable properties. Note the conservative levels of the design stress code allowables, which show a safety factor of around 2 for the “A” allowable properties,

Table 8 Minimum requirements, design code allowables and lower bound mechanical property data for normal and Weibull distributions for steels grouped according to ASTM A487 for grades and classes 4A, 4B and 4E.. Outliers have been removed.

	YS (ksi)						
Grade	Minimum Required	Code Allowable	"A" Allowable	"B" Allowable	Weibull "A"	Weibull "B"	3 Sigma
4A	60	25.7	65.8	74.9	60.6	74.2	59.9
4B	85	30.0	79.4	87.5	72.0	85.6	74.1
4E	95	32.9	88.4	95.4	79.4	92.6	84.0

	UTS (ksi)						
Grade	Minimum Required	Code Allowable	"A" Allowable	"B" Allowable	Weibull "A"	Weibull "B"	3 Sigma
4A	90	-	93.0	99.1	88.7	98.6	89.1
4B	105	-	100.4	107.8	93.3	106.2	95.6
4E	115	-	110.1	116.7	101.9	114.4	105.9

	Elongation (%)						
Grade	Minimum Required	Code Allowable	"A" Allowable	"B" Allowable	Weibull "A"	Weibull "B"	3 Sigma
4A	18	-	15.7	18.4	13.2	17.4	13.9
4B	17	-	13.8	16.4	11.9	15.8	12.0
4E	15	-	12.7	15.3	11.2	14.9	11.1

	Reduction of Area (%)						
Grade	Minimum Required	Code Allowable	"A" Allowable	"B" Allowable	Weibull "A"	Weibull "B"	3 Sigma
4A	-	-	33.1	41.6	30.4	41.3	27.7
4B	-	-	32.1	40.3	29.3	40.0	26.7
4E	-	-	29.8	37.7	27.0	37.2	24.7

and a safety factor of around 3 for the “B” allowable properties.

Study on the Prediction of Lower Bound Properties for 8630 Q&T Steel

Tensile test specimens produced from cast 8630 Q&T steel were machined from three test castings and a commercial casting. The tensile specimens were used in a study to develop a method to predict the tensile properties using casting and heat treatment simulation results. Following that, predictions of the lower bound properties for 8630 Q&T steel were developed using the statistics and lower bound properties determined from the SFSA member data for 8630 Q&T steel.

In Figures 13 to 15 images and a drawing of the three test castings used in the study are shown. A Y-block casting with a 4”x4” cross section from which eight specimens were machined was one source of the steel, shown in Figure 13a. The test specimens and their locations are shown in Figure 13b with the labels used identify them. Note that one specimen has a 0.5” diameter gage section (ID label 2A), and the others have 0.25” diameter gage sections. The keel block from which one specimen was taken is shown in the dimensioned drawings in Figure 14. The equivalent round (ER) casting used in 8630 Q&T property prediction study is shown in Figure 15. The location of the specimens taken from this casting is shown in the figure and is 1-1/8” from the surface. The commercial casting used as another source of material is not shown here, and its weight was about 362 pounds. The specimens taken from it were from heavy sections, at locations similar to specimens 3, 4 and 6 in the Y-block casting (see Figure 13b). All feeders were removed from the castings prior to heat treatment. The measured tensile test data from the cast 8630 Q&T steel specimens with the location IDs used are given in Table 9. In the table, the numbered “Location” IDs are from the Y-block, the “Standard Bar” is from the keel block, the specimens beginning with “ER” are from the equivalent round casting, and the specimen IDs beginning with “Part” are from the commercial casting. Note that one of the ER casting specimens is highlighted in red because the ductility data do not make physical sense, and the reduction of area is likely erroneous.

All castings were simulated using filling and solidification in *MAGMAsoft*, and the heat treatment was simulated using the *MAGMAsteel* module [5]. Models of the tensile test specimens were included in the simulations so that simulation results could be readily determined at the specimen locations (for example see Figure 13b). The *MAGMAsteel* module predicts microstructure and tensile properties resulting from the heat treatment process using the chemistry. The poured chemistry was used in the simulations. Selected results from the simulations using the *MAGMAsteel* module are shown in Figures 16 and 17 in the Y-block casting section and at specimen locations, respectively. The *MAGMAsteel* results show a bainitic microstructure at the center of the Y-block section (see Figure 16) that transitions to a martensitic structure nearer the surface (see Figure 17). These phases develop as a result of the quenching process and because heat transfer limits the effect of the quench to cool the casting. During the quench, the lower the cooling rate within the casting, the lower the amount of transition to martensite, and bainite forms instead in these simulation results. *MAGMAsteel* outputs tensile property predictions for yield strength (*YS*), ultimate strength (*UTS*), elongation (*EL*) and reduction of area (*RA*). The property prediction calculations use the predicted microstructure. For

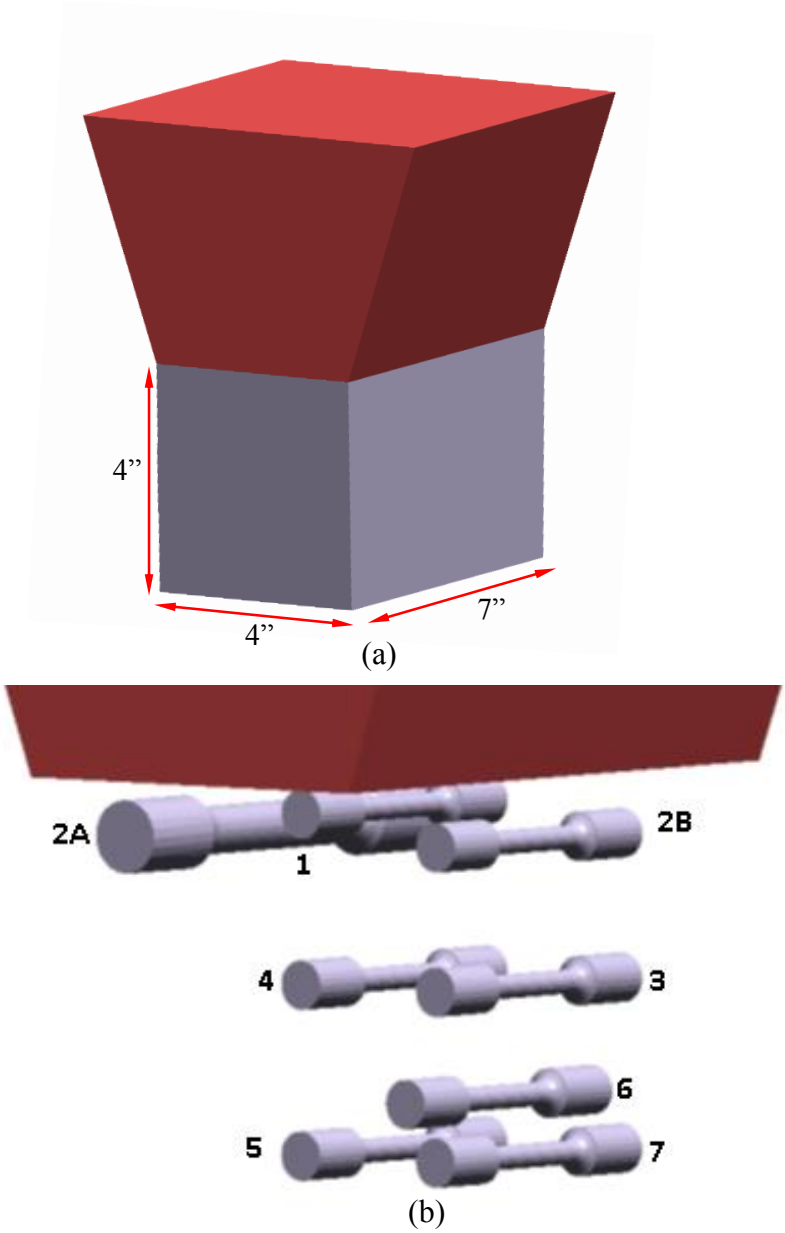

Figure 13 (a) Y-block casting and (b) the eight test specimens and their locations

the Y-block, because of this the yield strength prediction shown in Figure 17b has a similar appearance to the amount of martensite predicted in Figure 17a. In Figures18 and 19, the predicted versus measured yield and ultimate strengths for 8630 Q&T steel from *MAGMAsteel* compared to predictions and measurements for normalized WCB steel, just for comparison between these two grades and conditions. The symbols in the figures refer to the data in Table 9. Similarly, in Figures18 and 19, the predicted versus measured ductility data for 8630 Q&T steel from *MAGMAsteel* compared to predictions and measurements for normalized WCB steel. The vertical error bars in the figures give the data of data in a specimen. Generally, the strength data considering both grades show a good trend of agreement, but the 8630 data is slightly over predicted. Looking just at the 8630 Q&T strength data, much of the Y-block and the single keel block data point are the highest and the data from the commercial part and the ER casting are lower. Unfortunately the ductility data in Figures 20 and 21 show little variation in the predicted results, and do not agree with the measurements even in trend.

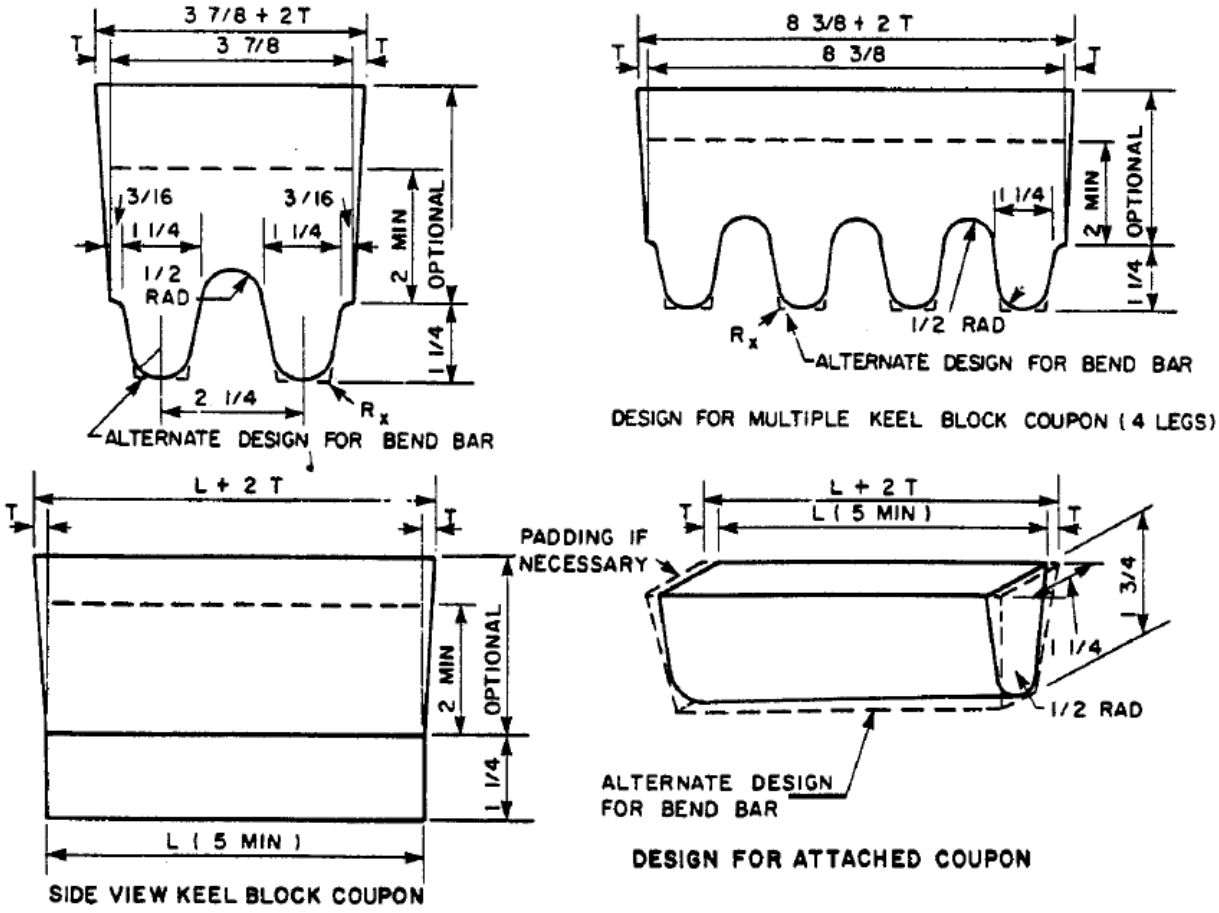

Figure 14 Keel block casting used in 8630 Q&T property study (dimensions in inches).

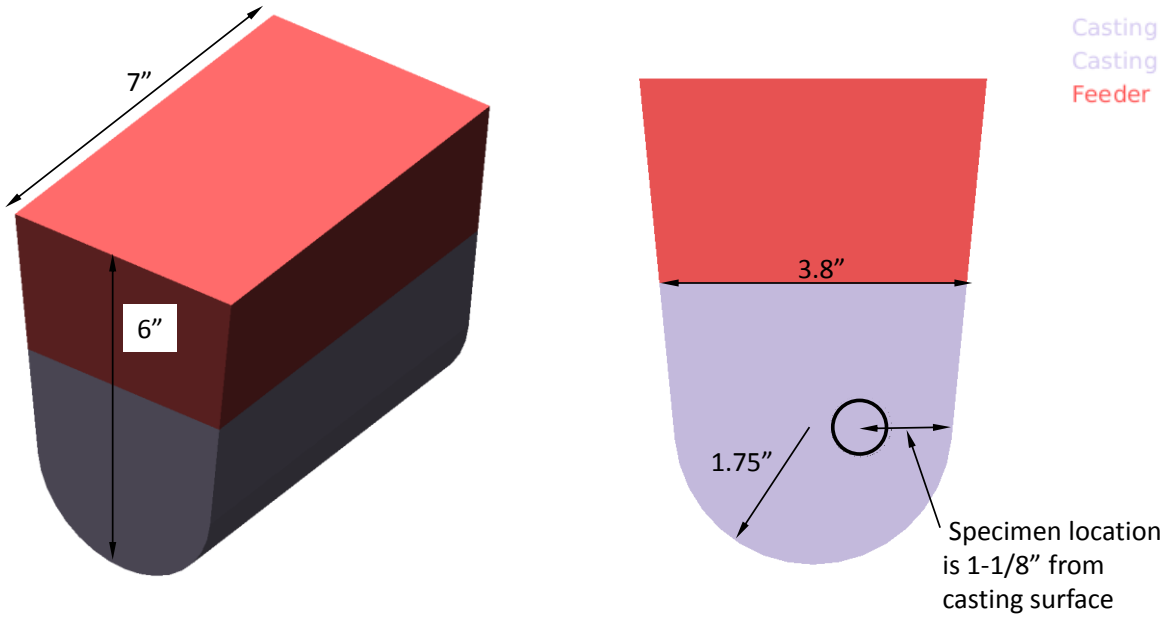

Figure 15 Equivalent round casting used in 8630 Q&T property prediction study.

Table 9 Measured tensile test data from the cast 8630 Q&T steel specimens with the location IDs used.

Location	Yield (ksi)	Tensile (ksi)	Elong (%)	RA (%)
1	113.2	129.5	5	13
2A	116.2	138.5	15	42
2B	108.9	134.9	15	35
3	100.2	129.1	13	42
4	94.3	123	16	39
5	103.3	129.2	16	42
6	97.8	125.5	14	27
7	117.5	140.8	16	49
Standard Bar	103.318	132.459	22	42.4
ER bar 1.13"	65.5	96.6	11.5	**12.2**
ER bar surface	85.6	114.1	10	16.8
Part 0°	86.8	110.6	9	10.1
Part 45°	78.5	104.5	9.5	11.5
Part 1/2" Red	83.7	108.4	15	26.9
Part 1/2" Blue	91.9	113	9	11.3
ER bar 1.13"	86.6	115	14	23.6
ER bar surface	88.2	115.4	14	21.7
Part 1/2" Red	95.5	117.5	16	24.5
Part 1/2" Blue	97.6	119.4	15.5	26.4

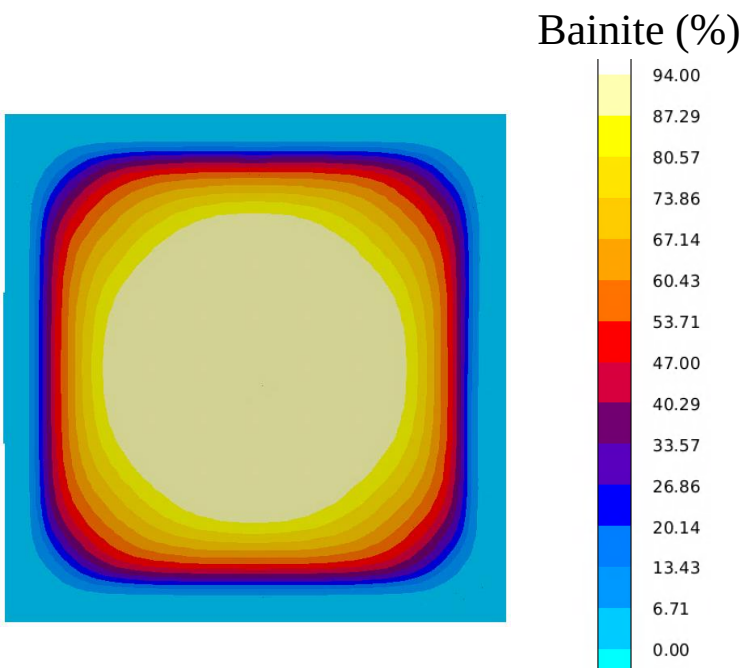

Figure 16 Microstructure prediction from the *MAGMAsteel* module for the final bainite phase percentage in the 8630 Q&T Y-block casting section.

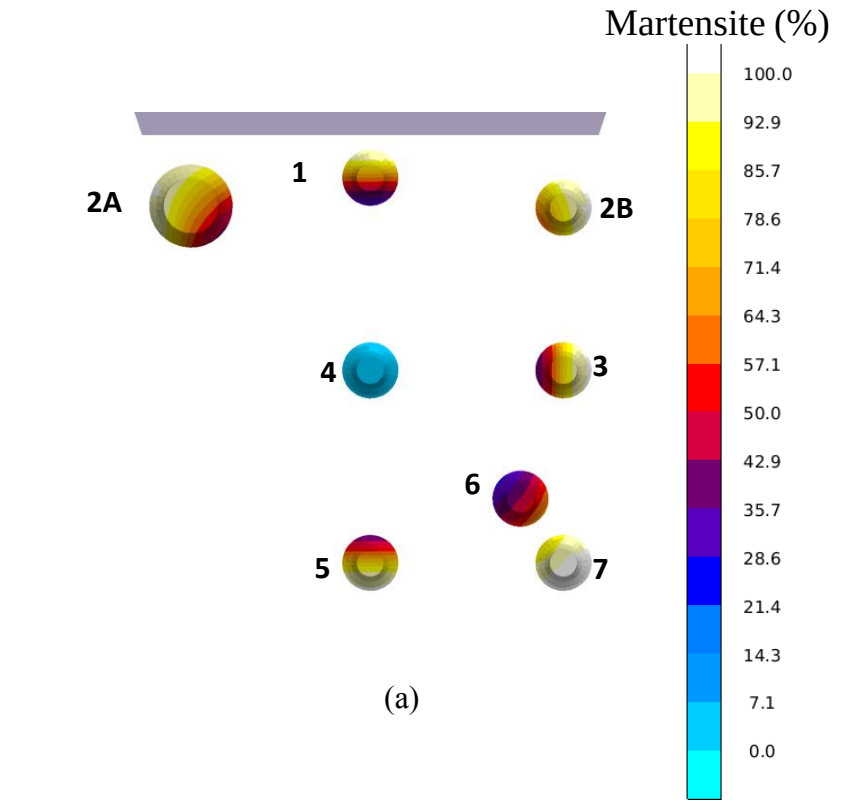

(a)

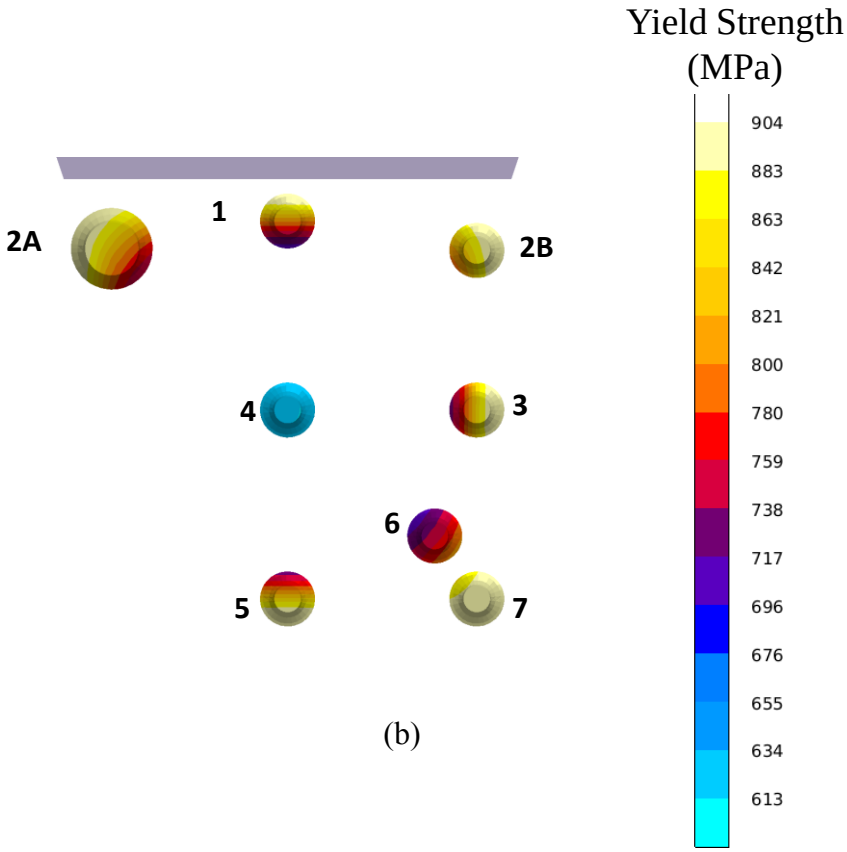

(b)

Figure 17 (a) Microstructure prediction from the *MAGMAsteel* module showing the final martensite phase percentage and (b) yield strength prediction from the *MAGMAsteel* module at the specimen locations in the 8630 Q&T Y-block casting.

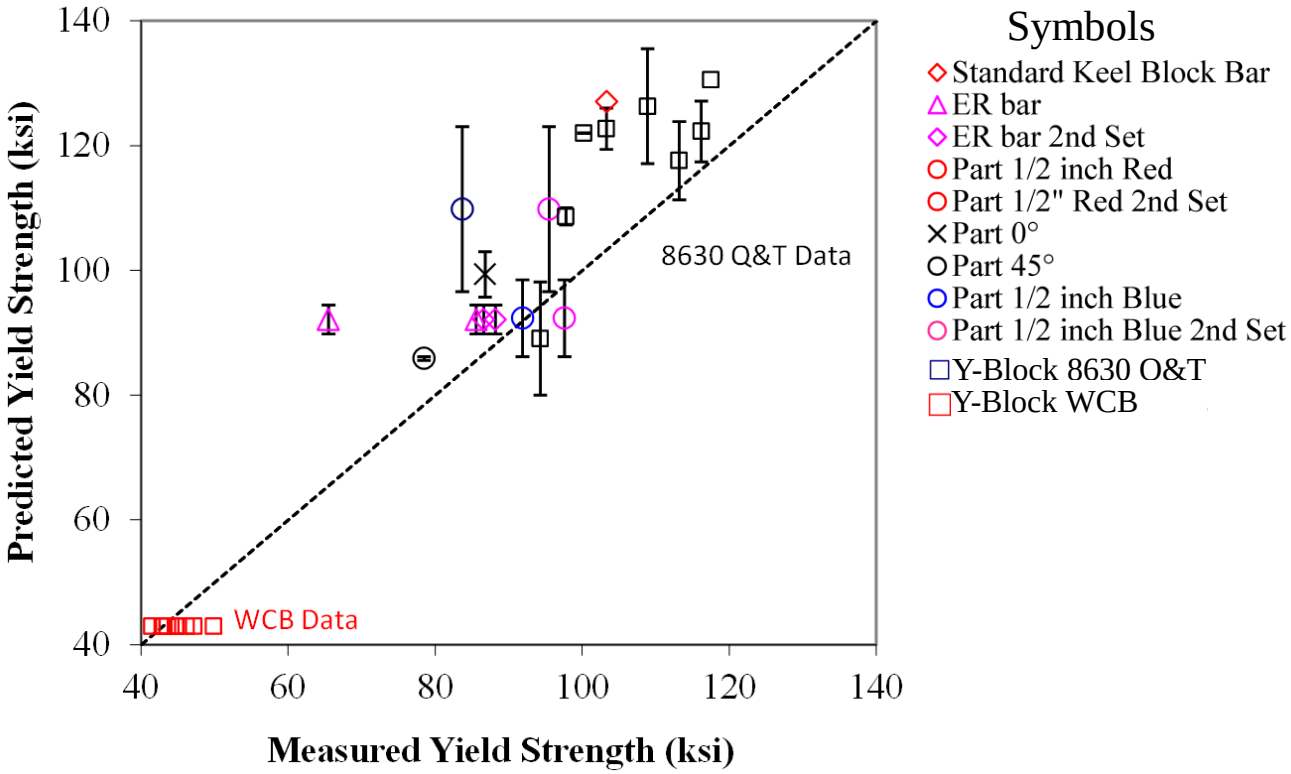

Figure 18 Predicted versus measured yield strengths for the 8630 Q&T steel from *MAGMAsteel* compared to predictions and measurements for WCB steel.

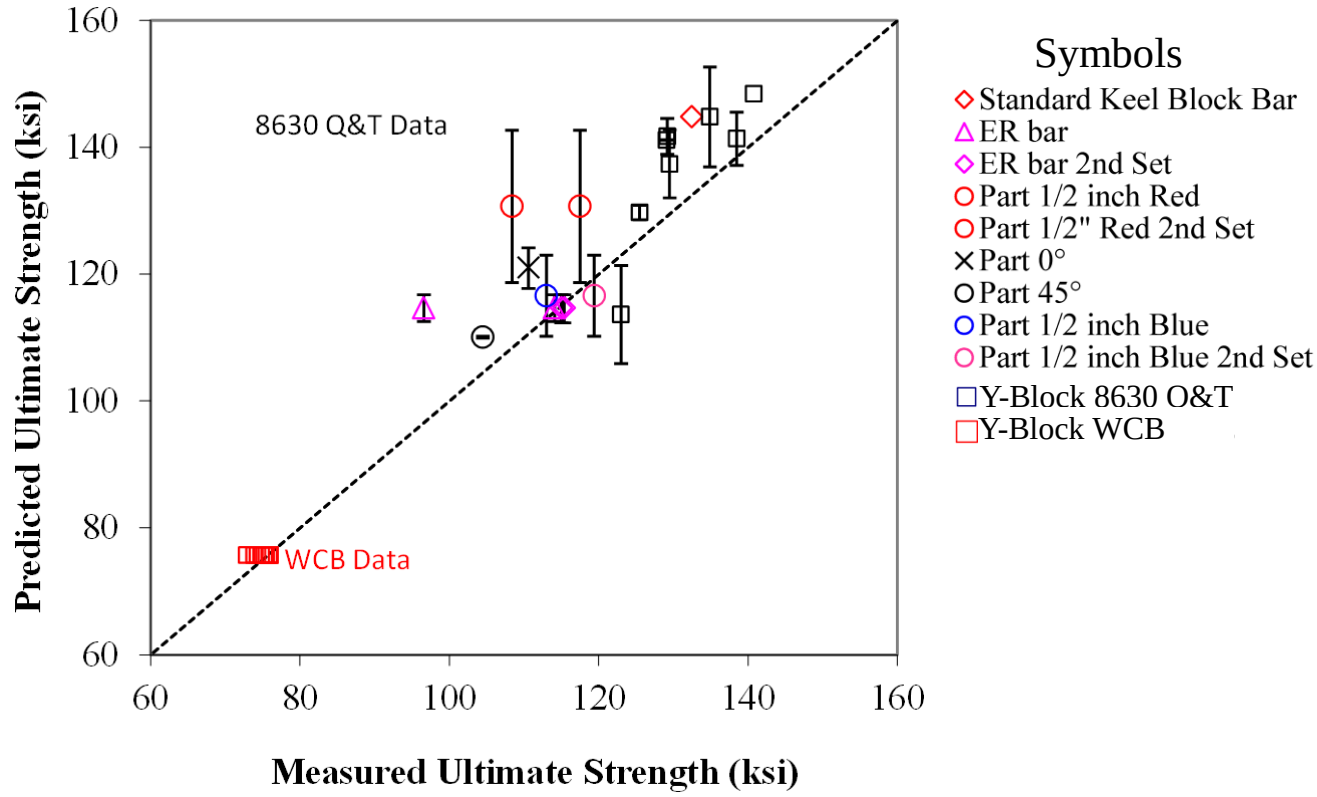

Figure 19 Predicted versus measured ultimate strengths for the 8630 Q&T steel from *MAGMAsteel* compared to predictions and measurements for WCB steel.

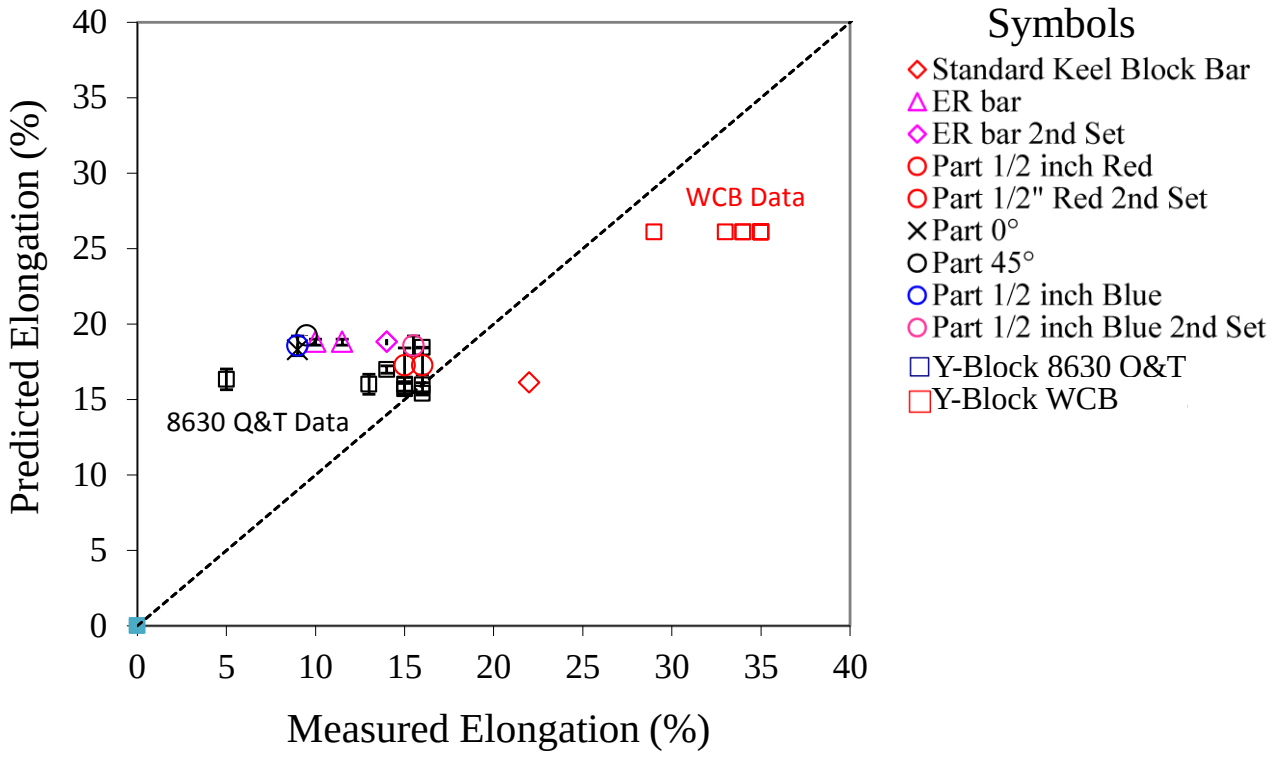

Figure 20 Predicted versus measured reduction of area for 8630 Q&T steel from *MAGMAsteel* compared to predictions and measurements for WCB steel.

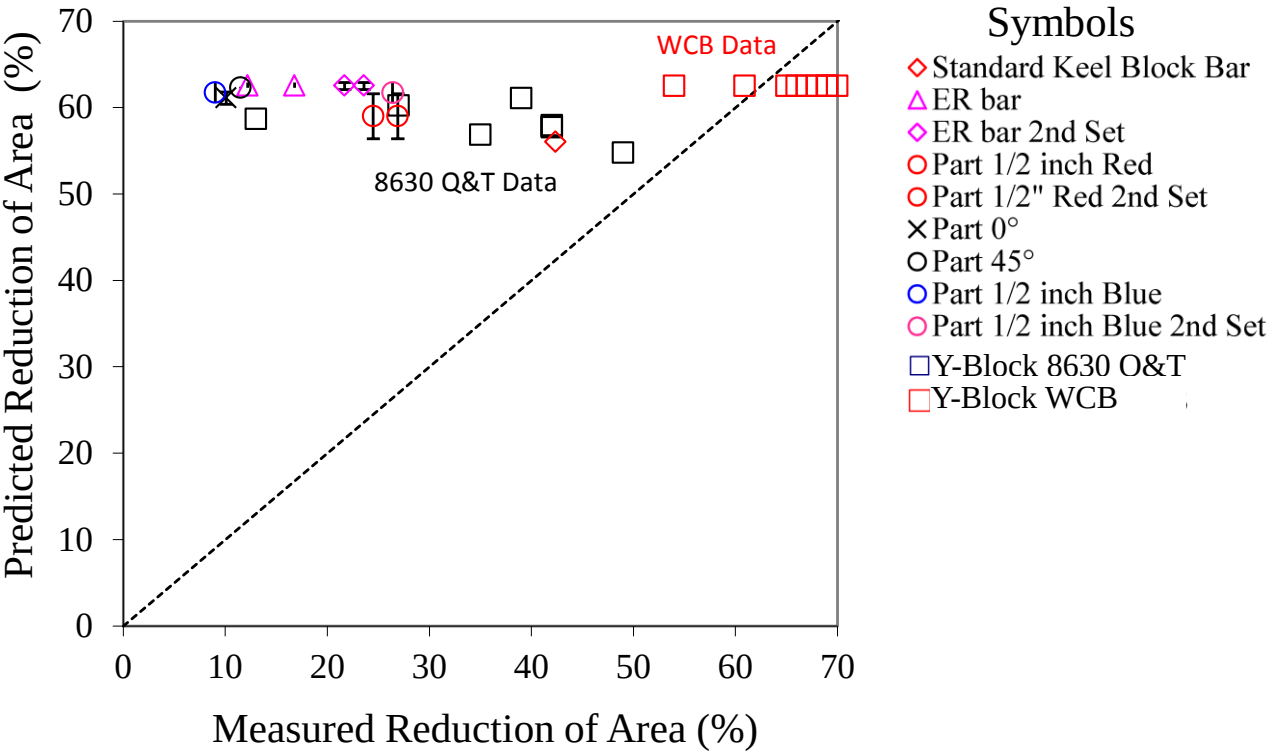

Figure 21 Predicted versus measured reduction of area for 8630 Q&T steel from *MAGMAsteel* compared to predictions and measurements for WCB steel.

In order to improve property predictions resulting from the *MAGMAsteel* module and using the results from solidification, studies were performed using numerous results and curve fits to the measured data. The results from *MAGMAsteel* property predictions and *MAGMAsoft* (such as solidification and cooling rates, thermal gradient, porosity, Niyama criterion) were explored using multivariable curve fitting using linear and non-linear equations for the fits. In some cases, complex form of the fitting equations using three or for parameters produced very good results having lower standard errors than the equations presented here. It was decided to use simple equations with a limited number of parameters (only two) to provide an improvement in the agreement between the predictions and the measurements. For yield strength *YS* the equation used was

$$YS = 0.881 YS_{MAGMAsteel} + 3.52\ \nabla T \tag{1}$$

where $YS_{MAGMAsteel}$ is the yield strength from *MAGMAsteel* and ∇T is the temperature gradient during solidification (used in calculating the Niyama criterion). Similarly the equation having a simple form that was found to improve the ultimate strength *UTS* prediction was

$$UTS = 0.939 UTS_{MAGMAsteel} + 2.15\ \nabla T \tag{2}$$

where $UTS_{MAGMAsteel}$ is the ultimate strength from *MAGMAsteel*. The predictions for the 8630 Q&T steel using the *MAGMAsteel* results in combination with temperature gradient are shown in Figure 22. In the figure the predicted versus measured yield and ultimate strengths have a much better agreement than those from the results from *MAGMAsteel* in Figures 18 and 19. Equations 1 and 2 can be defined as a user result in the software and used and viewed as any other result. For the ductility results, reduction of area *RA* and elongation *EL*, the result (if restricted to selecting only one result) from the solidification modeling which improved the best fit to the measurements was the solidification rate $\dot{T}$. Since $\dot{T}$ is a primary variable in determining the secondary dendrite arm spacing, using it makes physical sense, as it is related to the cast microstructure. The equations used to improve the RA and EL predictions are

$$RA = 253 - 3.79\ RA_{MAGMAsteel} + 13.2\ \dot{T} \tag{3}$$

and

$$EL = 20.6 - 56.8\ EL_{MAGMAsteel} + 29.4\ \dot{T} \tag{4}$$

where $EL_{MAGMAsteel}$ and $RA_{MAGMAsteel}$ are the elongation and reduction of area from *MAGMAsteel*, respectively. As shown in Figure 23, there was not a great improvement in the agreement between the elongation measurements and predictions. Although, the keel block data point at 22% elongation no appears to be correctly predicted with the addition of the cooling rate. For the reduction of area, adding the cooling rate to the prediction, Equation 3, the data follows a much better trend and agreement that the original *MAGMAsteel* result for *RA*.

Equations 1 to 4 are best fit equations using the local simulation results describing the average of the local variation of the measured tensile data. So these equations provide us with a prediction of the mean property value resulting from the solidification and heat treatment conditions locally in the casting. Using the mean and standard deviation from the statistical

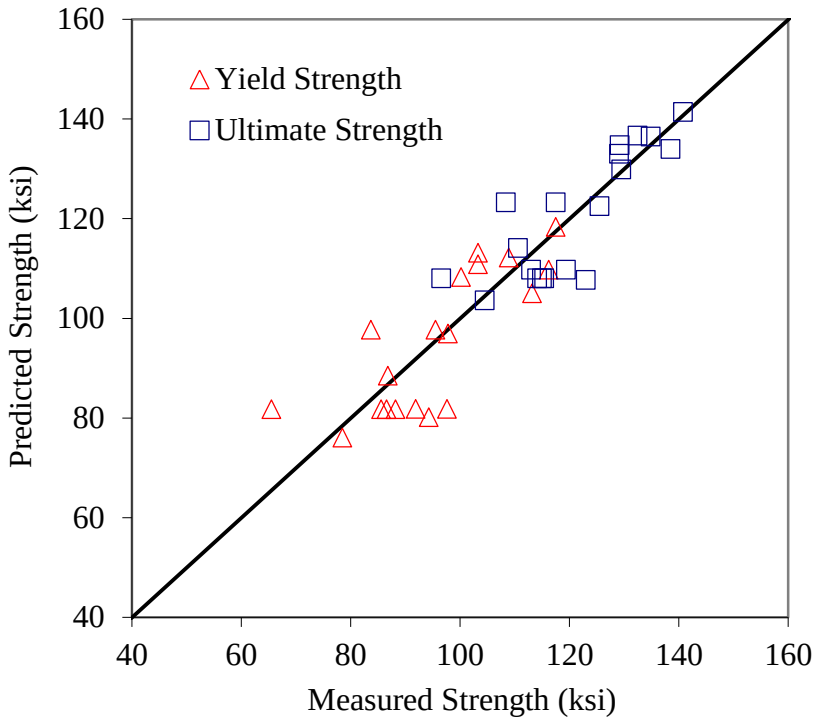

Figure 22 Predicted versus measured yield and ultimate strengths. The predictions use the *MAGMAsteel* results in combination with temperature gradient.

distribution of the SFSA member 8630 Q&T data, and the z-scores calculated at the 1st and 10th percentiles corresponding to the lower bound properties, the results from the mean property predictions can be converted to lower bound property predictions. For example, consider the yield strength for 8630 Q&T steel from the SFSA member data, the mean is 108.8 ksi, the standard deviation is 13.7 ksi, and the lower bound data at the 10th percentile is 94.4 ksi and at the 1st percentile is 82.3 ksi. The z-score for the 10th percentile is -1.05 (from (94.4 – 108.8)/13.7) and the z-score at the 1st percentile is -1.93. The lower bound prediction is then determined by calculating the reduction in a property from the results of Equations 1 to 4 to the z-score for the lower bound level. For yield stress using the result of Equation 1 this is, YS – (1.05)(13.7) for the 10th percentile lower bound, and YS – (1.93)(13.7) for the 1st percentile lower bound. For each property, its mean, standard deviation and lower bound properties are used to calculate the z-scores at the 10th and 1st percentiles. Then the relevant property prediction from Equations 1 to 4, the standard deviation and resulting z-scores, are used to calculate the lower bound properties. The lower bound property prediction results for the strength data is presented in Figure 25 for the 10th percentile level (analogous to the "B" design allowable level), and in Figure 26 for the 1st percentile level (analogous to the "A" design allowable level). Note that since the predictions in these figures include the local property variations one would find in commercial castings, they are more conservative than the lower bound properties determined from the SFSA member data, where specimens come from keel and other test block castings. Equation 1 to 4, and the approach used to calculate lower bound properties at two level of conservatism, will serve as a basis to link the performance of casting designs to their production process.

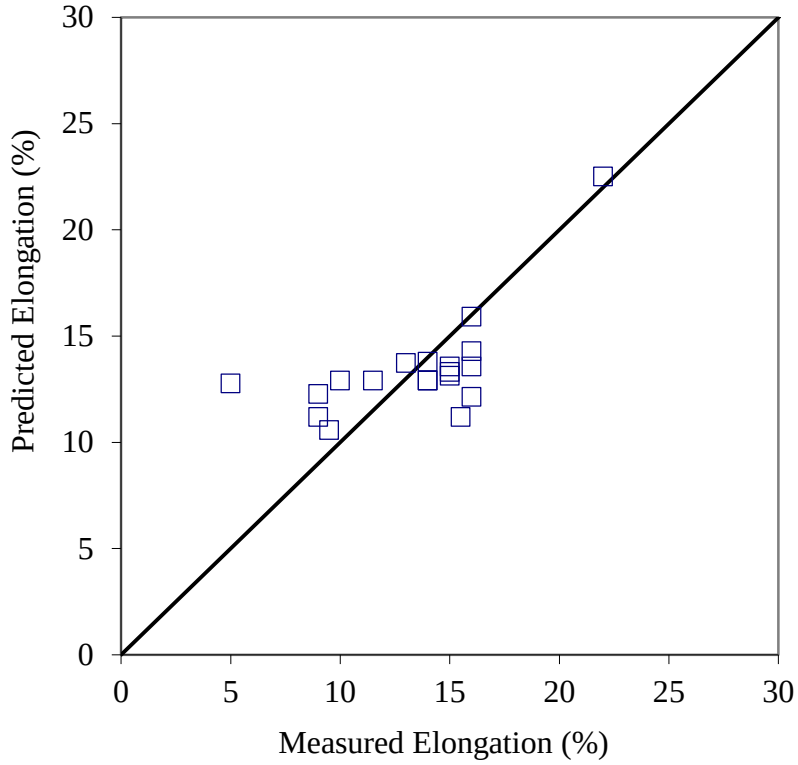

Figure 23 Predicted versus measured elongation. The predictions use the *MAGMAsteel* results in combination with the solidification rate.

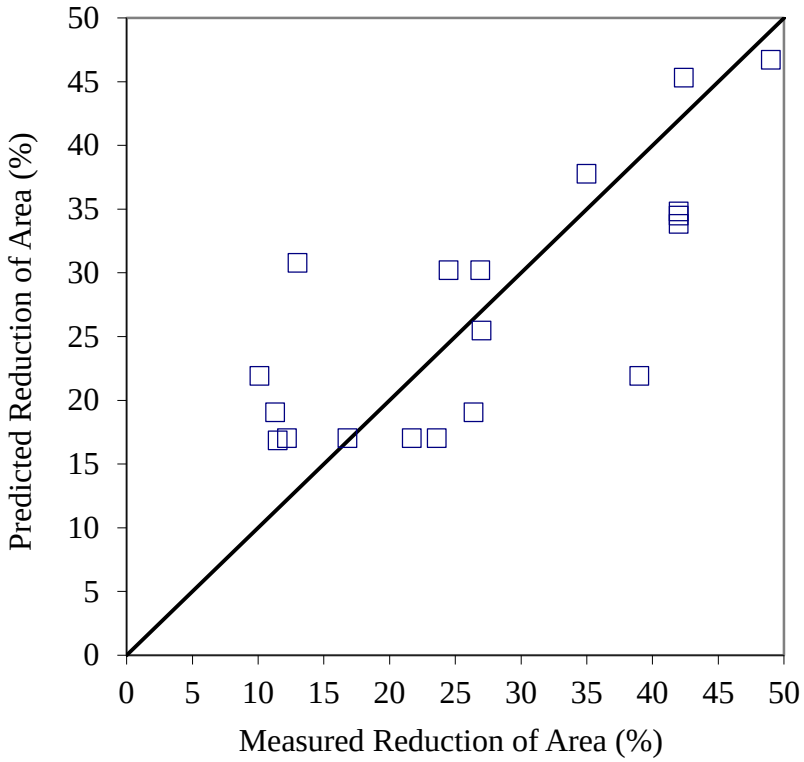

Figure 24 Predicted versus measured reduction of area. The predictions use the *MAGMAsteel* results in combination with the solidification rate.

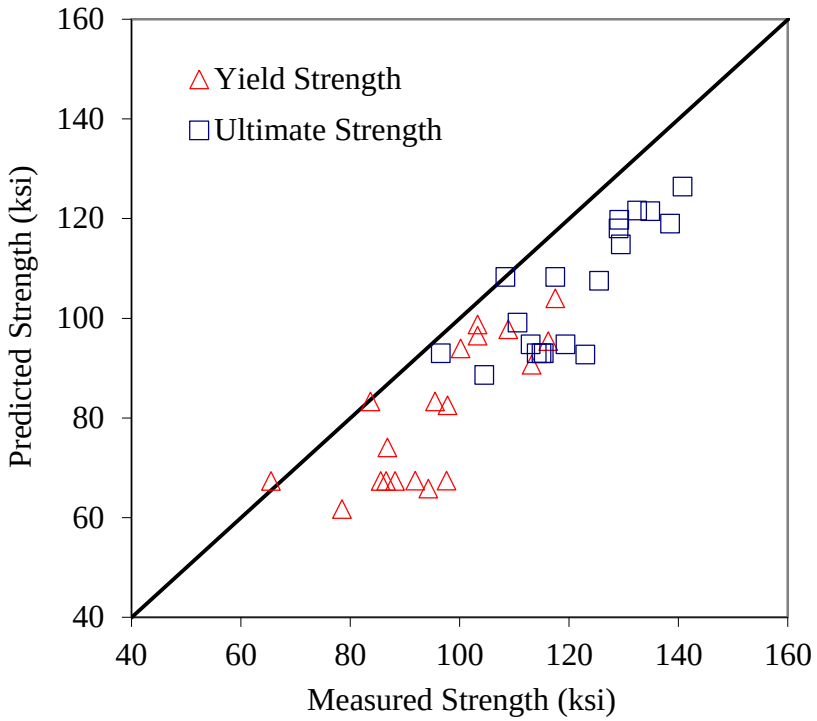

Figure 25 Lower bound property prediction results for the 8630 Q&T strength data at the 10th percentile compared to the measured data.

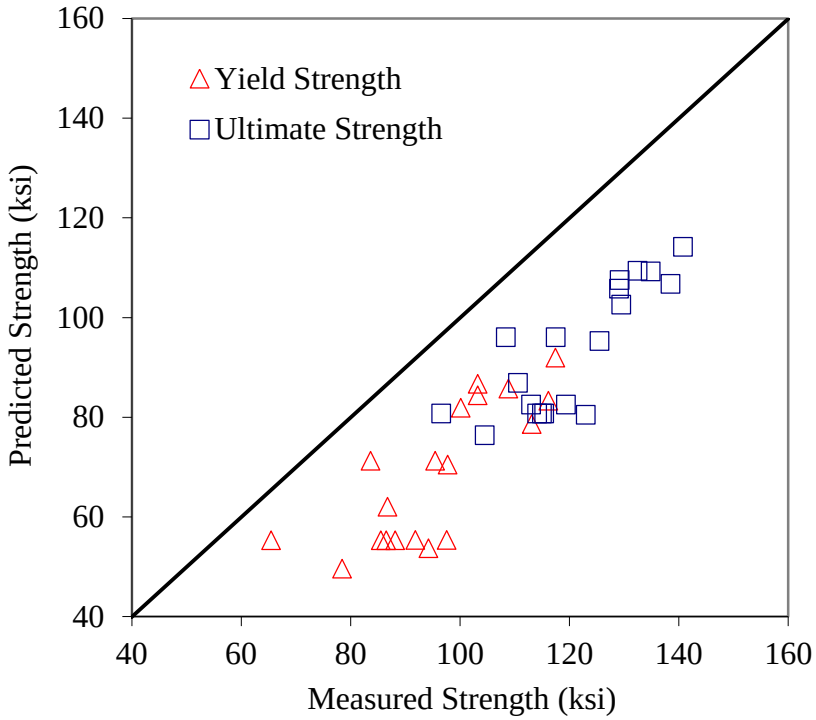

Figure 26 Lower bound property prediction results for the 8630 Q&T strength data at the 1st percentile compared to the measured data.

Conclusions

Lower bound properties are determined based on statistical analysis of mechanical test data for ten grades of cast steel. They provide engineers with a rational framework for selecting conservative, reliable design stresses, or design allowables, for use in the design of components and structures. Two statistical levels used to establish the lower bound properties presented here, and based on the MMPDS approach. The levels used for determining the lower bound properties are the 1st and 10th percentiles of the normal distribution at the lower 95% confidence level of each percentile. The more conservative property level (1^{st} percentile) is termed in the "A" design allowable and the less conservative property level (10^{th} percentile) is termed in the "B" design allowable.

Mechanical test data was grouped by the SFSA by grade, heat treatment and class according to two specifications; ASTM A958, and ASTM A487. For the data for grouped by grade and heat treatment according to the ASTM A958 standard, the property data presented here are for; 8620, 8625 and 8630 in normalized and tempered condition (N&T), and 8620, 8625, 8630 and 8635 in quenched and tempered heat treatment condition (Q&T). For the data analyzed and grouped according to ASTM A487lower bound allowables for grades and classes 4A, 4B and 4E are determined. Outlier data was identified in the data sets. The z-score of a data point was used as the basis for selecting it as an outlier. The z-score values below -2 and above 2 were removed as outliers.

For the ASTM A958 steels, the minimum lower bound yield strength (at the "A" allowable level) for N&T steel is about 40 ksi and for the Q&T steels it is about 65 ksi. The minimum lower bound ultimate strength (at the "A" allowable level) for N&T steel is about 72 ksi and for the Q&T steels it is about 92 ksi. The ductility data show the 8635 Q&T steel has a low ductility relative to the others. The ductility decreases when using Q&T heat treatment and with increasing carbon content. Just looking at elongation as a ductility measure, the "A" allowable lower bound data range from 10% to 15%, and the "B" allowable lower bound data range from 13% to 19%.

There is evidence of compliance bias in the data for the steels grouped by the A487 grade 4 and classes A, B and E. The biases in the data correspond to the minimum requirements, and are evidenced by the large number of samples observed at these requirements. For these steels, the only grade meeting the minimum required strengths is 4A, and none of the elongation minimum requirements are met. For the "B" allowable data (at 10% lower bound) all the strength minimum requirements are met except for the 4E steel. It is interesting that the 4E steel has virtually no difference between the "A" and "B" lower bound allowables for yield strength.

The prediction of lower bound properties is based on tensile test specimens produced from cast 8630 Q&T steel that were machined from three test castings and a commercial casting. The tensile specimens were used to develop a method to predict the tensile properties using simulation results. All castings were simulated using filling and solidification and the heat treatment process was simulated to predict final phase amounts and properties. The strength data

shows a good trend in agreement between measured and predicted data but is slightly over predicted. Y-block and the keel block data were found to have the best properties compared to the data from the commercial part and the ER castings. The predicted ductility shows little variation in the results, and do not agree with the measurements even in trend. Best fit equations are determined giving predictions of the mean properties resulting from the solidification and heat treatment conditions locally in the casting. These equations use local simulation results to calculate the local variation of properties, and agree well with the average of the measured tensile data. Using the mean and standard deviation from the statistical distribution of the SFSA member 8630 Q&T data, and the z-scores calculated at the 1^{st} and 10^{th} percentiles corresponding to the lower bound properties, a method is proposed to calculate lower bound properties using the "mean" property predictions. The approach used to calculate lower bound properties is demonstrated at two levels of conservatism (corresponding to the "A" and "B" allowables). The approach is proposed to serve as a basis linking the performance of casting designs to their production process.

Acknowledgements

This research is sponsored by the DLA-Troop Support, Philadelphia, PA and the Defense Logistics Agency Information Operations, J62LB, Research & Development , Ft. Belvoir, VA.

.

References

1. "Metallic Materials Properties Development and Standardization (MMPDS)," Department of Transportation Report DOT/FAA/AR-MMPDS-01, January 2003.

2. Rice, R. C., Goode, R., Bakuckas, J., and Thompson, S., "Development of MMPDS Handbook Aircraft Design Allowables," Proceedings of the7th Joint DOD/FAA/NASA Conference on Aging Aircraft, New Orleans, LA, Sept. 2003.

3. *SAS* software, Version 7.15 of the SAS System for Windows, SAS Institute Inc., 2017.

4. *Minitab* 19 Statistical Software, Minitab, Inc. (www.minitab.com), State College, PA, 2019.

5. *MAGMAsoft*, MAGMA Gmbh, Kackerstrasse 11, 52072 Aachen, Germany.

Appendix A Histograms, Normal Distributions and Statistical Measures of Property Data

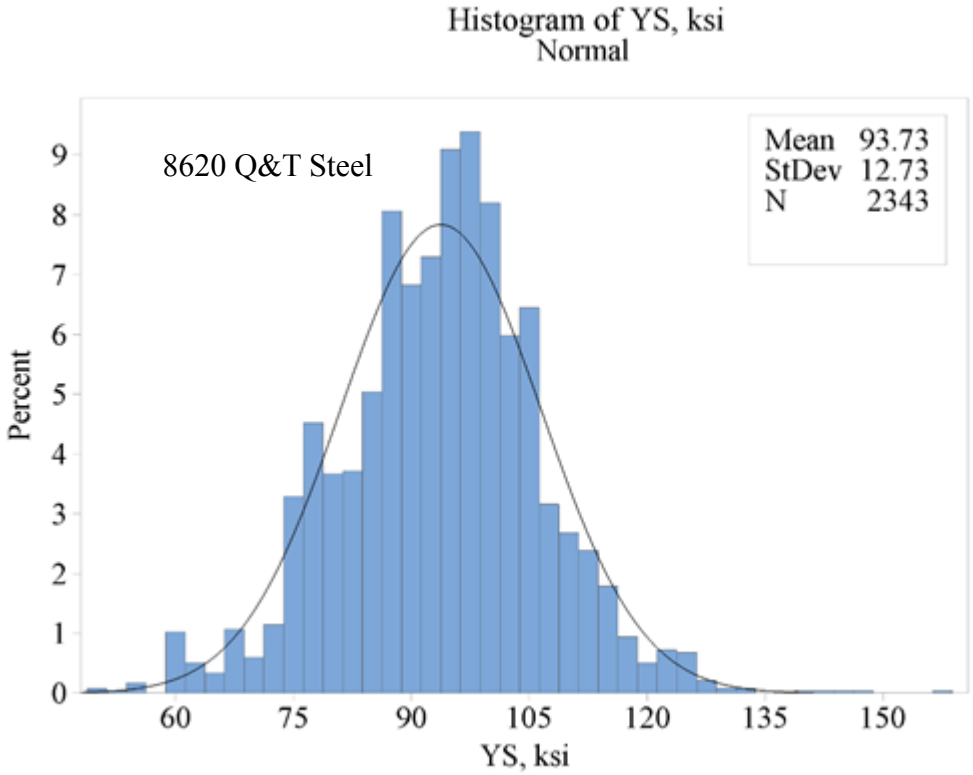

Figure A1. Normal distribution and histogram of yield stress data for 8620 quenched and tempered cast steel.

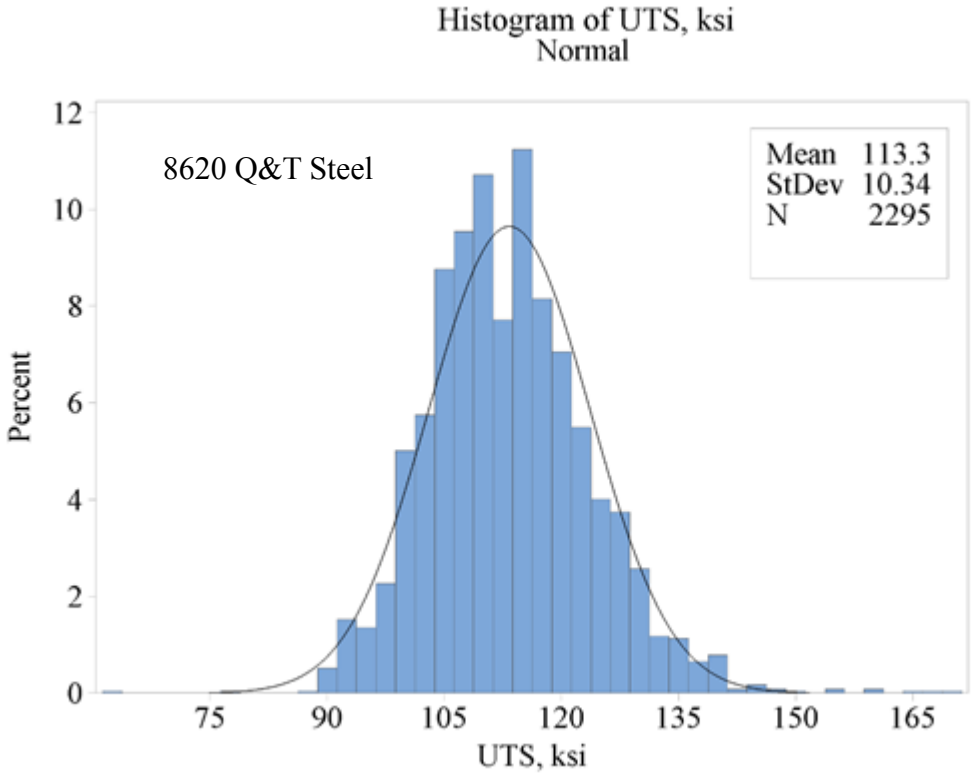

Figure A2. Normal distribution and histogram of ultimate stress data for 8620 quenched and tempered cast steel.

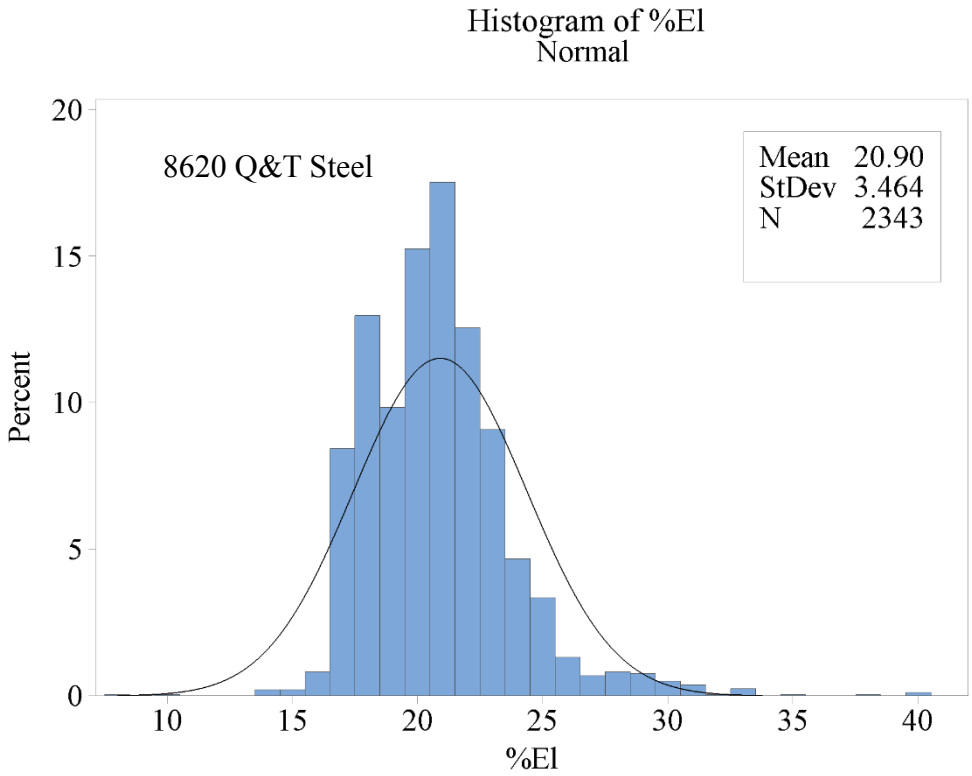

Figure A3. Normal distribution and histogram of elongation data for 8620 quenched and tempered cast steel.

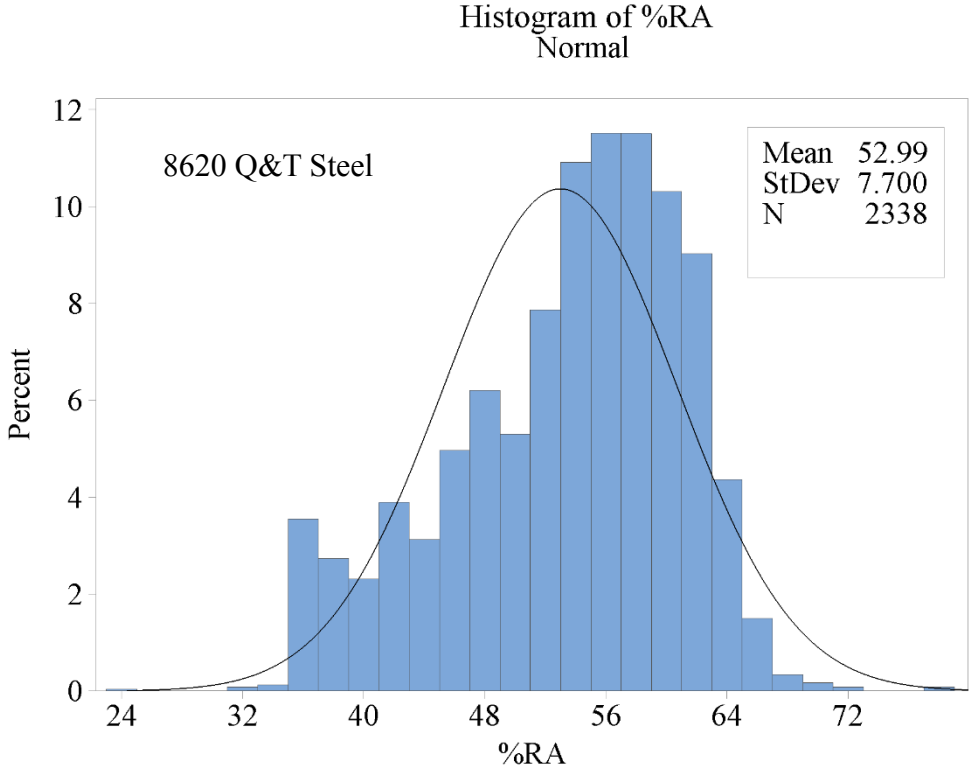

Figure A4. Normal distribution and histogram of reduction of area data for 8620 quenched and tempered cast steel.

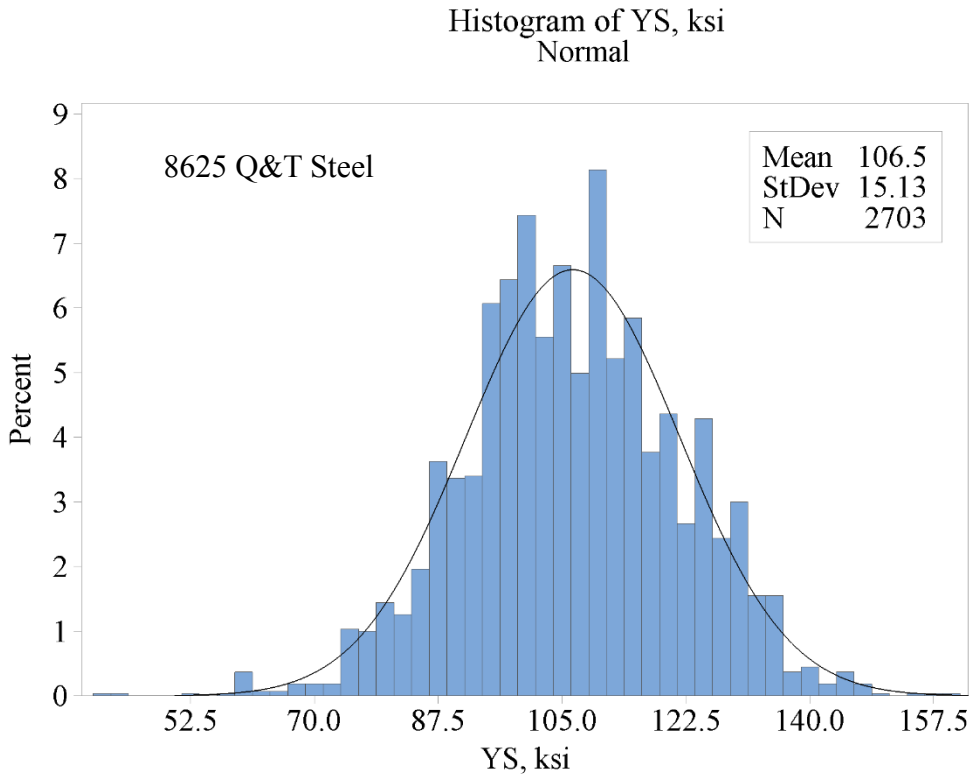

Figure A5. Normal distribution and histogram of yield stress data for 8625 quenched and tempered cast steel.

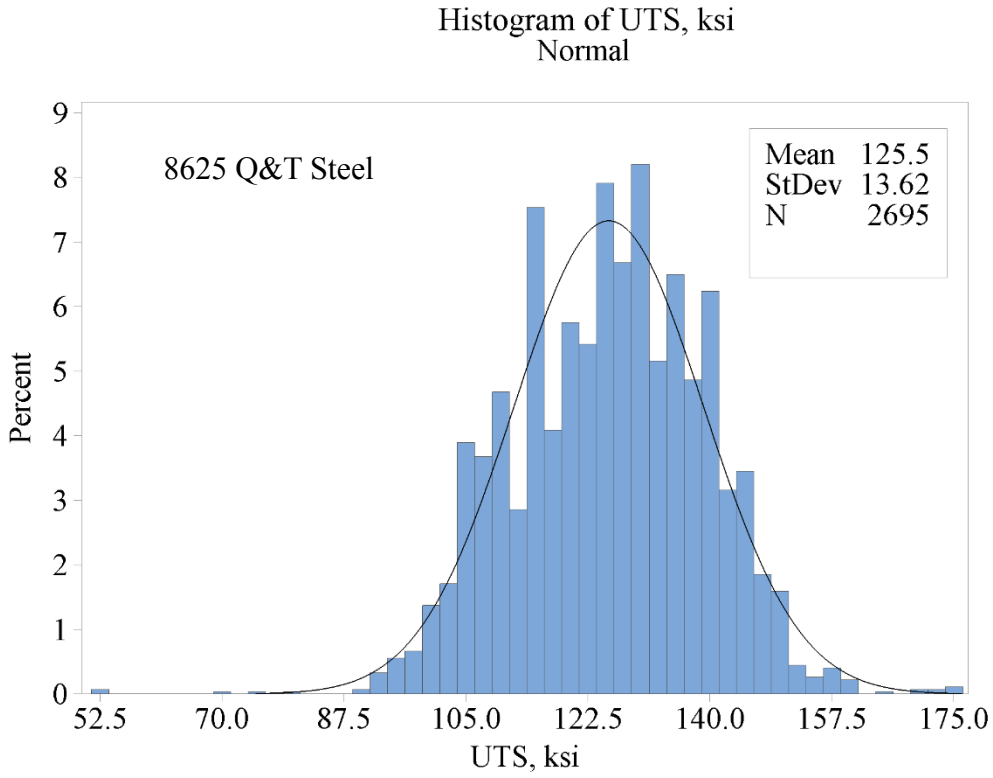

Figure A6. Normal distribution and histogram of ultimate stress data for 8625 quenched and tempered cast steel.

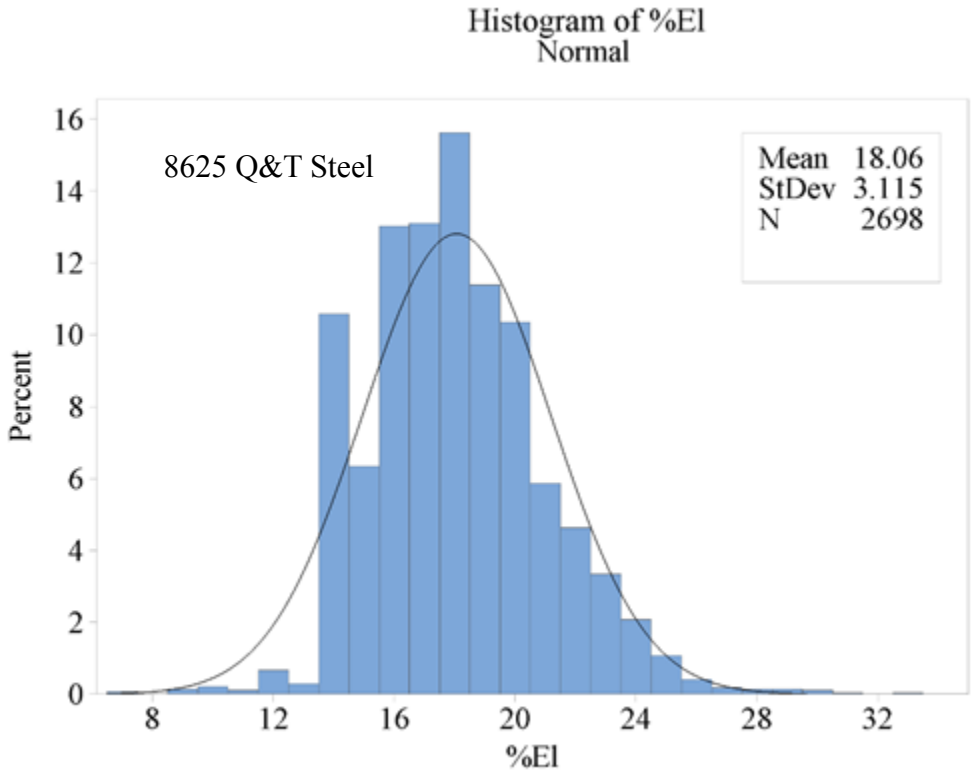

Figure A7. Normal distribution and histogram of elongation data for 8625 quenched and tempered cast steel.

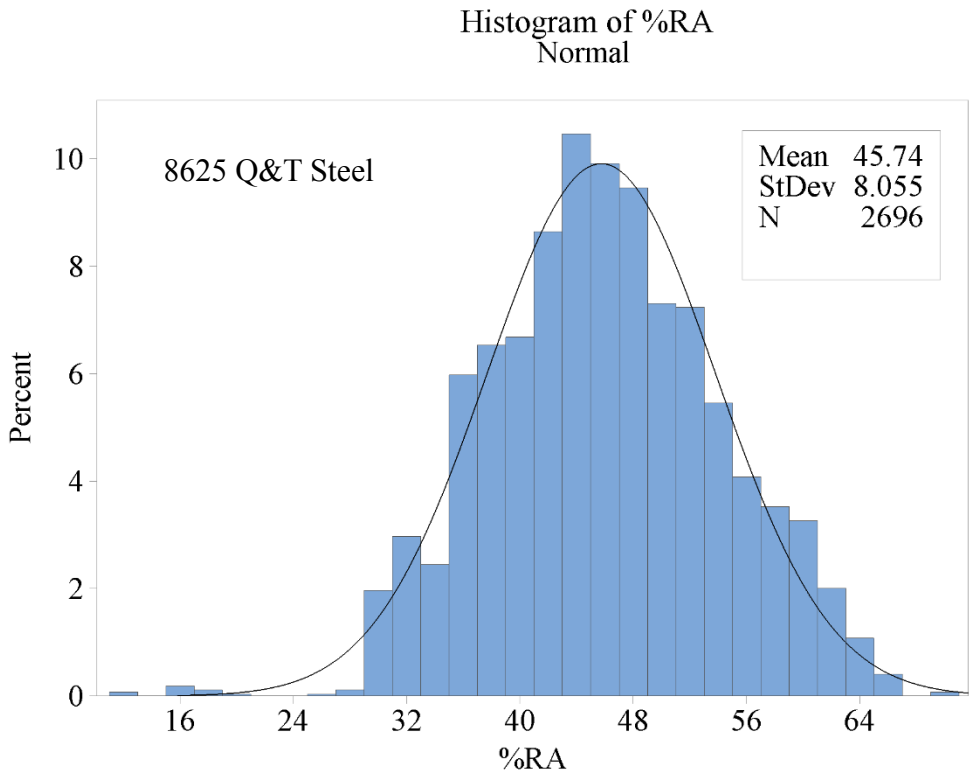

Figure A8. Normal distribution and histogram of reduction of area data for 8625 quenched and tempered cast steel.

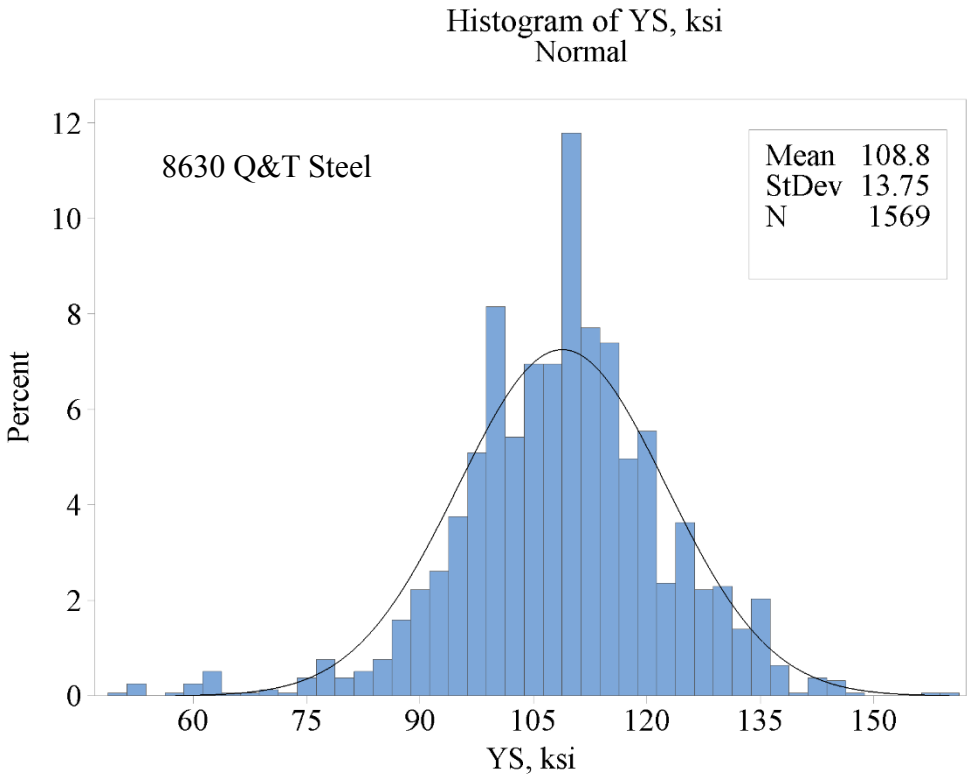

Figure A9. Normal distribution and histogram of yield stress data for 8630 quenched and tempered cast steel.

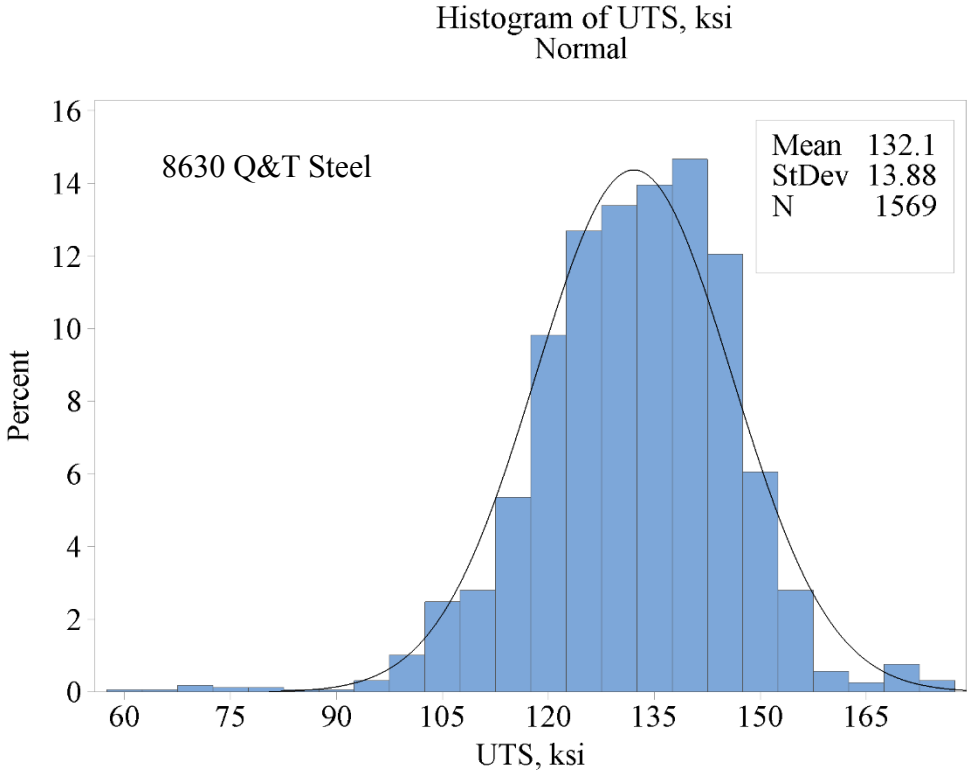

Figure A10. Normal distribution and histogram of ultimate stress data for 8630 quenched and tempered cast steel.

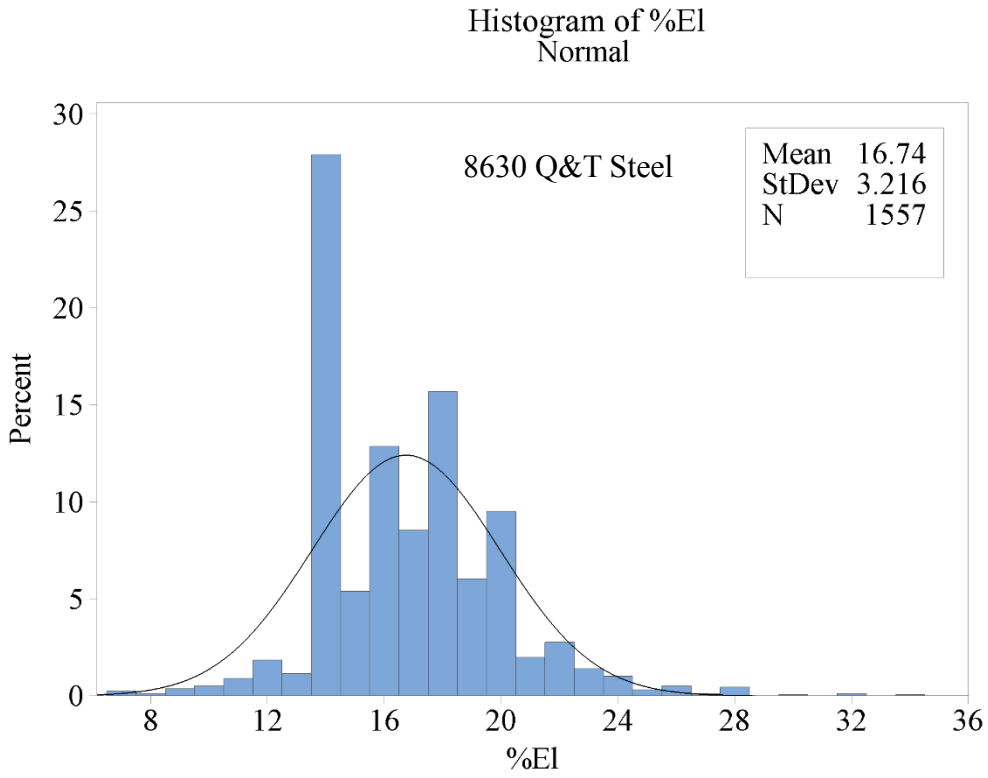

Figure A11. Normal distribution and histogram of elongation data for 8630 quenched and tempered cast steel.

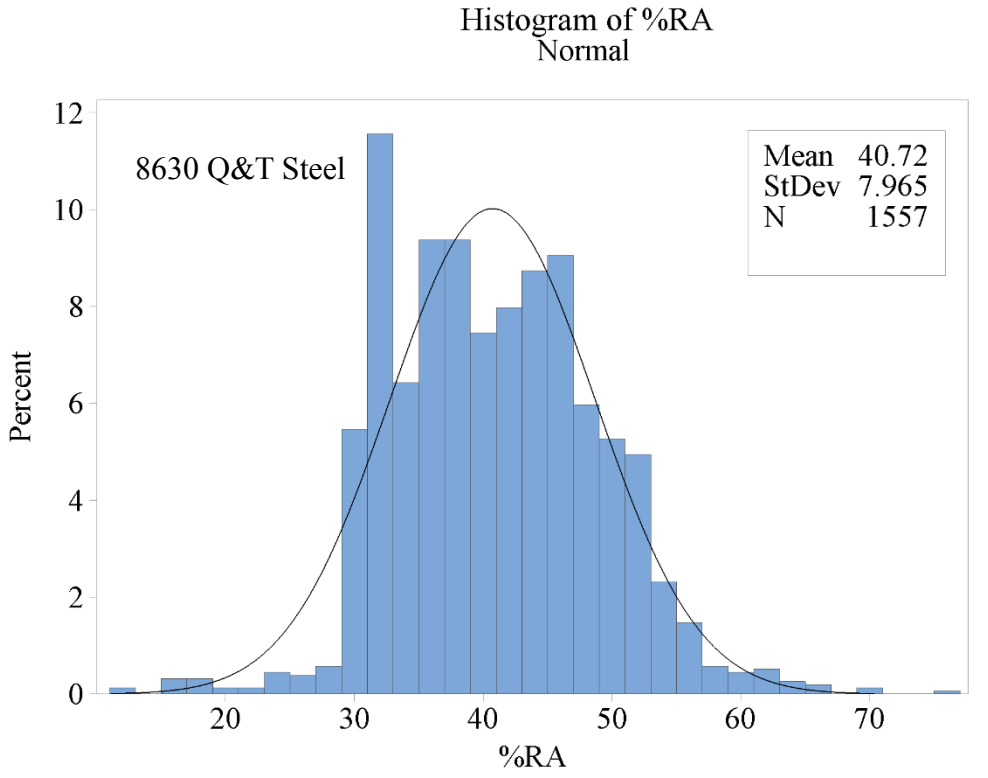

Figure A12. Normal distribution and histogram of reduction of area data for 8630 quenched and tempered cast steel.

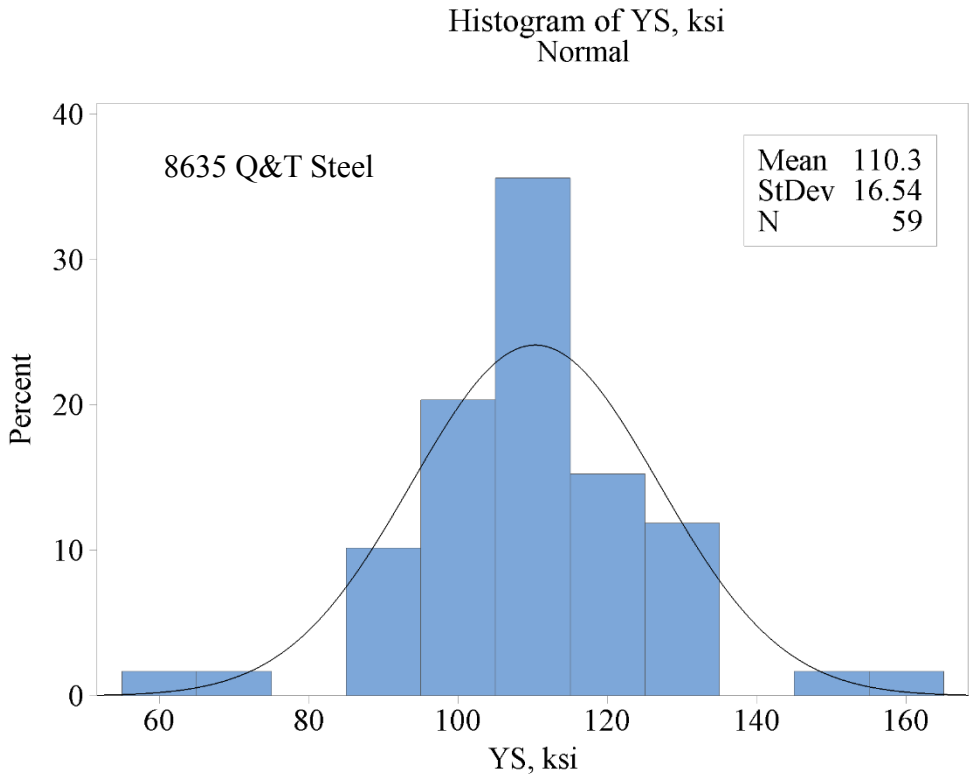

Figure A13. Normal distribution and histogram of yield stress data for 8635 quenched and tempered cast steel.

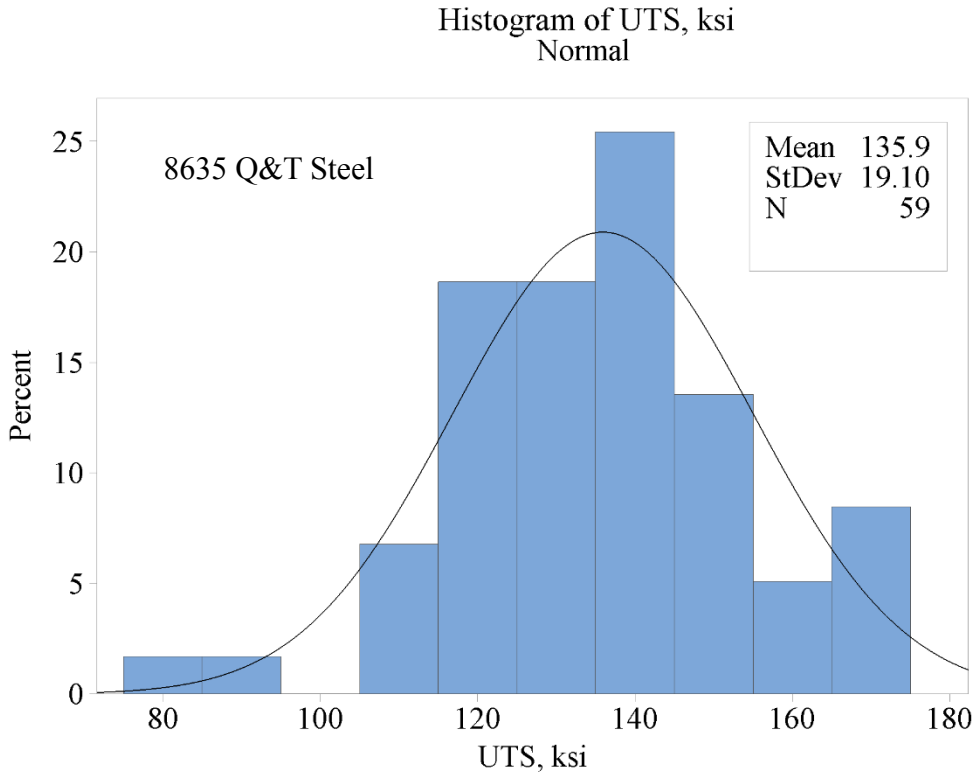

Figure A14. Normal distribution and histogram of ultimate stress data for 8635 quenched and tempered cast steel.

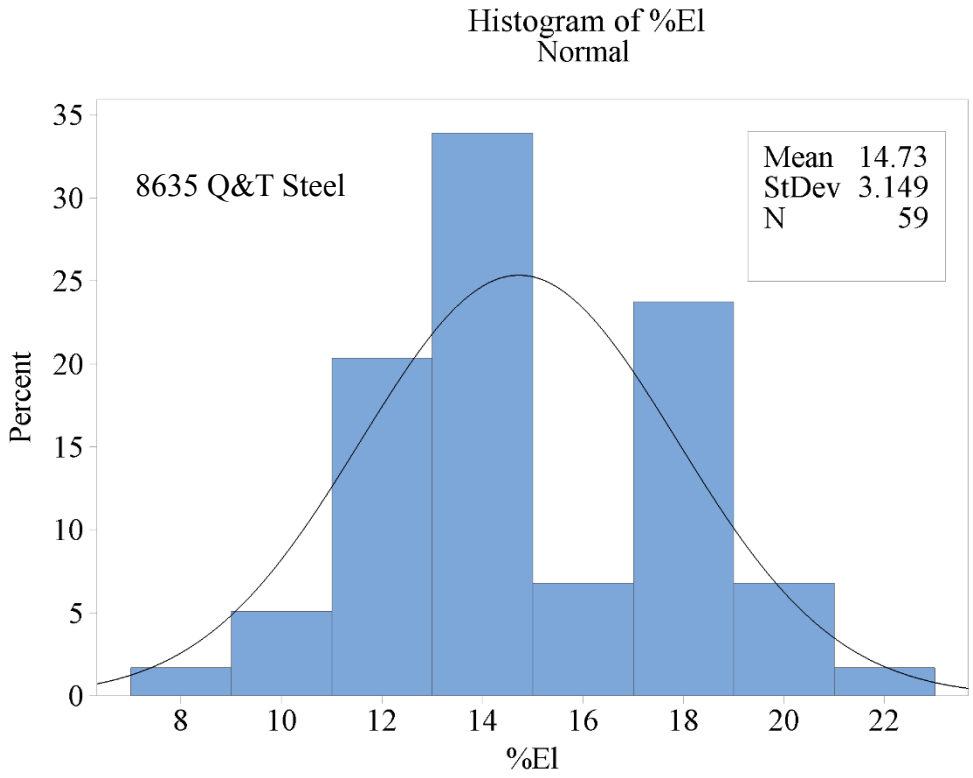

Figure A15. Normal distribution and histogram of elongation data for 8635 quenched and tempered cast steel.

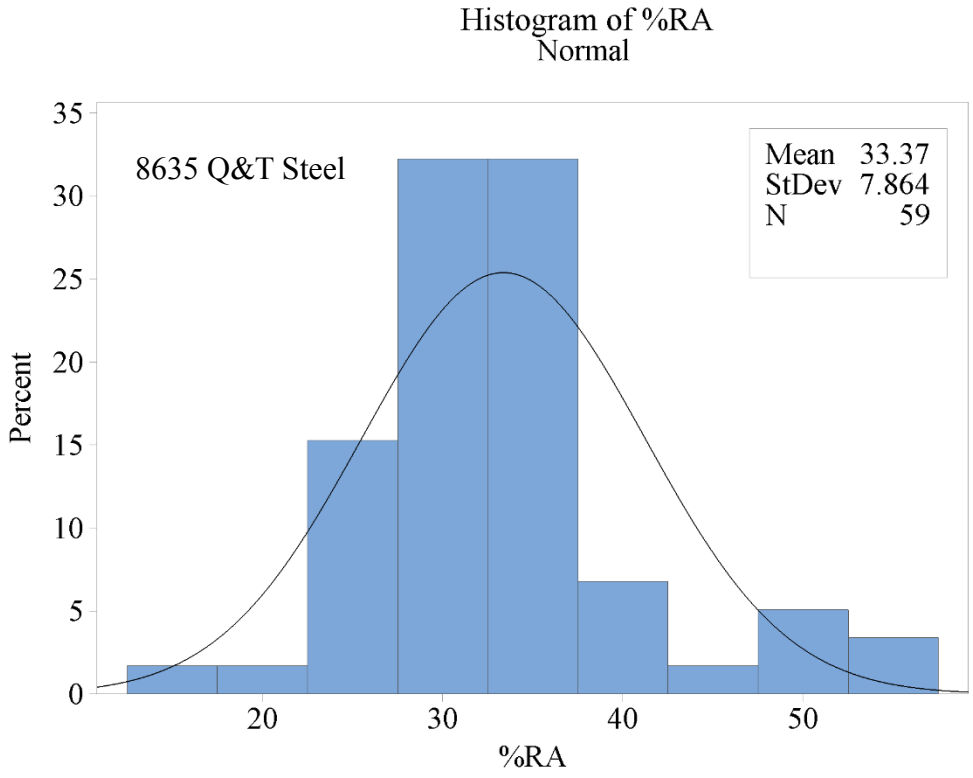

Figure A16. Normal distribution and histogram of reduction of area data for 8635 quenched and tempered cast steel.

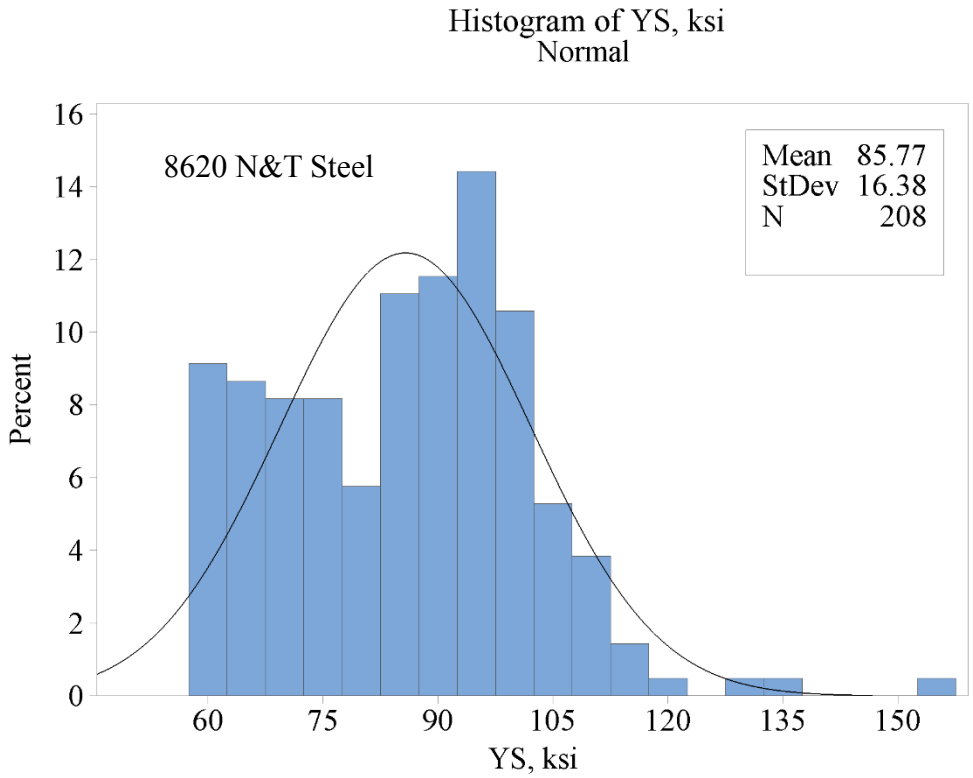

Figure A17. Normal distribution and histogram of yield stress data for 8620 normalized and tempered cast steel.

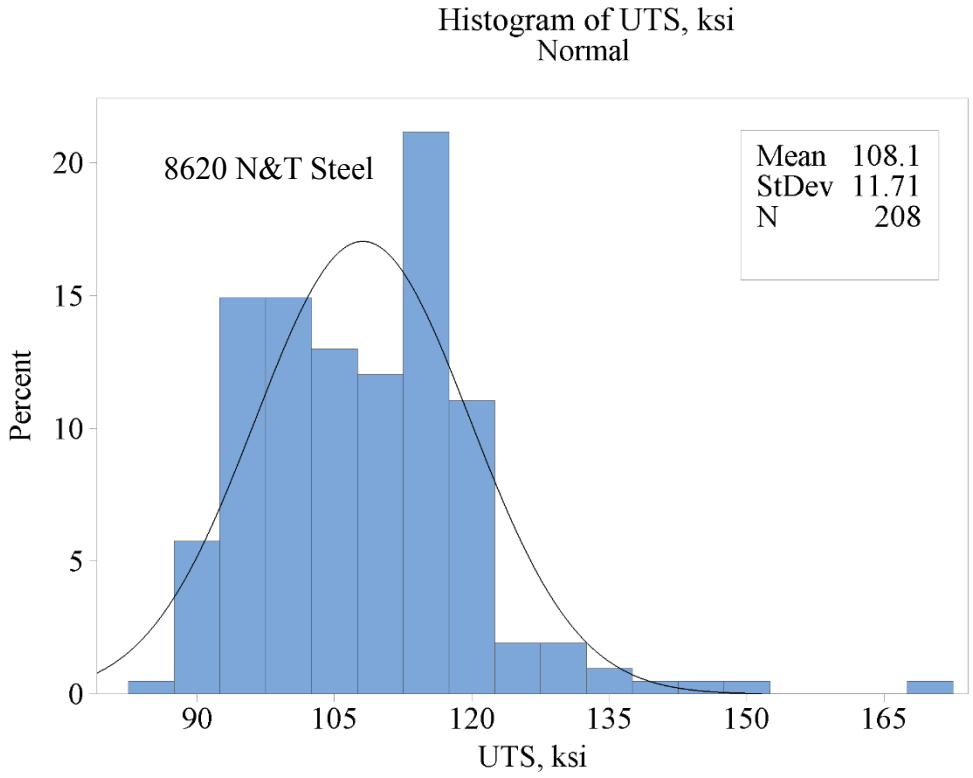

Figure A18. Normal distribution and histogram of ultimate stress data for 8620 normalized and tempered cast steel.

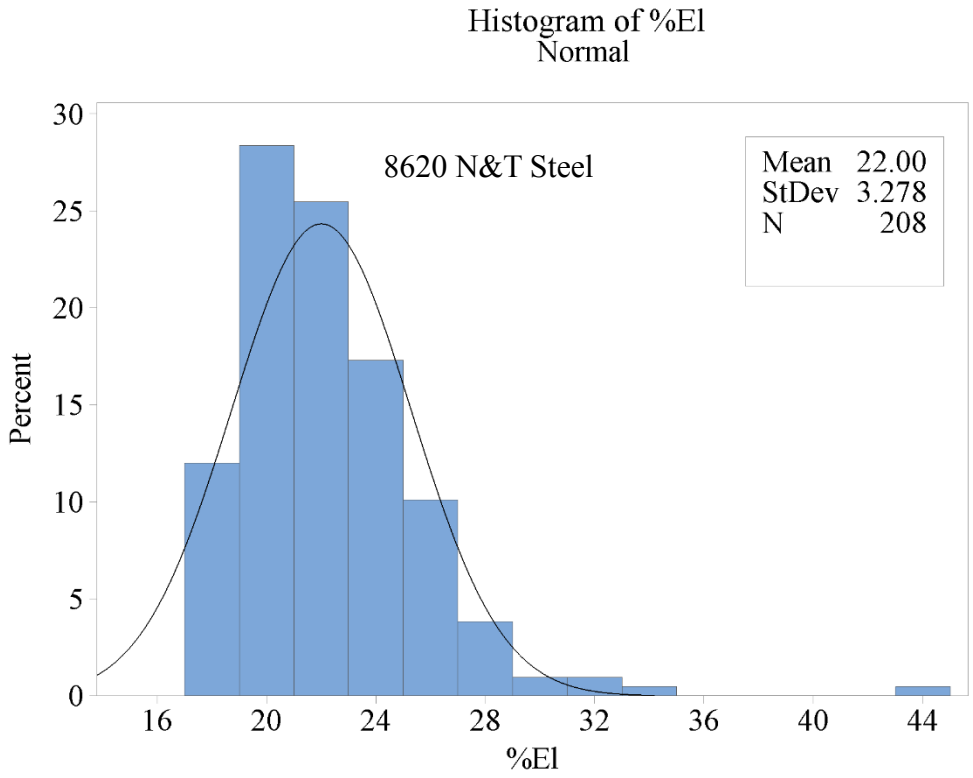

Figure A19. Normal distribution and histogram of elongation data for 8620 normalized and tempered cast steel.

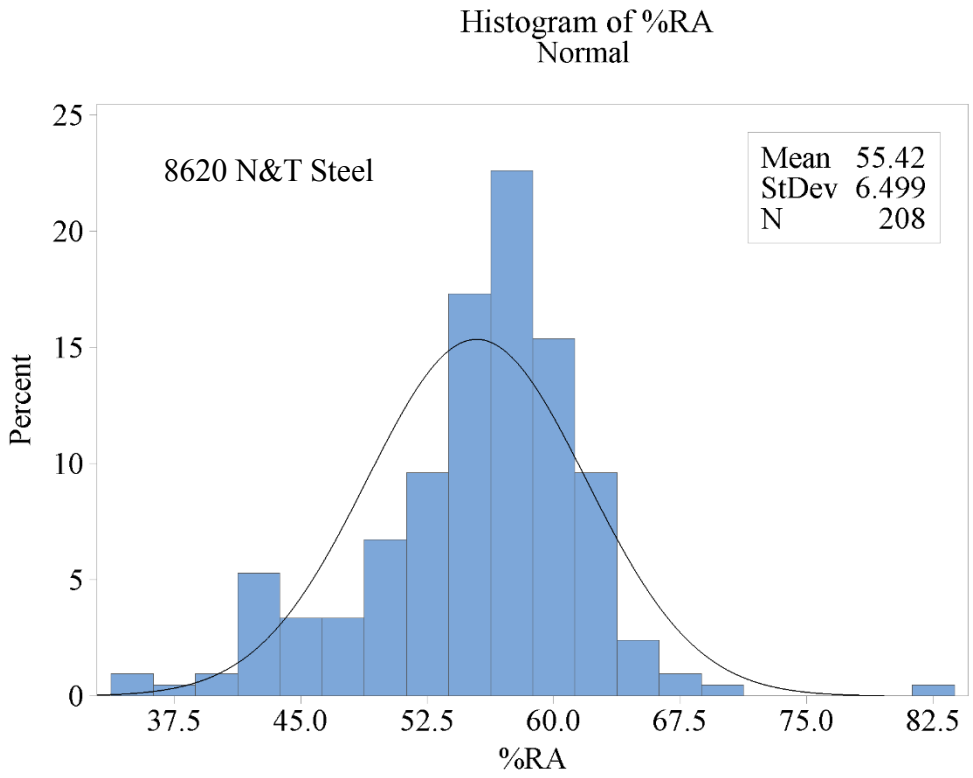

Figure A20. Normal distribution and histogram of reduction of area data for 8620 normalized and tempered cast steel.

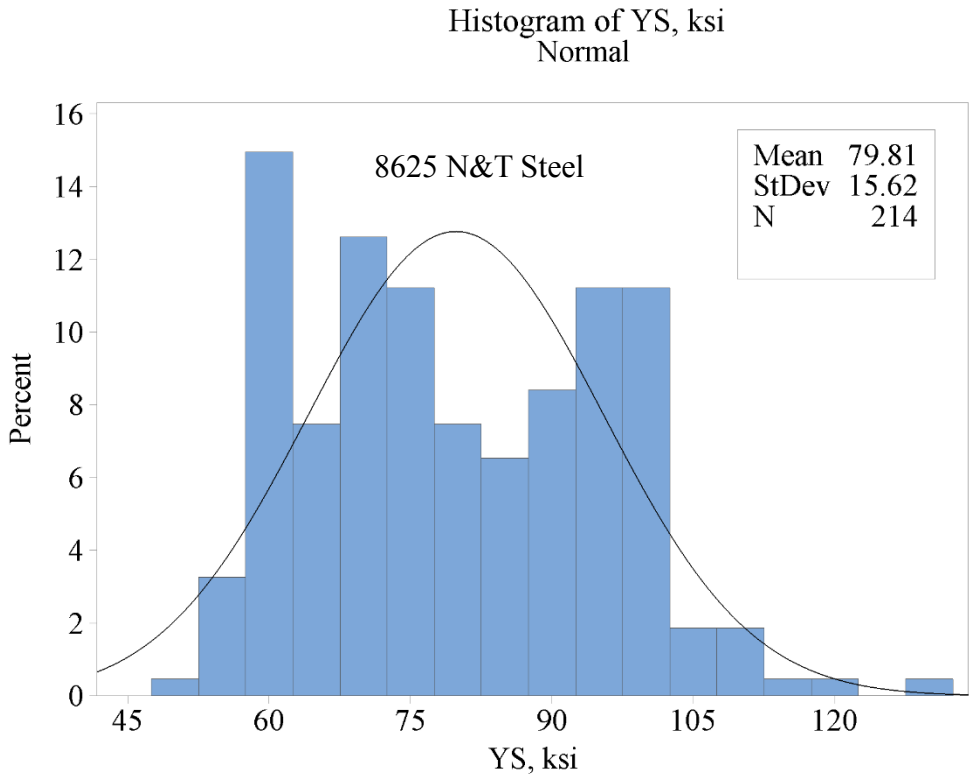

Figure A21. Normal distribution and histogram of yield stress data for 8625 normalized and tempered cast steel.

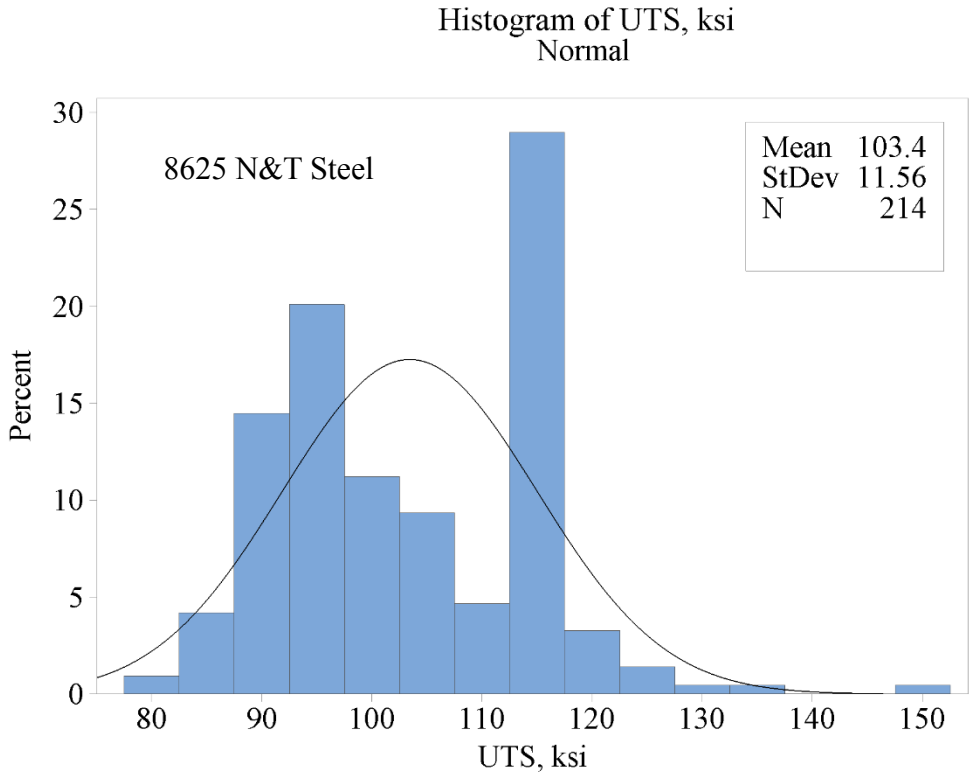

Figure A22. Normal distribution and histogram of ultimate stress data for 8625 normalized and tempered cast steel.

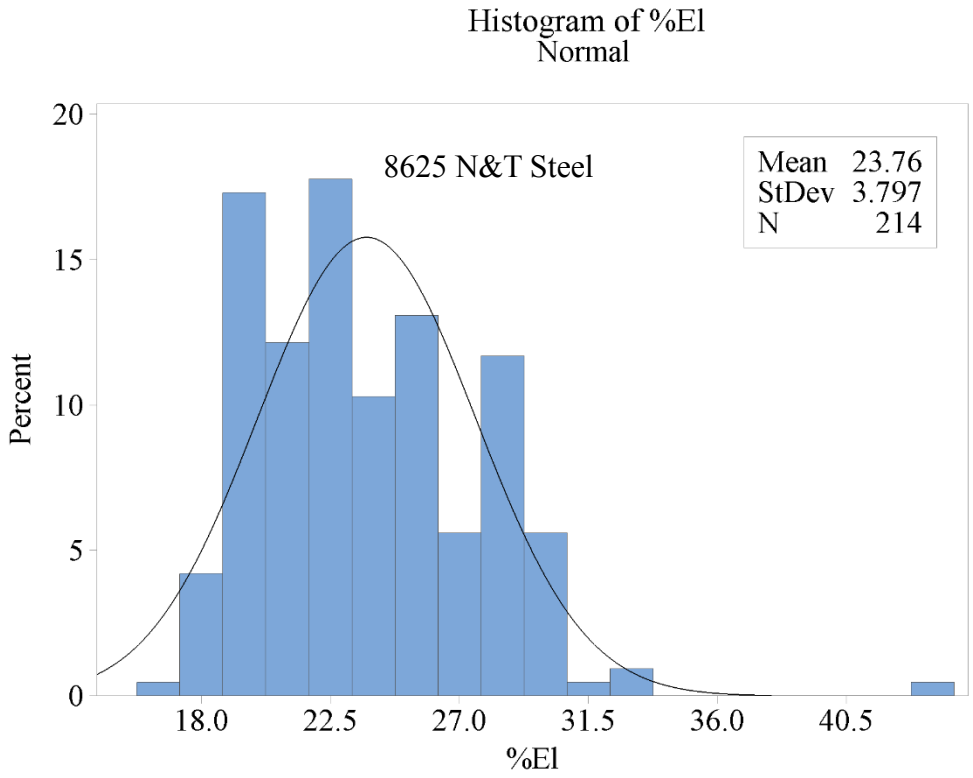

Figure A23. Normal distribution and histogram of elongation data for 8625 normalized and tempered cast steel.

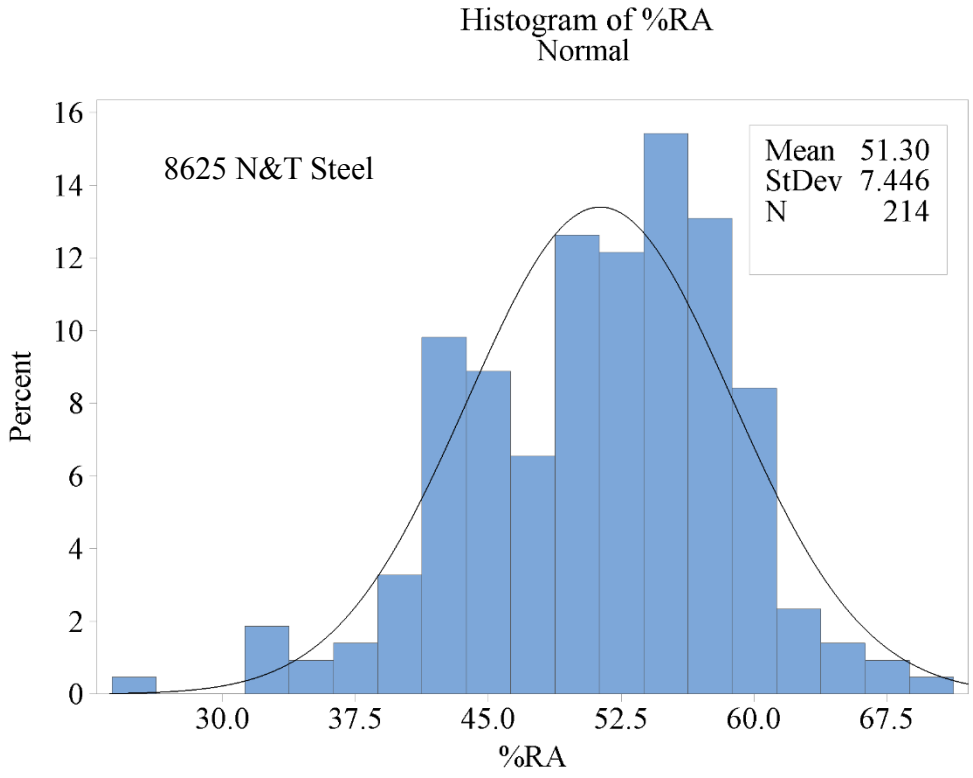

Figure A24. Normal distribution and histogram of reduction of area data for 8625 normalized and tempered cast steel.

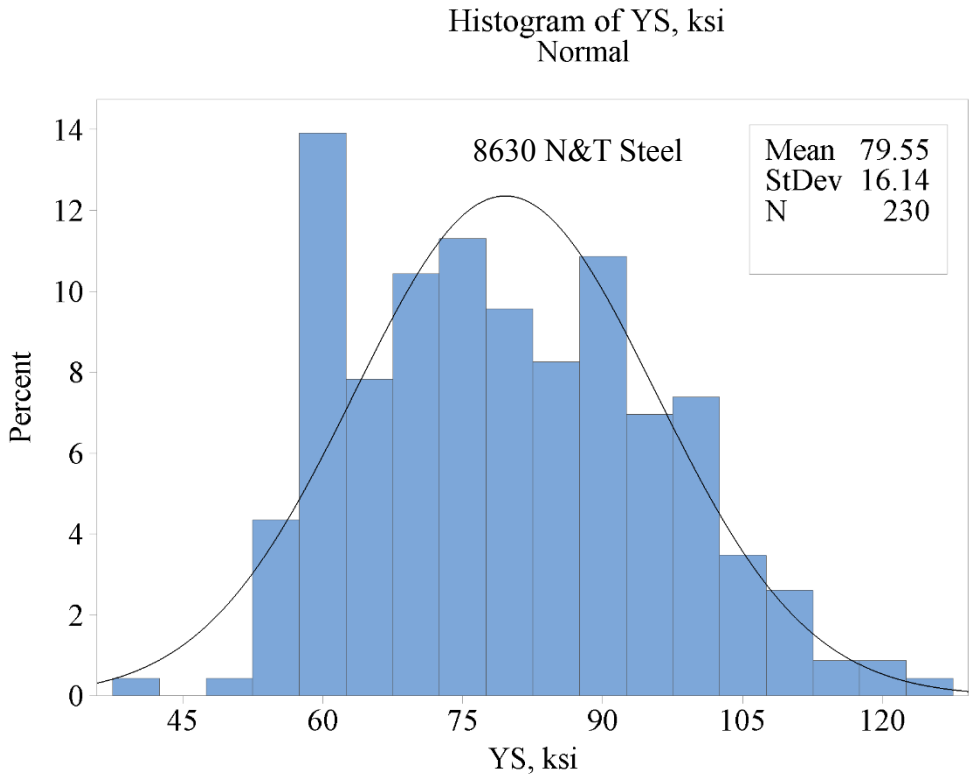

Figure A25. Normal distribution and histogram of yield stress data for 8630 normalized and tempered cast steel.

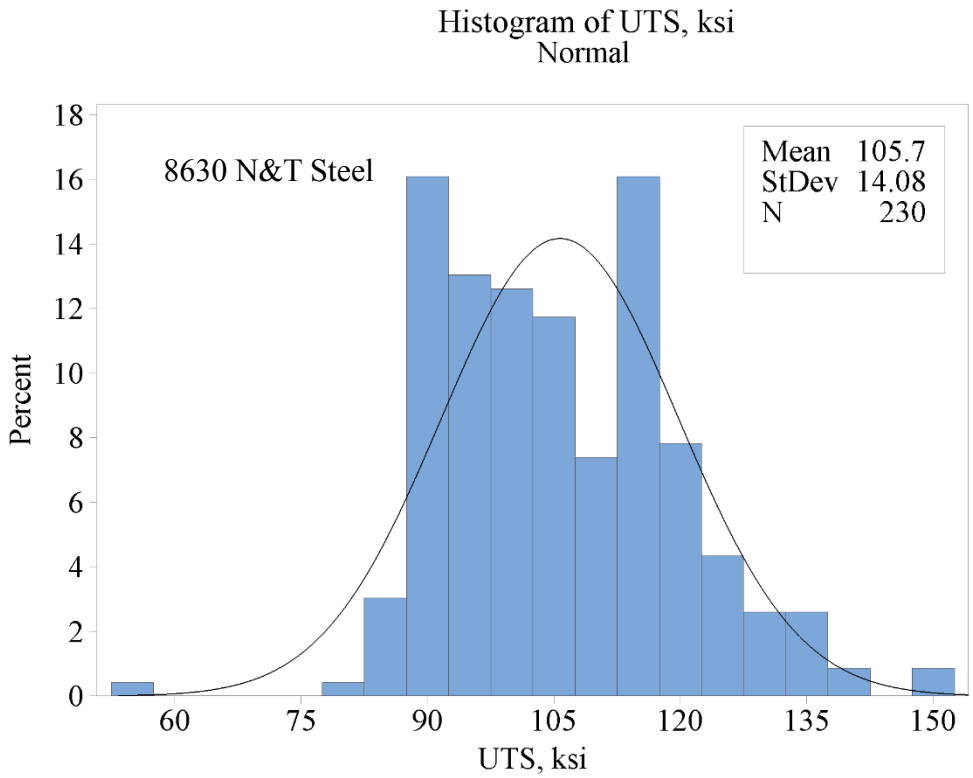

Figure A26. Normal distribution and histogram of ultimate stress data for 8630 normalized and tempered cast steel.

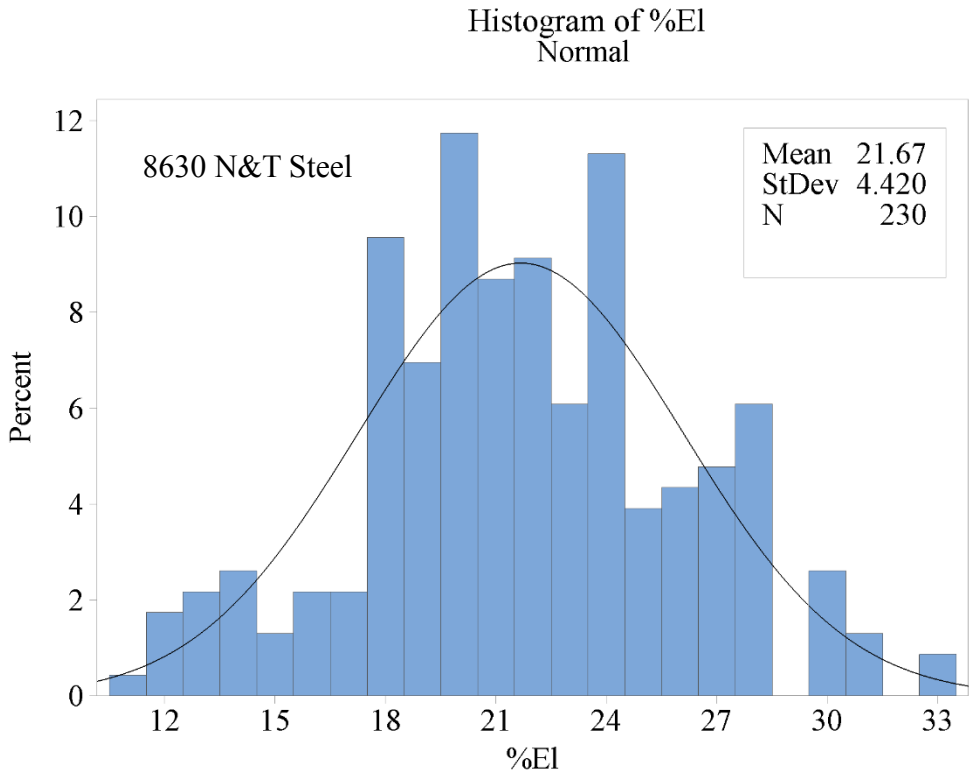

Figure A27. Normal distribution and histogram of elongation data for 8630 normalized and tempered cast steel.

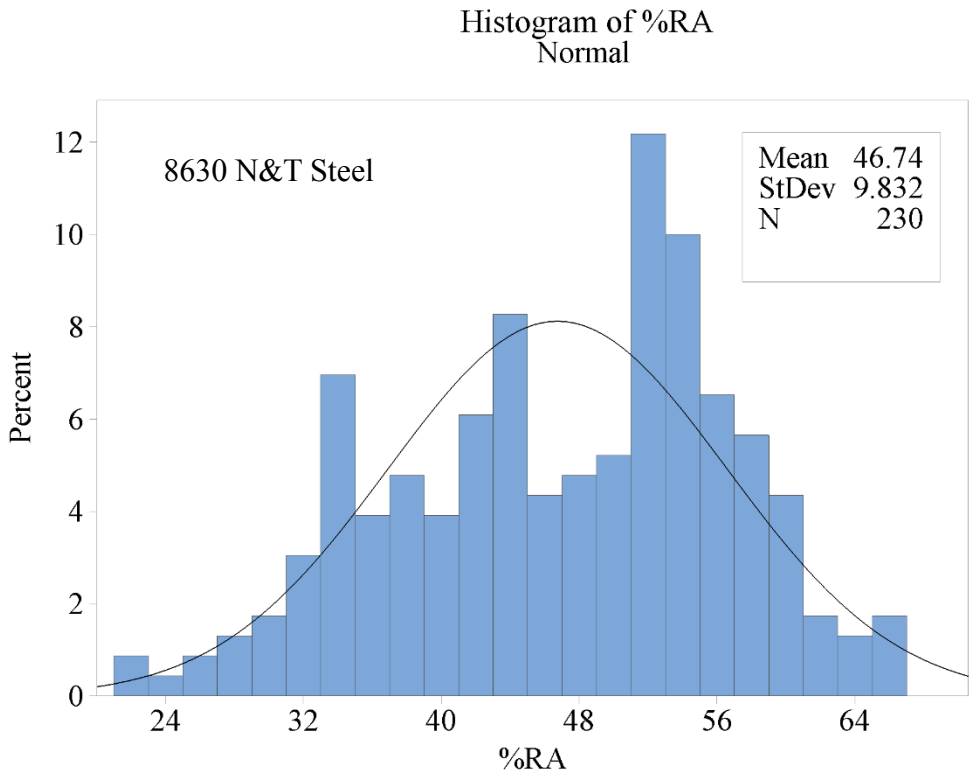

Figure A28. Normal distribution and histogram of reduction of area data for 8630 normalized and tempered cast steel.

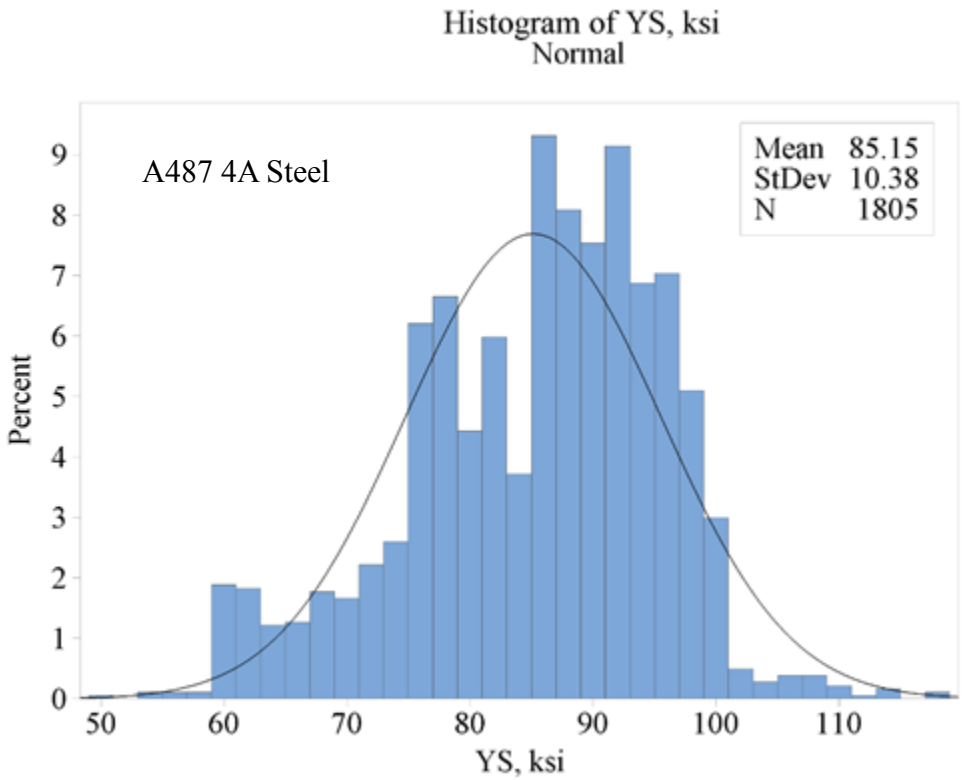

Figure A29. Normal distribution and histogram of yield stress data for A487 4A cast steel.

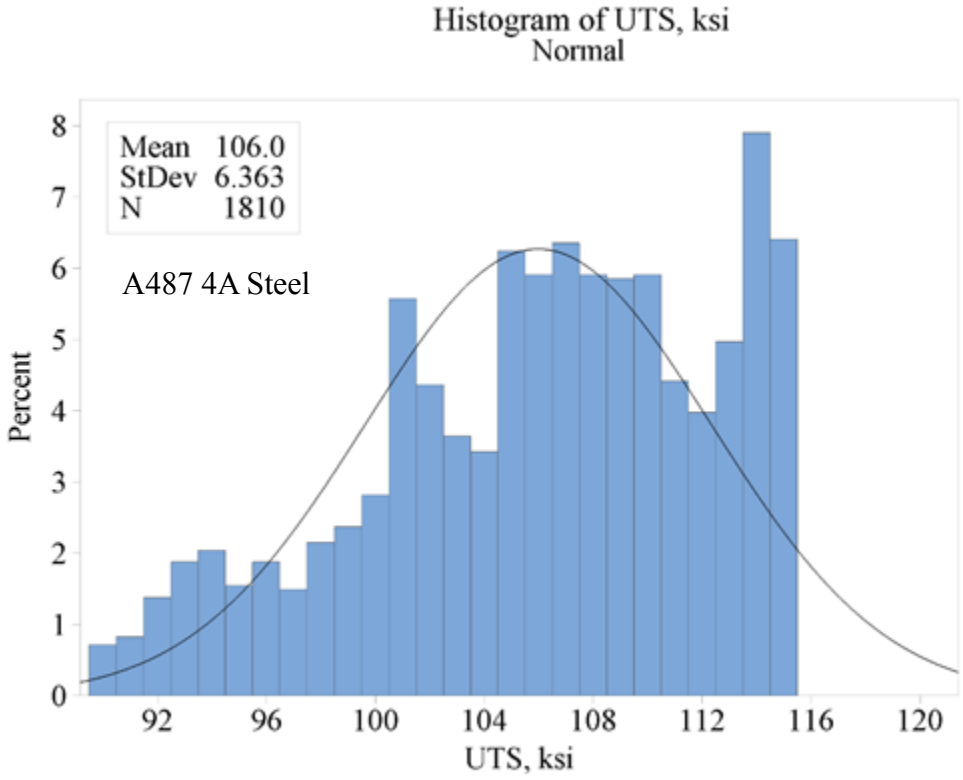

Figure A30. Normal distribution and histogram of ultimate stress data for A487 4A cast steel.

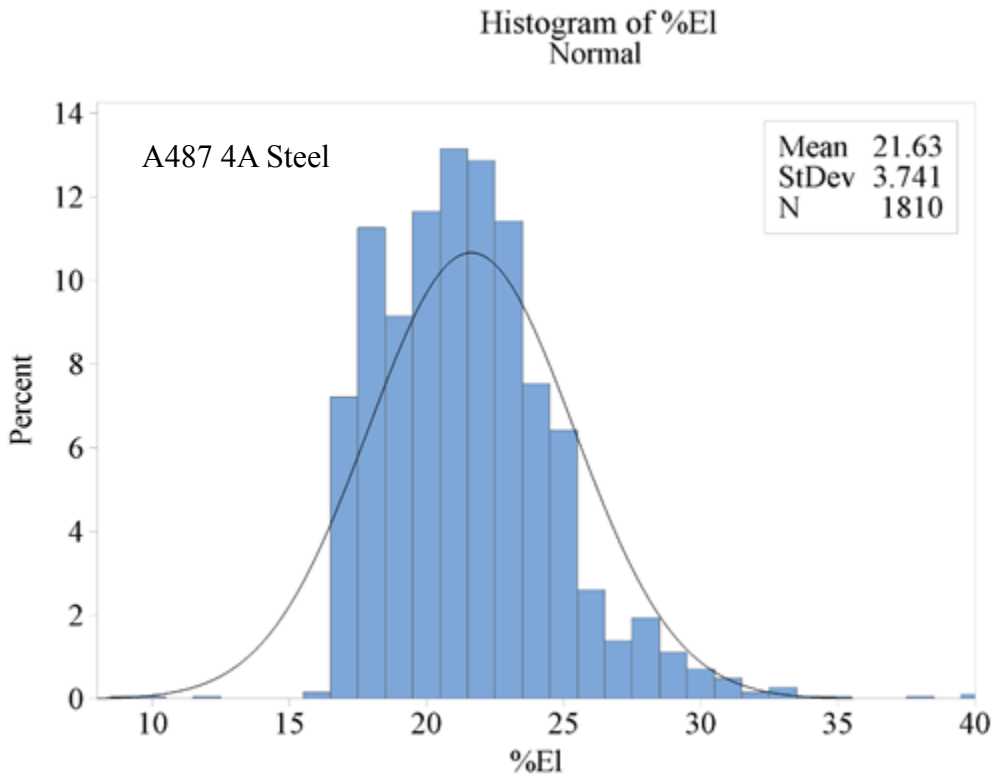

Figure A31. Normal distribution and histogram of elongation data for A487 4A cast steel.

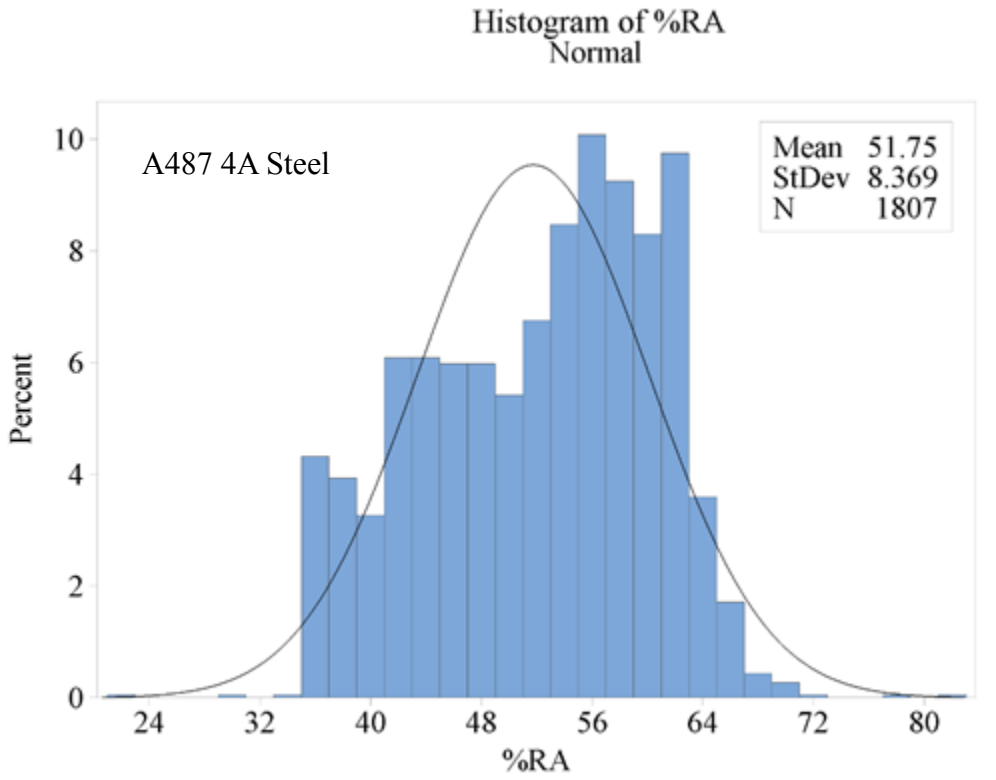

Figure A32. Normal distribution and histogram of reduction of area data for A487 4A cast steel.

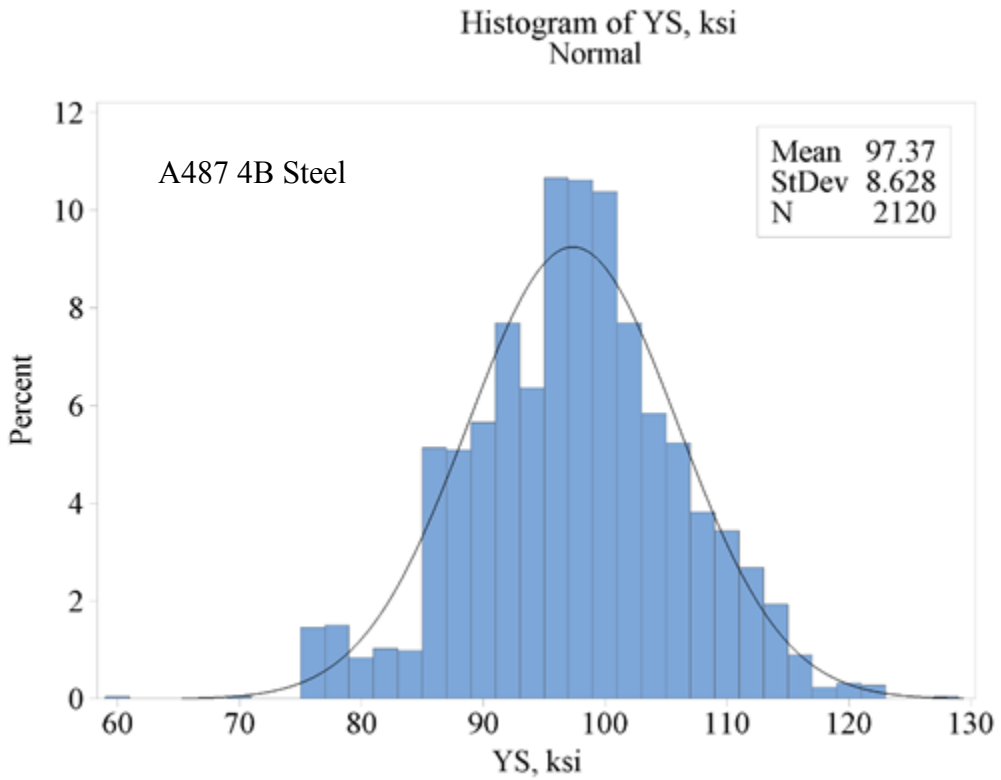

Figure A33. Normal distribution and histogram of yield stress data for A487 4B cast steel.

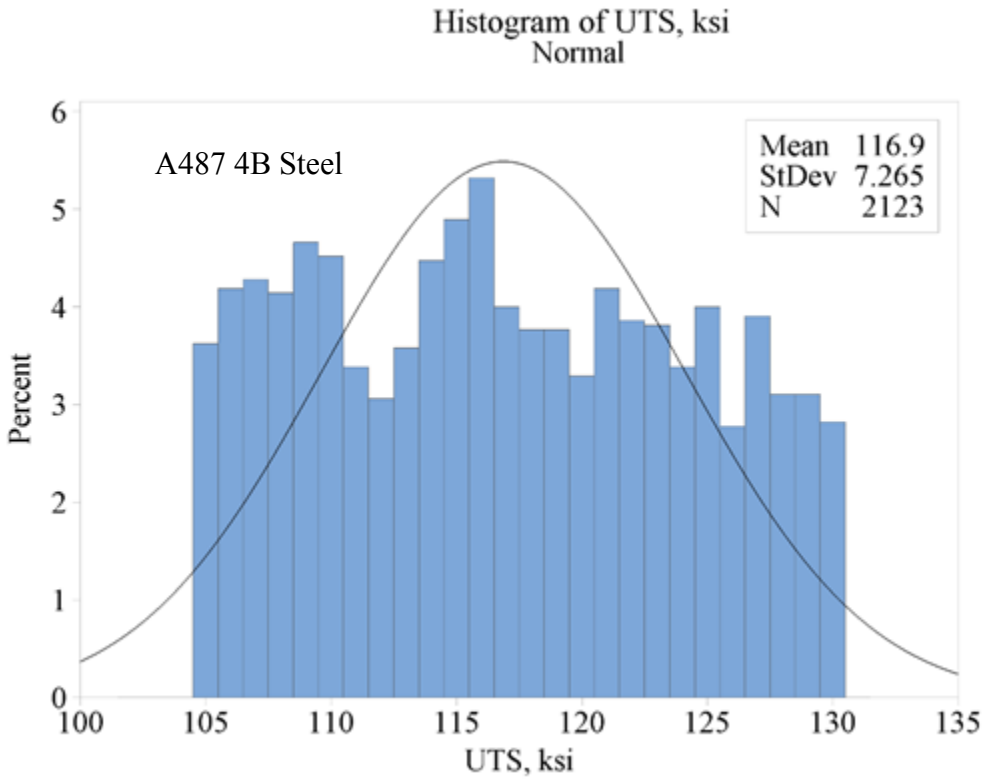

Figure A34. Normal distribution and histogram of ultimate stress data for A487 4B cast steel.

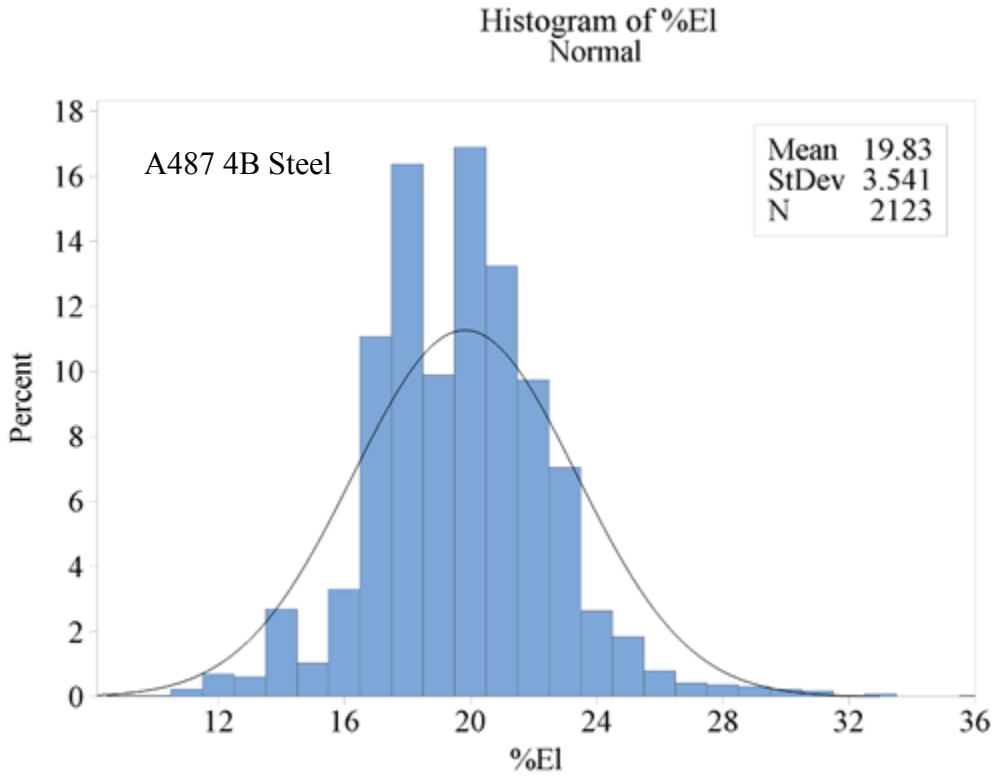

Figure A35. Normal distribution and histogram of elongation data for A487 4B cast steel.

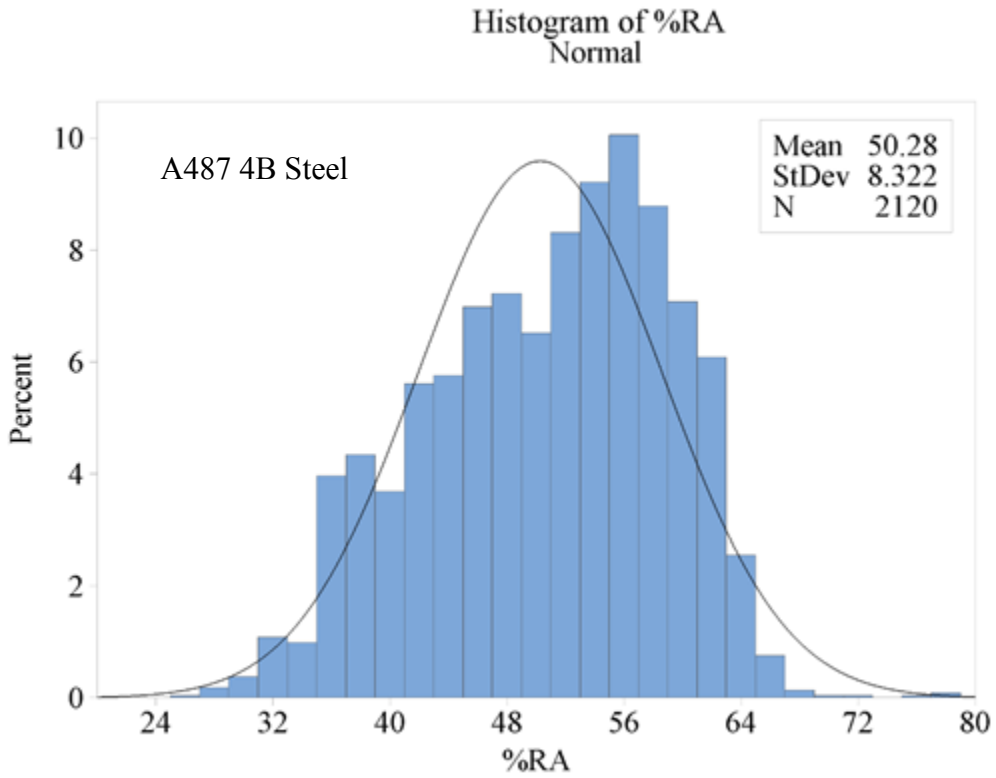

Figure A36. Normal distribution and histogram of reduction of area data for A487 4B cast steel.

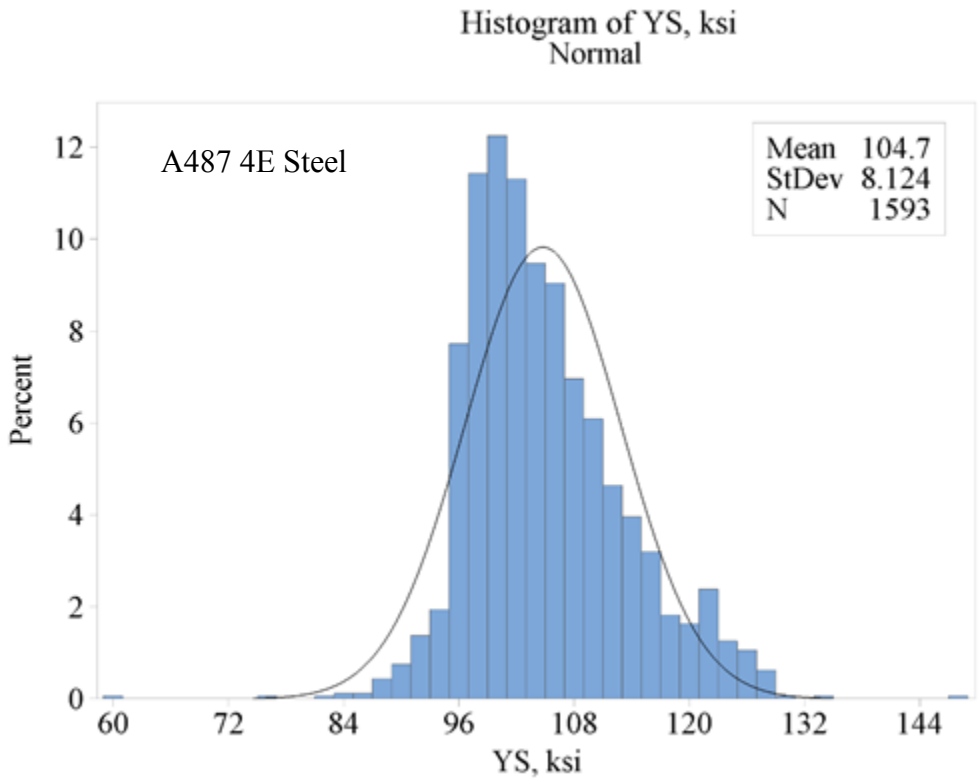

Figure A37. Normal distribution and histogram of yield stress data for A487 4E cast steel.

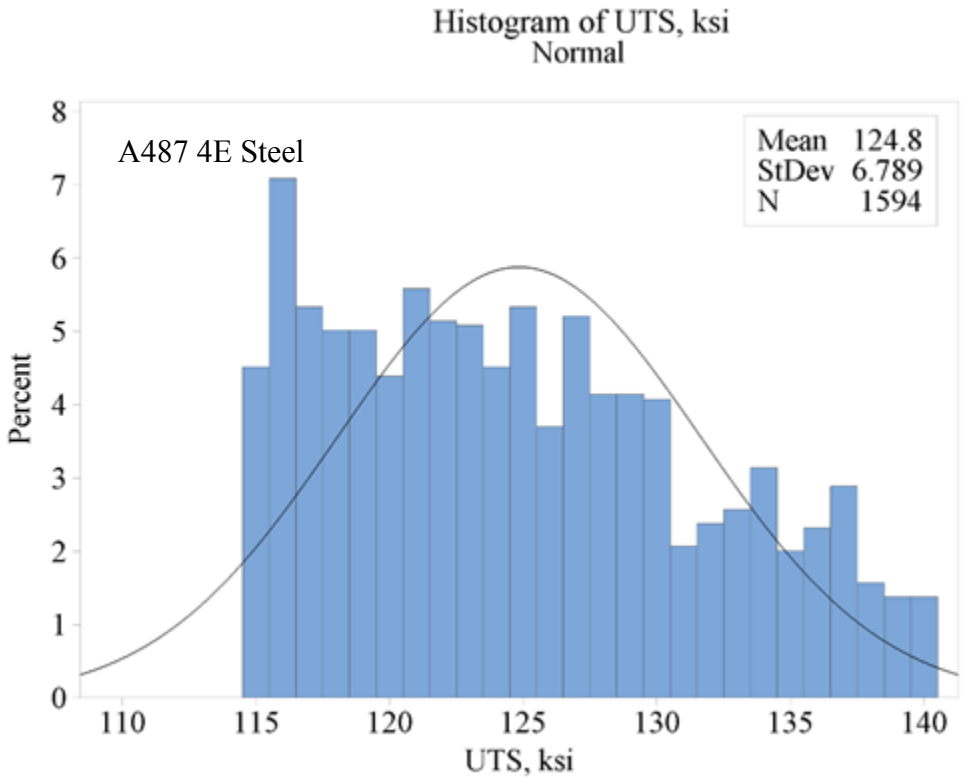

Figure A38. Normal distribution and histogram of ultimate stress data for A487 4E cast steel.

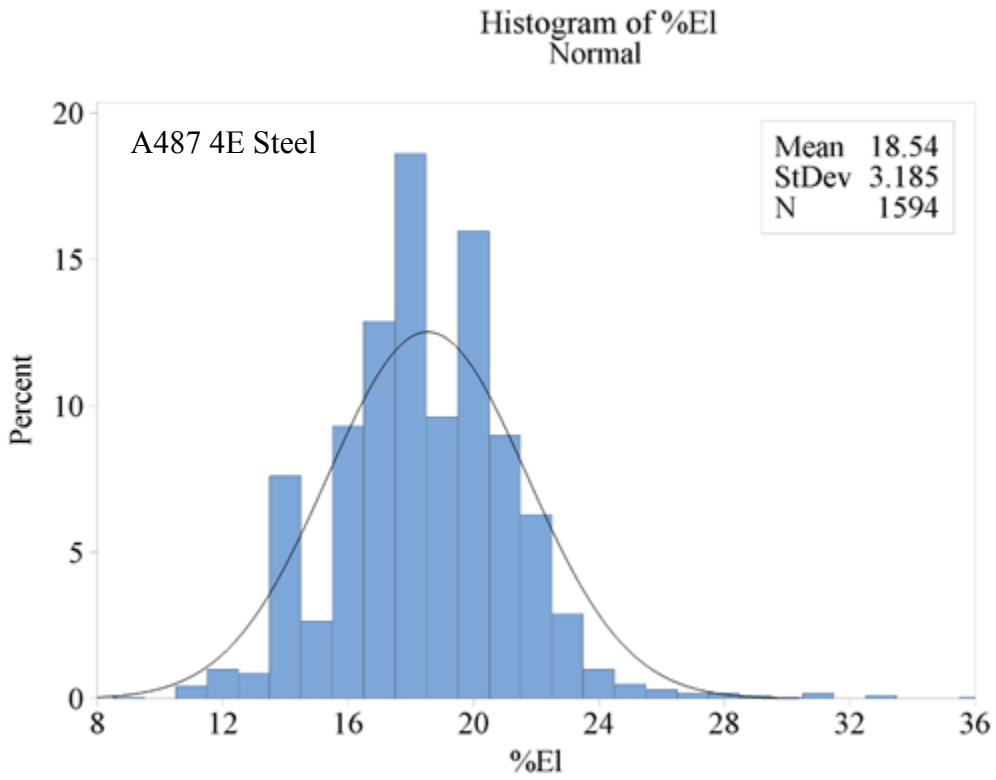

Figure A39. Normal distribution and histogram of elongation data for A487 4E cast steel.

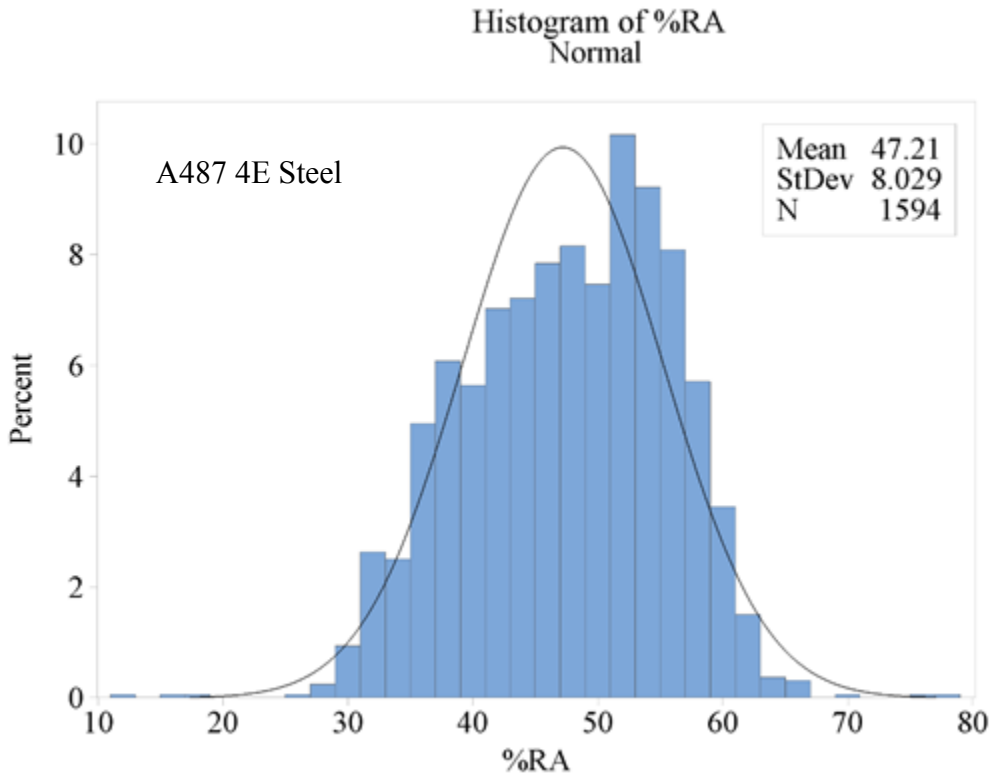

Figure A40. Normal distribution and histogram of reduction of area data for A487 4E cast steel.

Appendix B Probability Plots Using Normal Distribution and All Property Data

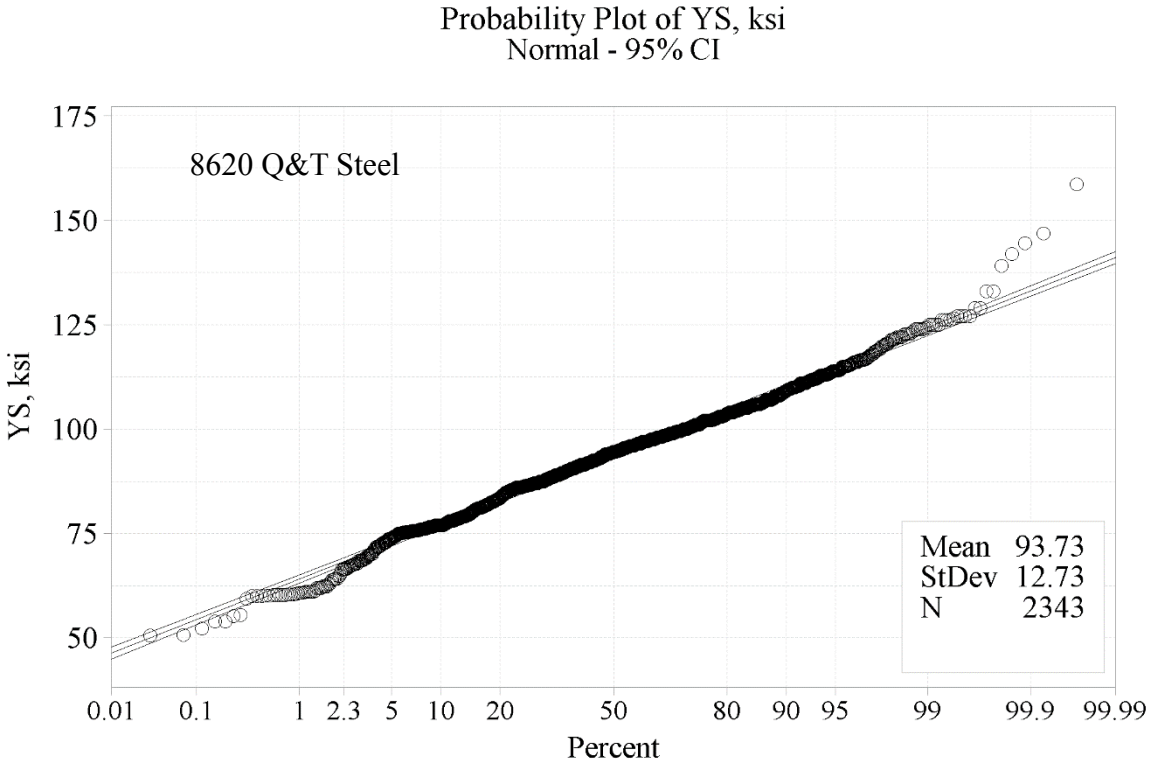

Figure B1. Normal distribution probability plot of yield strength data for 8620 quenched and tempered cast steel.

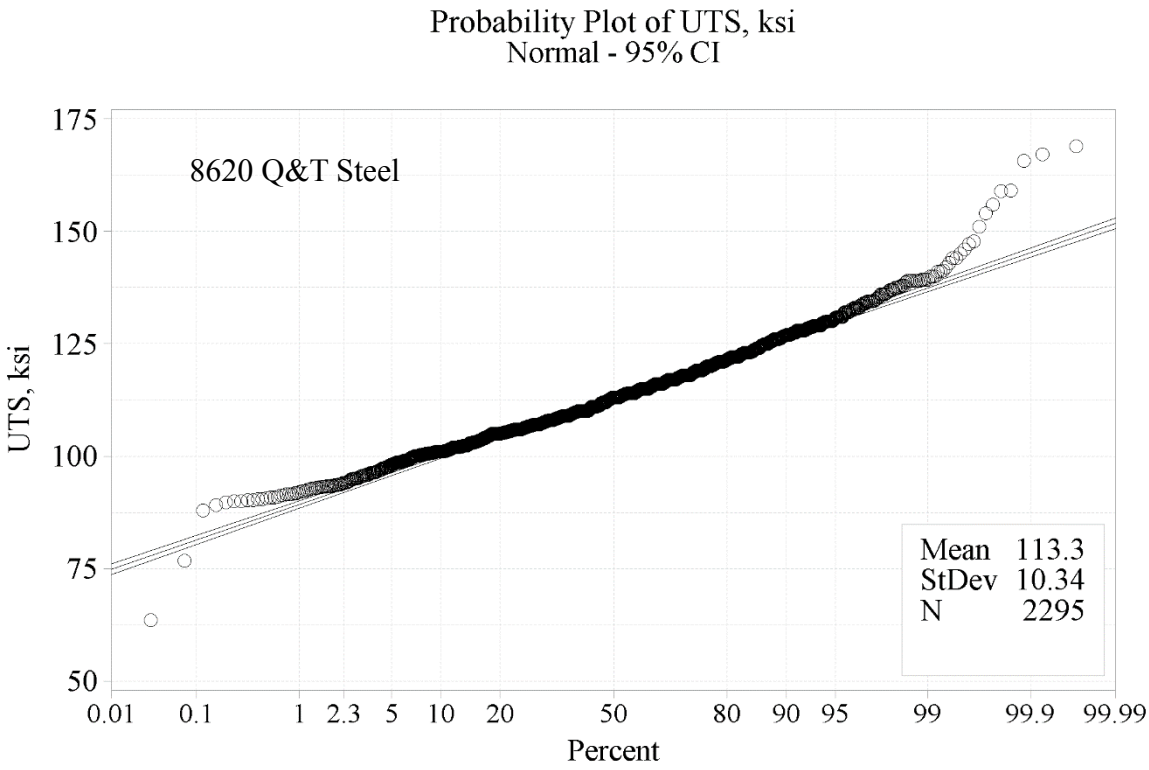

Figure B2. Normal distribution probability plot of ultimate strength data for 8620 quenched and tempered cast steel.

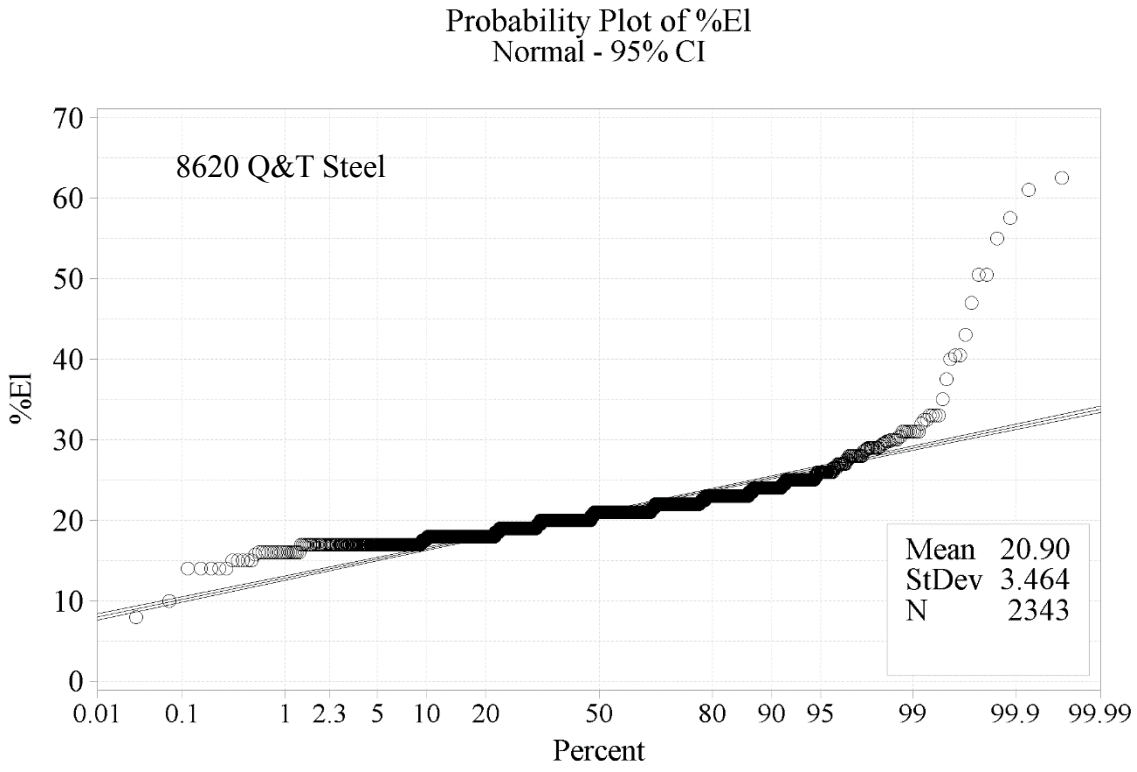

Figure B3. Normal distribution probability plot of elongation data for 8620 quenched and tempered cast steel.

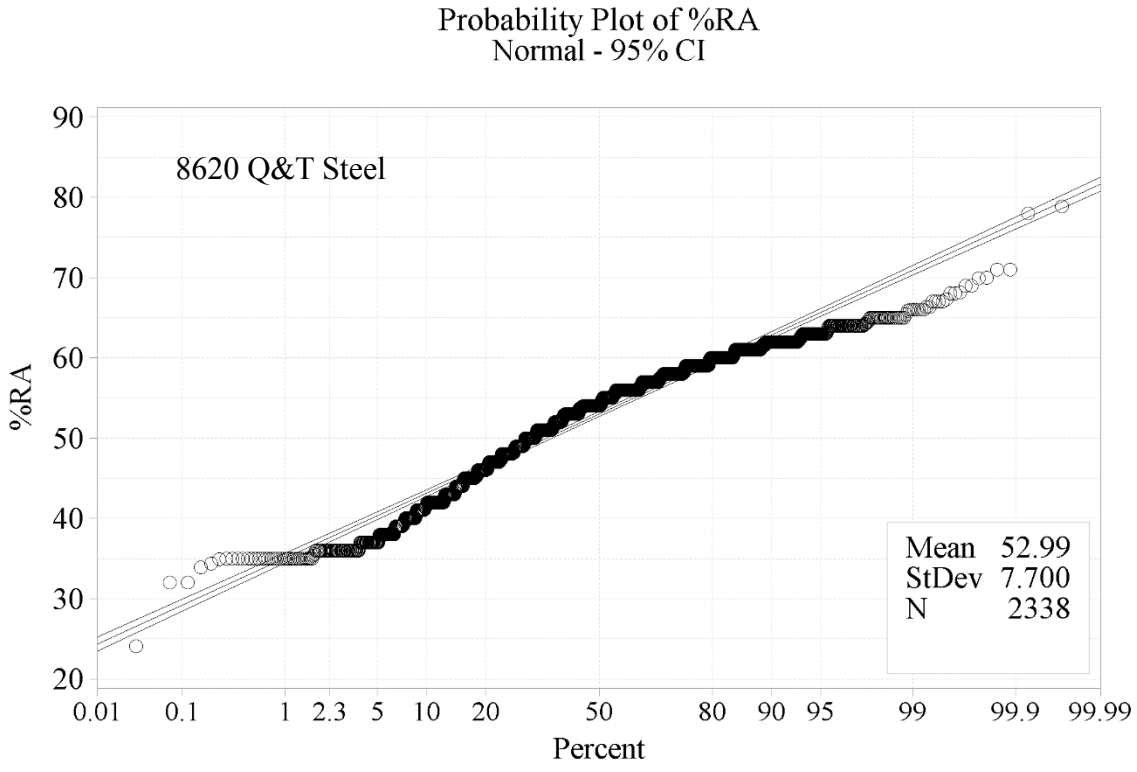

Figure B4. Normal distribution probability plot of reduction of area data for 8620 quenched and tempered cast steel.

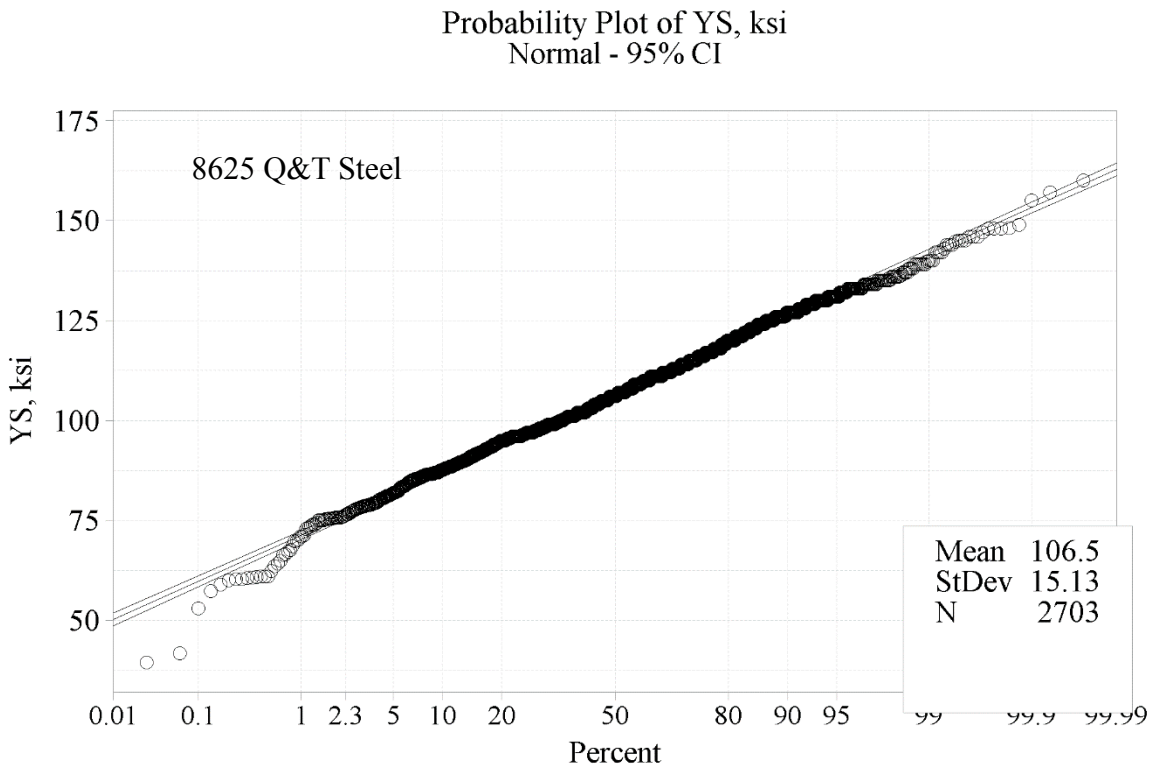

Figure B5. Normal distribution probability plot of yield strength data for 8625 quenched and tempered cast steel.

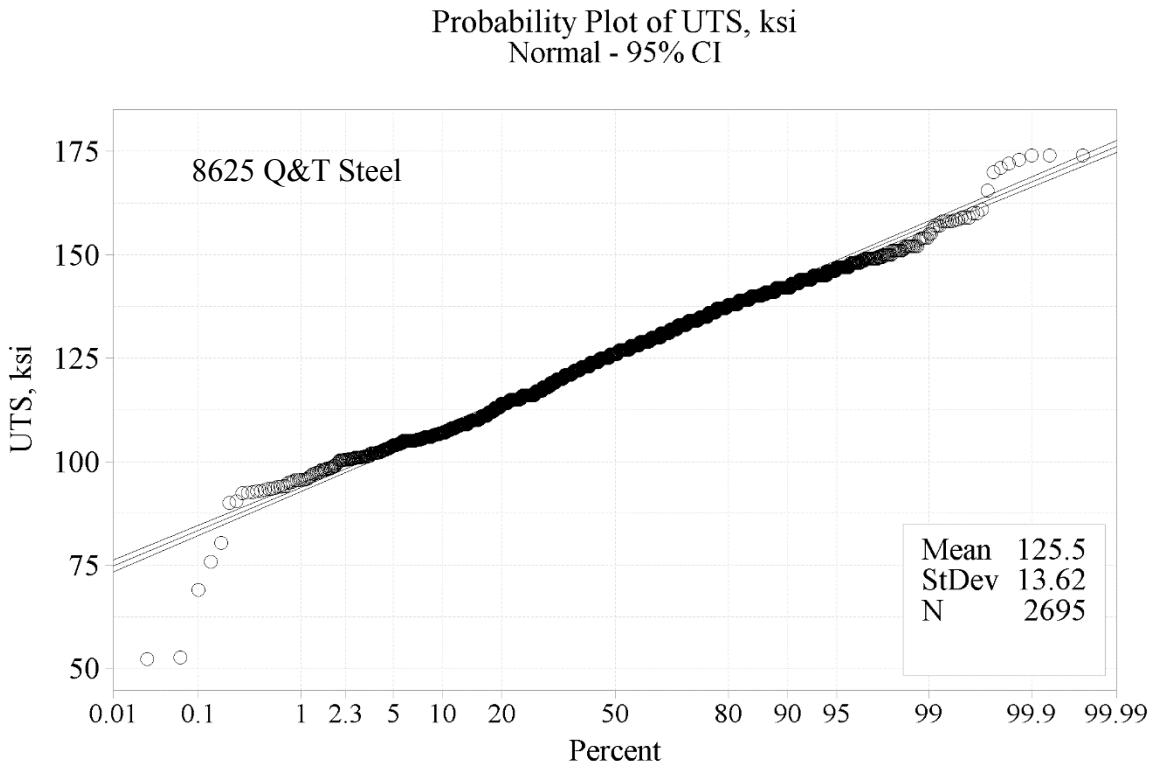

Figure B6. Normal distribution probability plot of ultimate strength data for 8625 quenched and tempered cast steel.

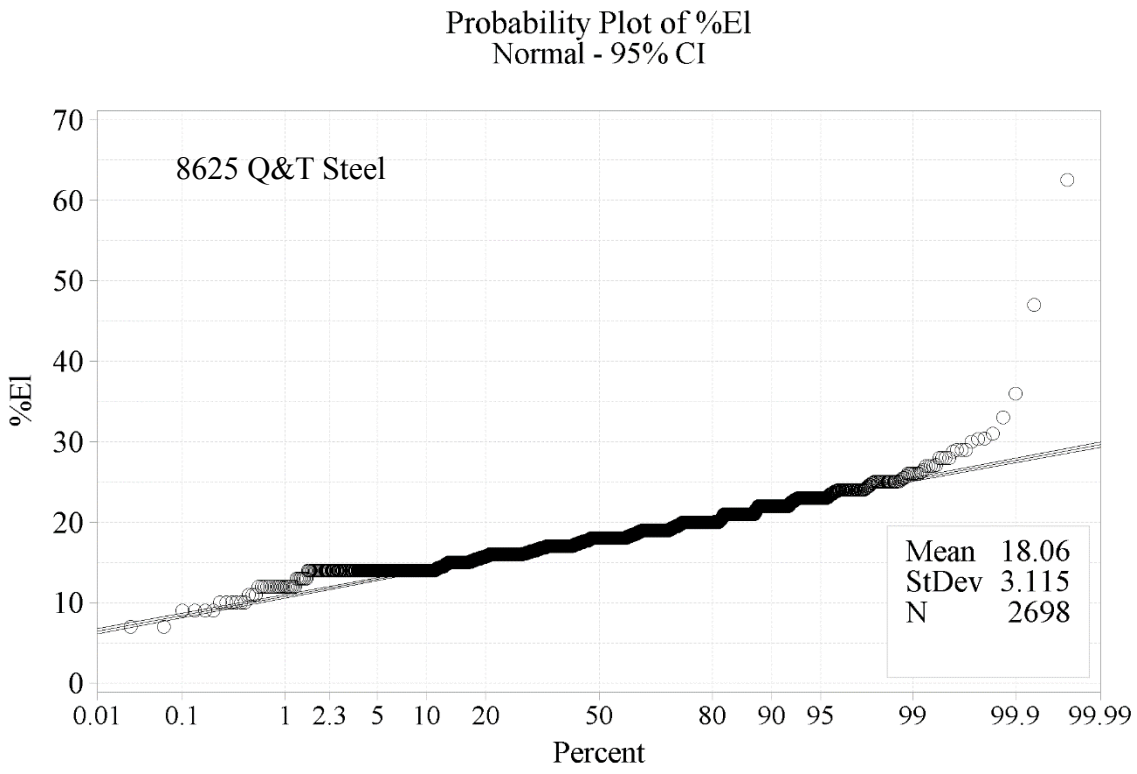

Figure B7. Normal distribution probability plot of elongation data for 8625 quenched and tempered cast steel.

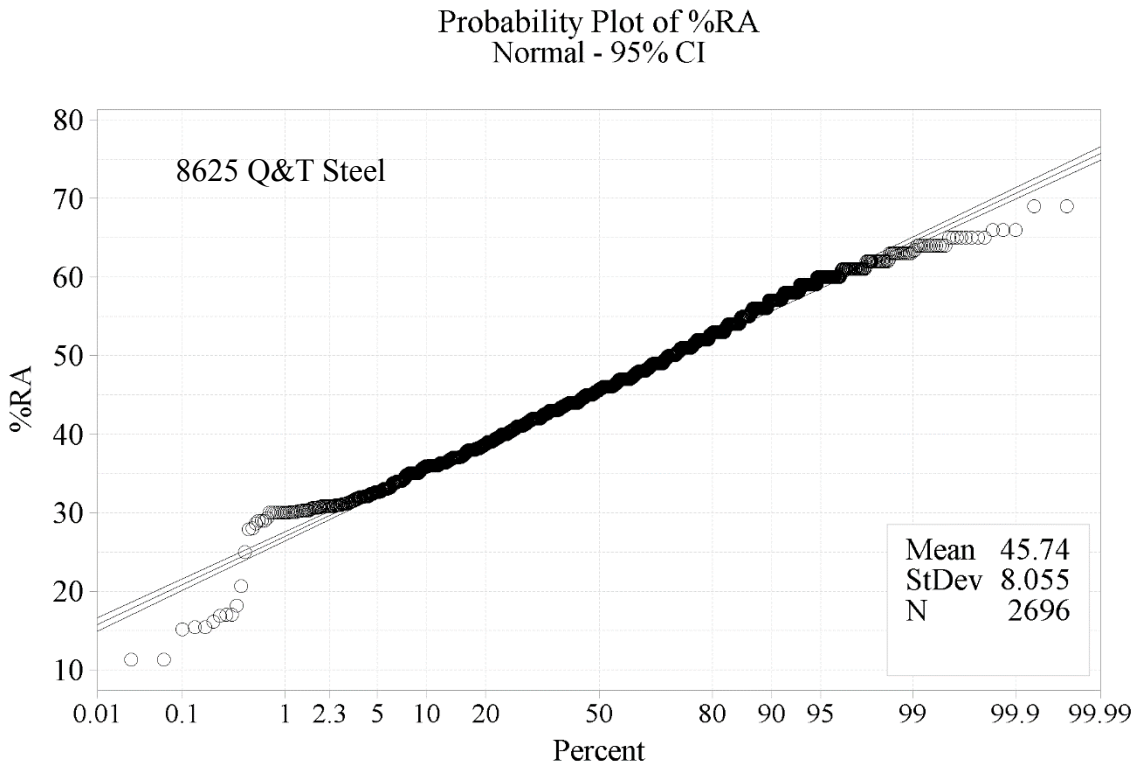

Figure B8. Normal distribution probability plot of reduction of area data for 8625 quenched and tempered cast steel.

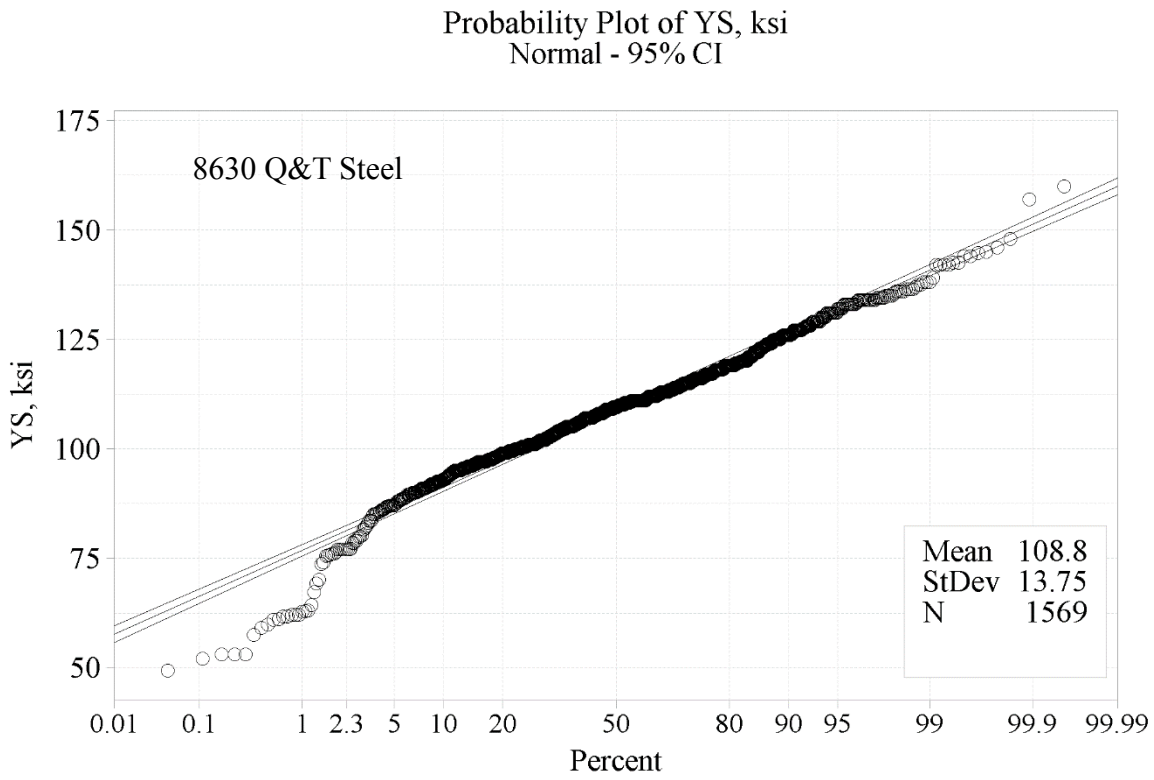

Figure B9. Normal distribution probability plot of yield strength data for 8630 quenched and tempered cast steel.

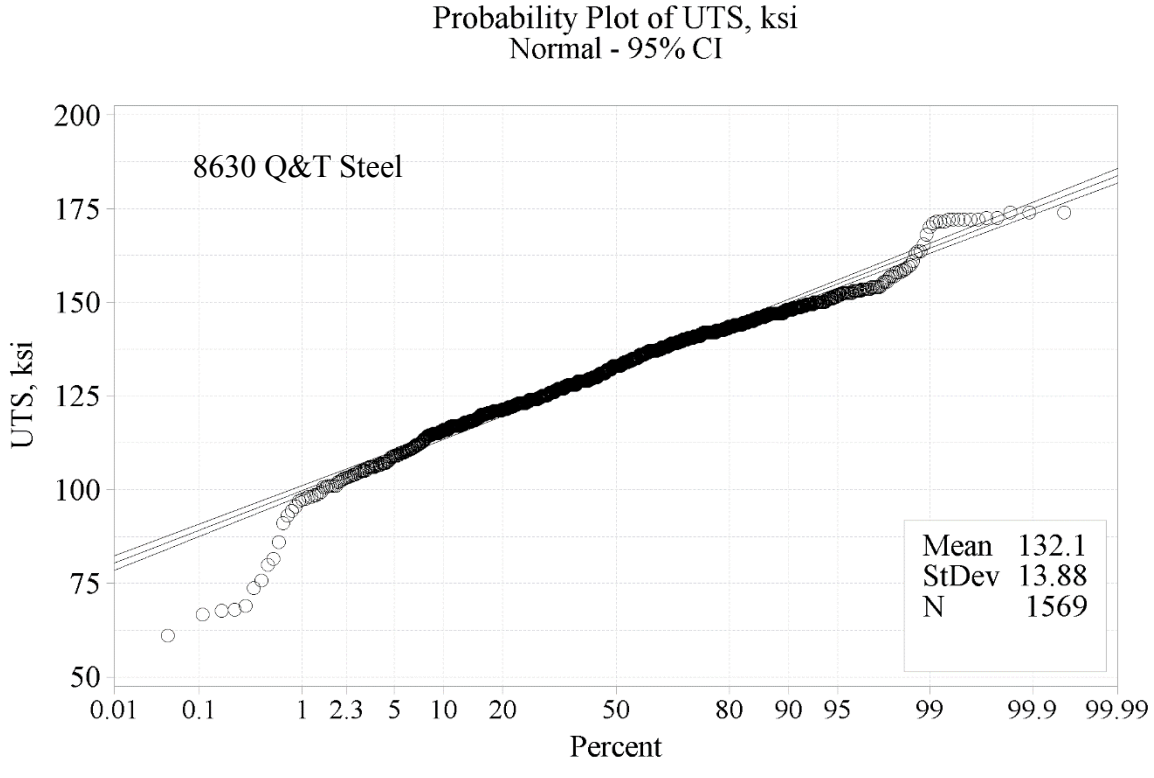

Figure B10. Normal distribution probability plot of ultimate strength data for 8630 quenched and tempered cast steel.

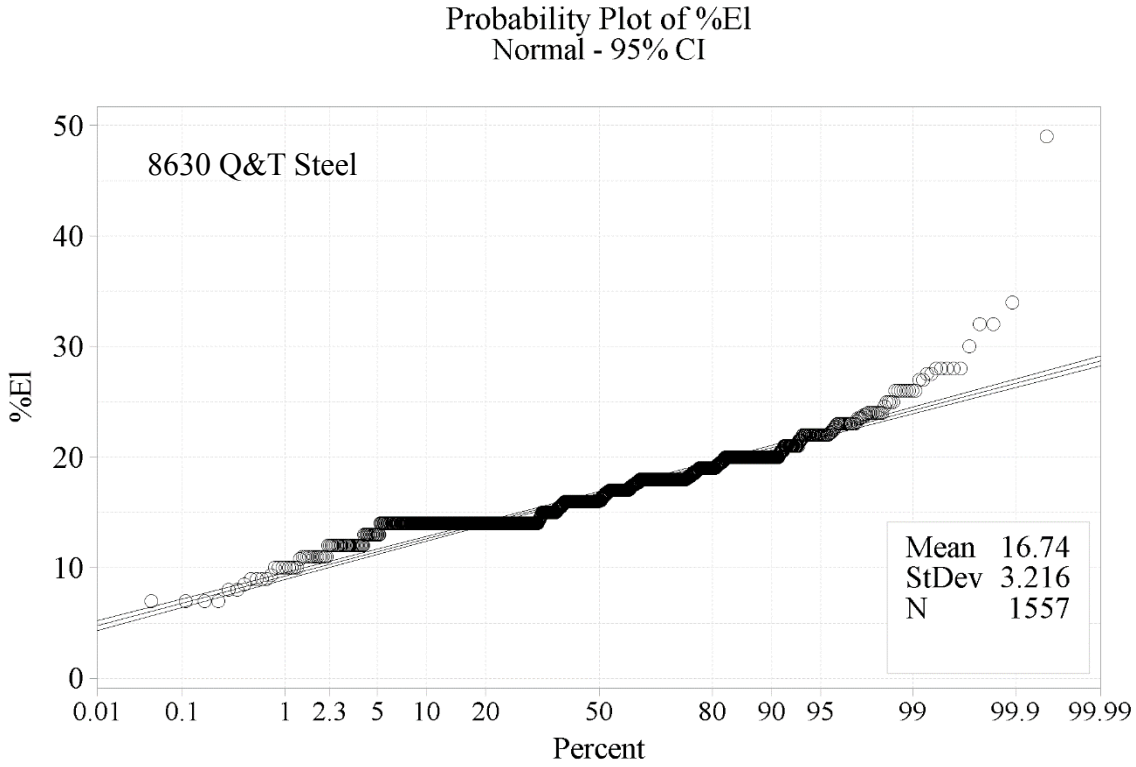

Figure B11. Normal distribution probability plot of elongation data for 8630 quenched and tempered cast steel.

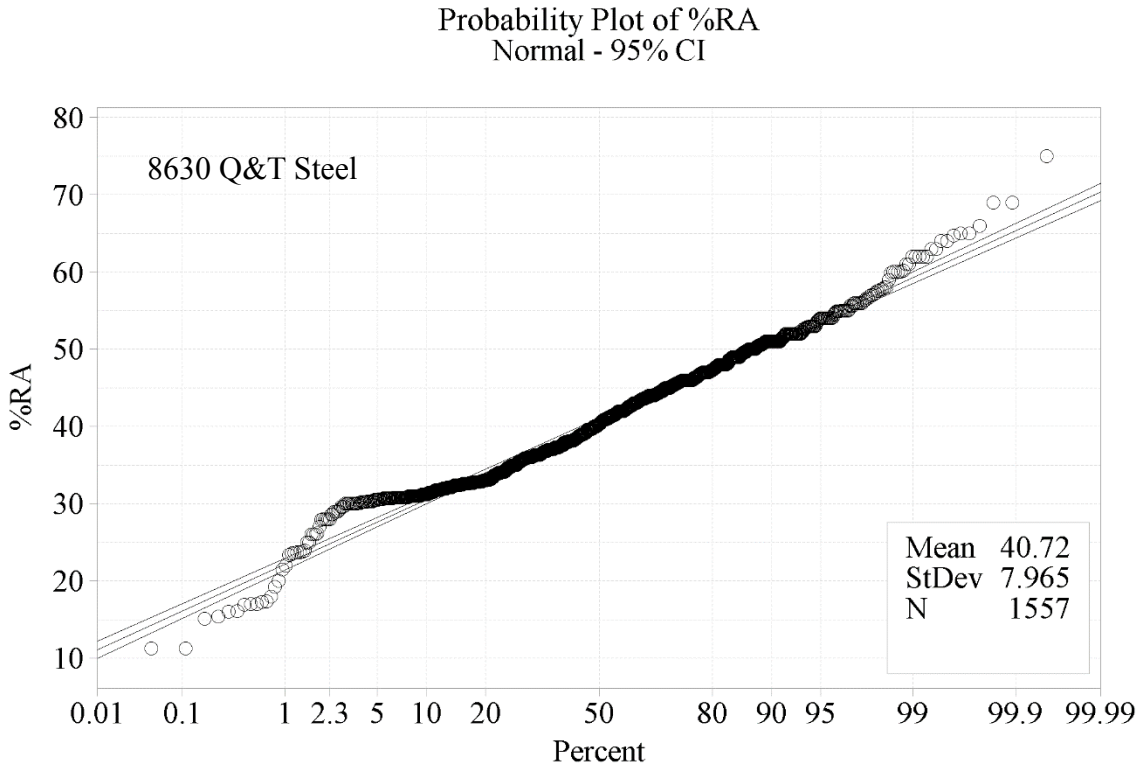

Figure B12. Normal distribution probability plot of reduction of area data for 8630 quenched and tempered cast steel.

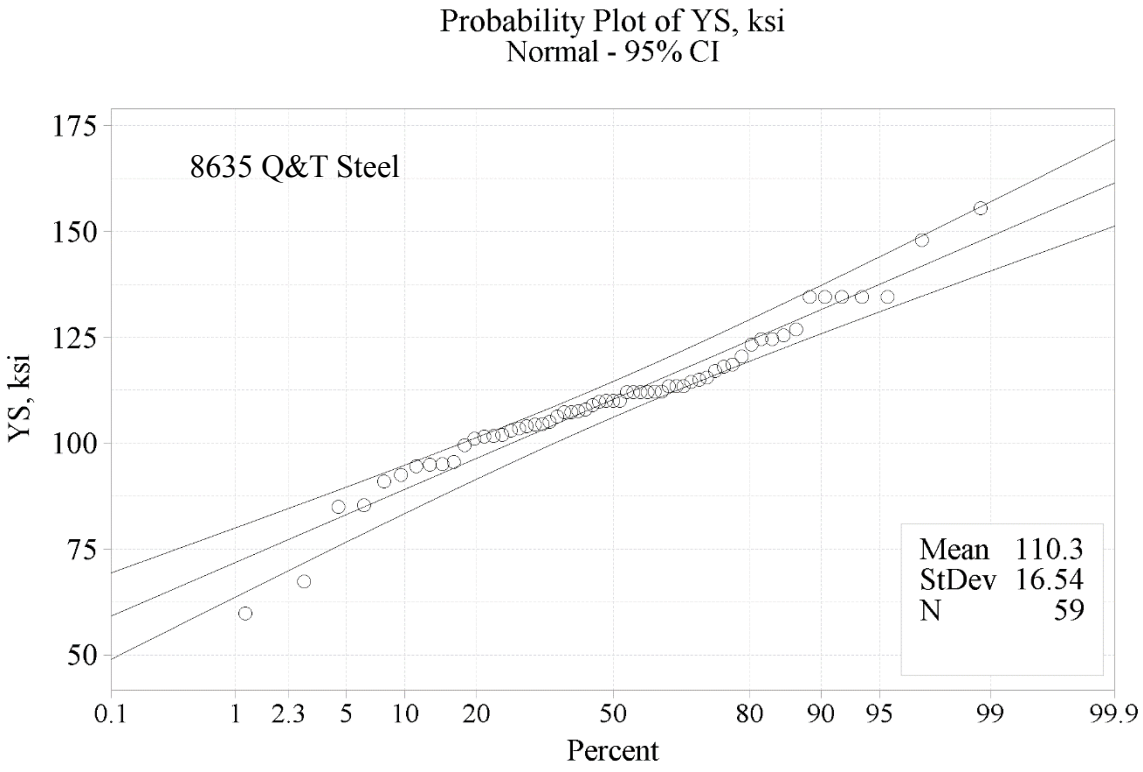

Figure B13. Normal distribution probability plot of yield stress data for 8635 quenched and tempered cast steel.

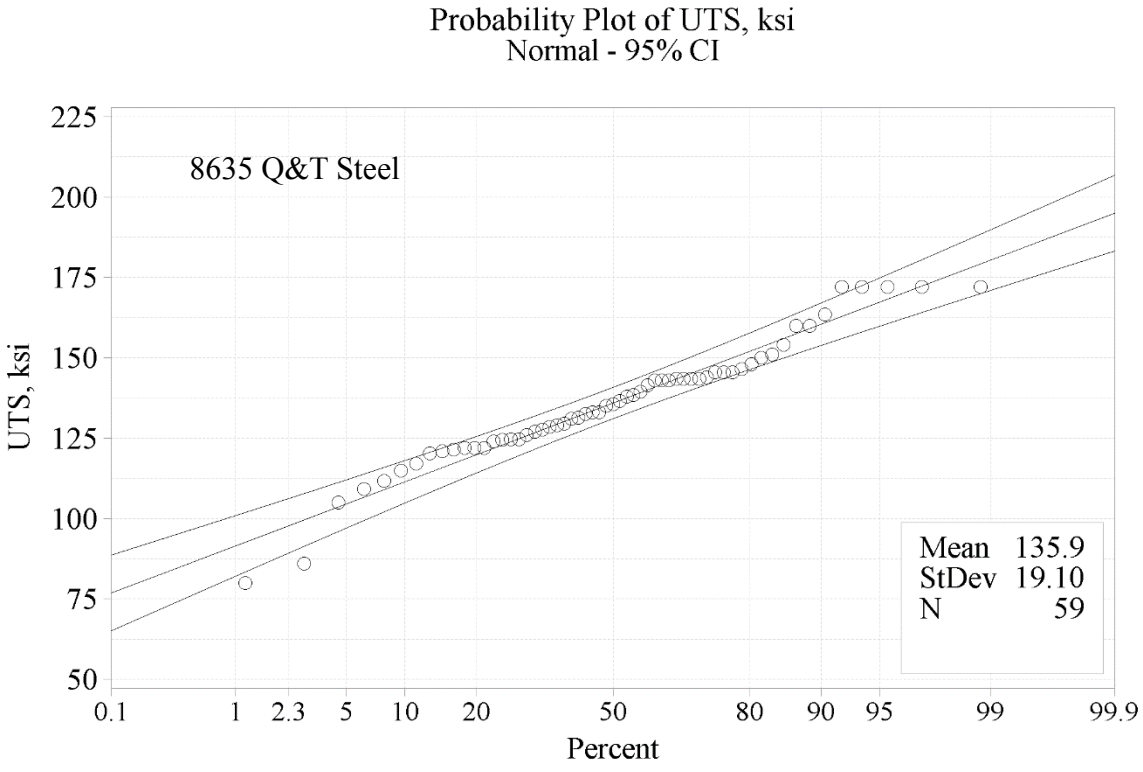

Figure B14. Normal distribution probability plot of ultimate strength data for 8635 quenched and tempered cast steel.

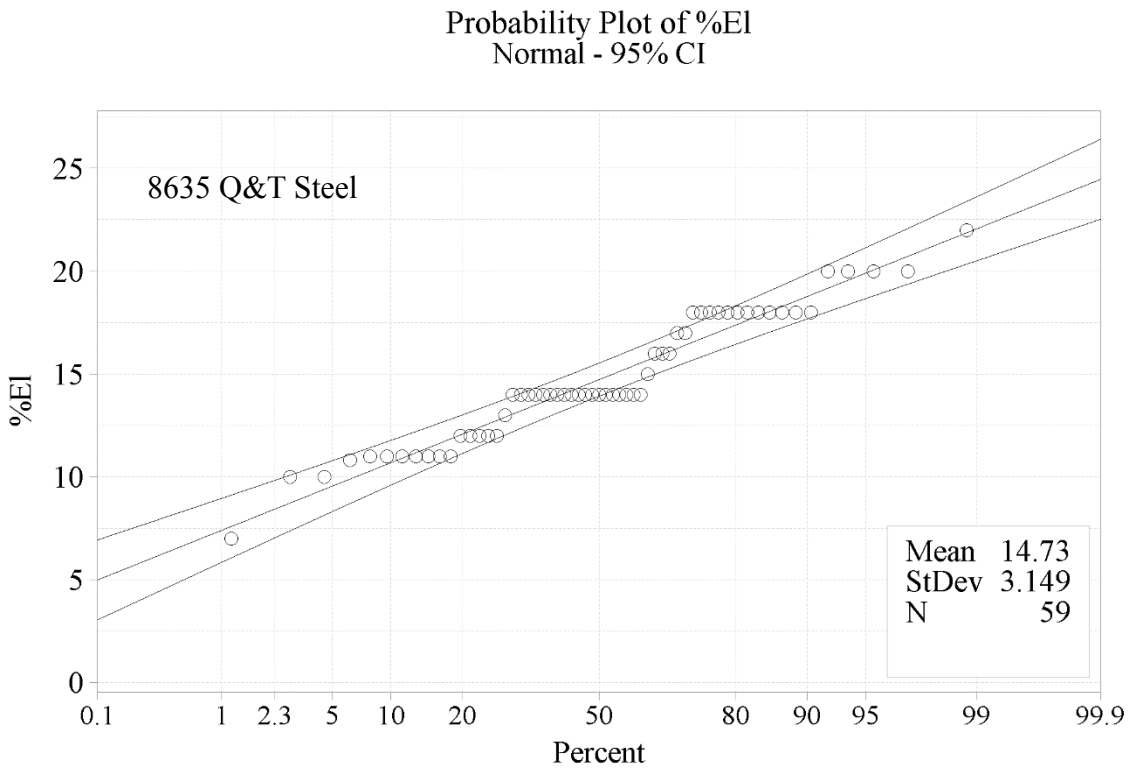

Figure B15. Normal distribution probability plot of elongation data for 8635 quenched and tempered cast steel.

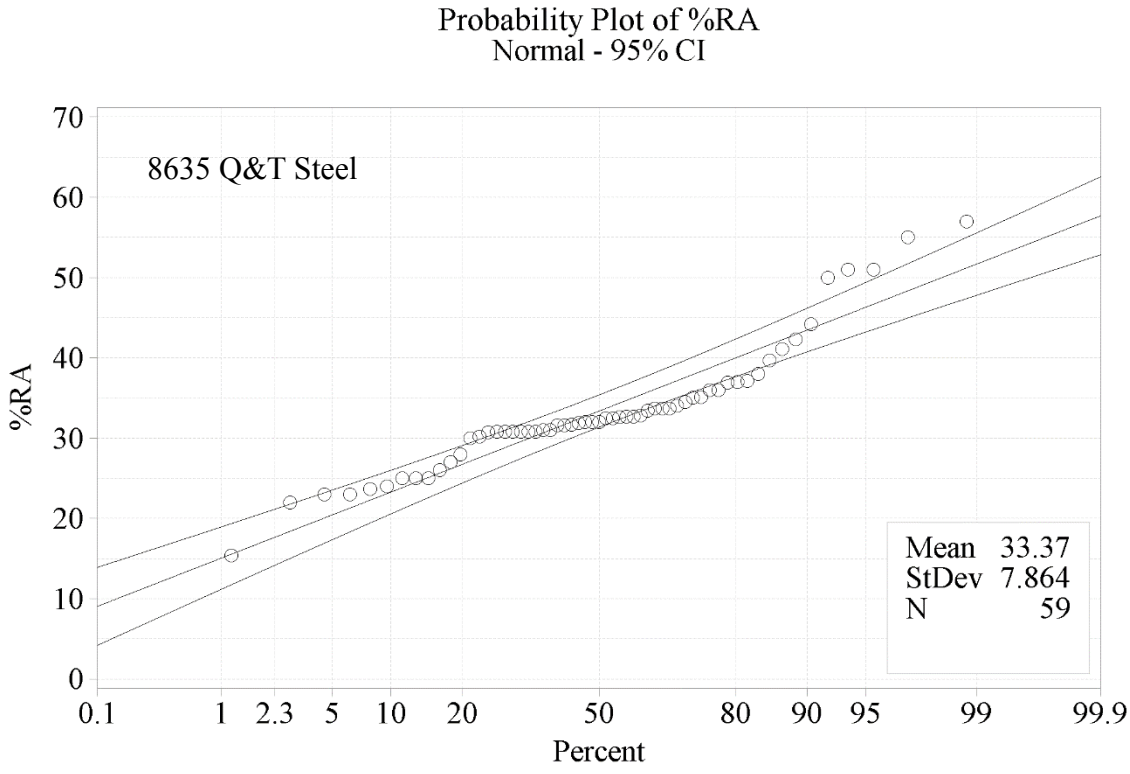

Figure B16. Normal distribution probability plot of reduction of area data for 8635 quenched and tempered cast steel.

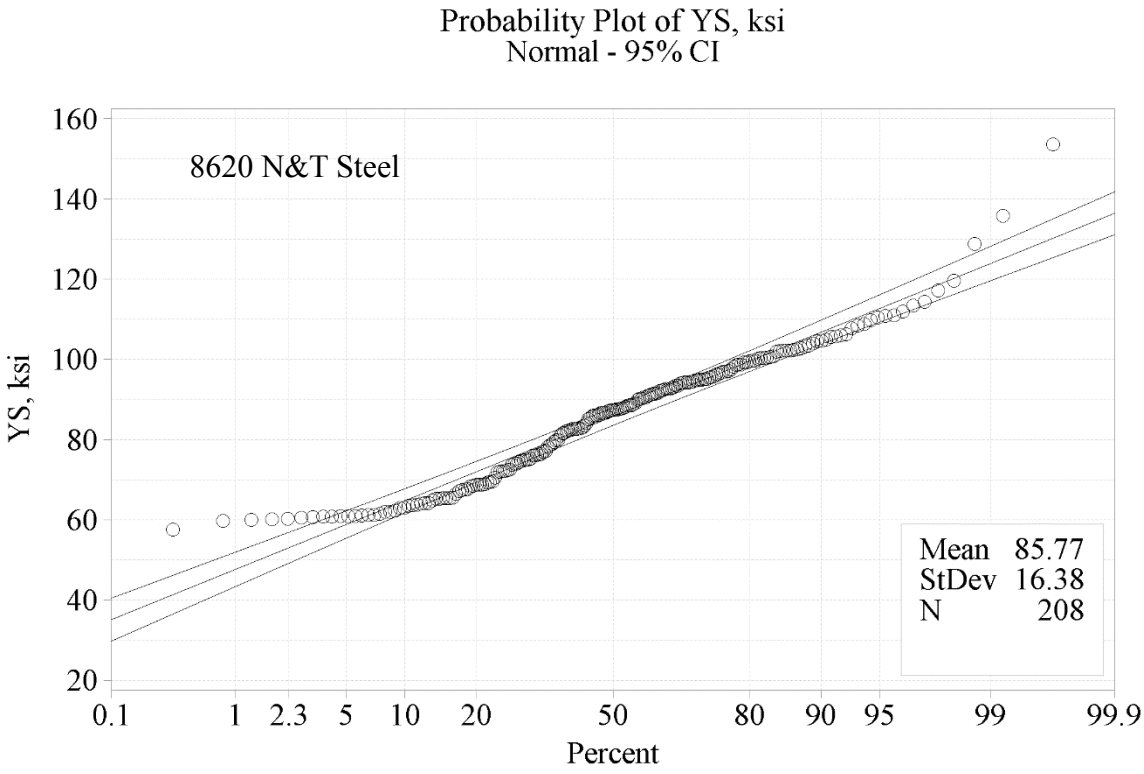

Figure B17. Normal distribution probability plot of yield strength data for 8620 normalized and tempered cast steel.

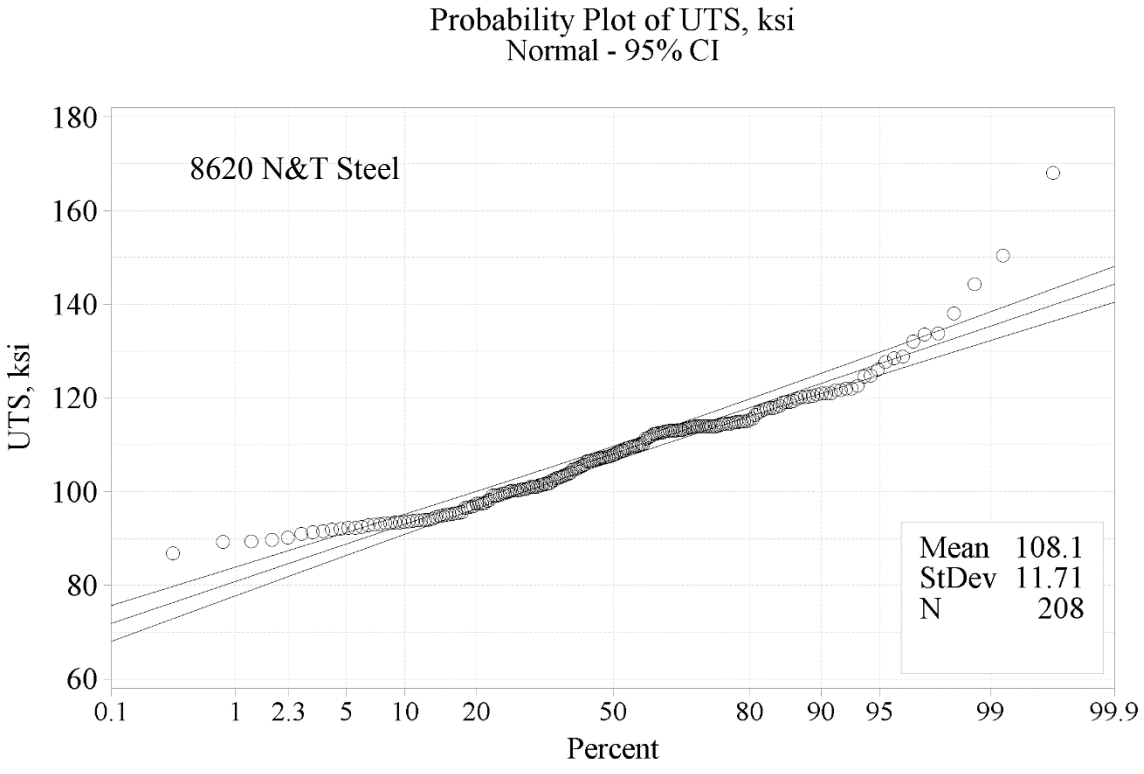

Figure B18. Normal distribution probability plot of ultimate strength data for 8620 normalized and tempered cast steel.

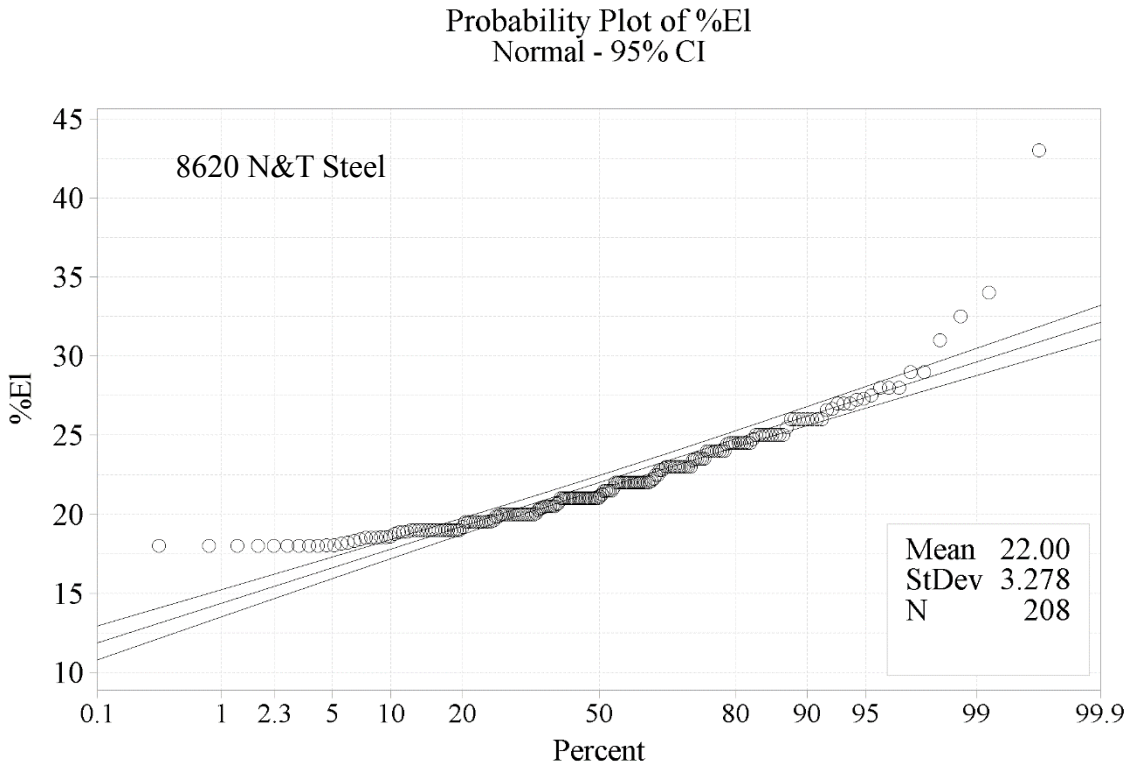

Figure B19. Normal distribution probability plot of elongation data for 8620 normalized and tempered cast steel.

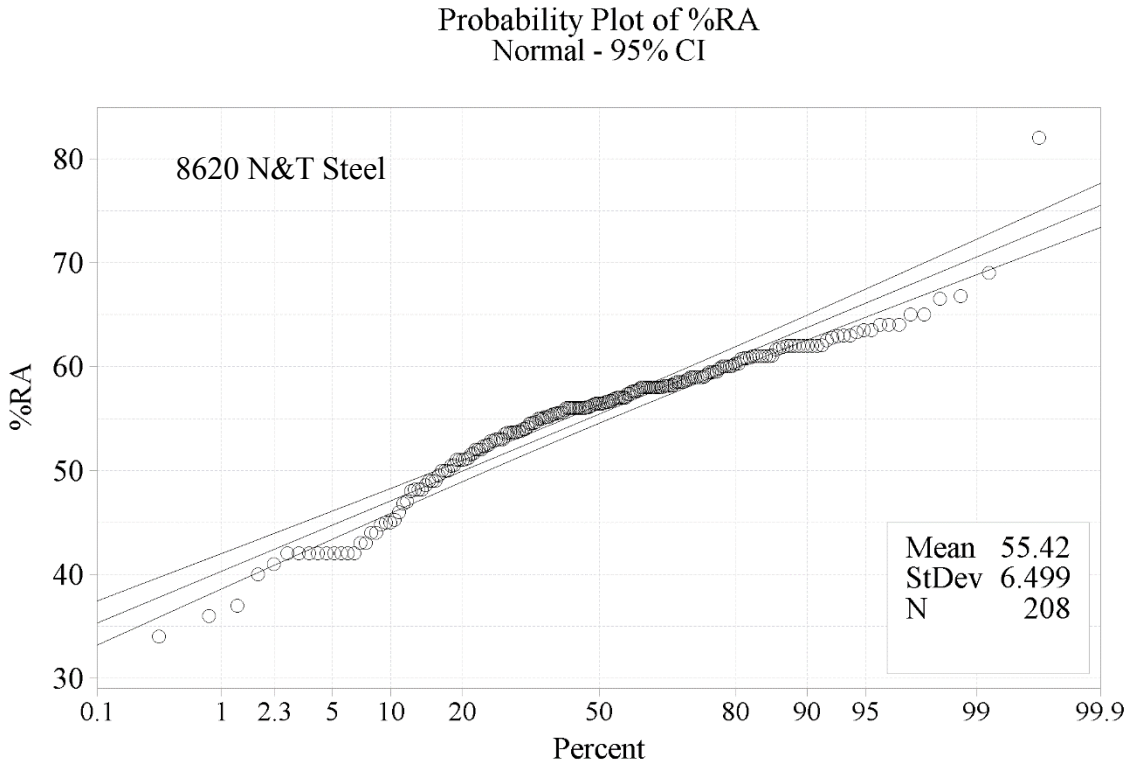

Figure B20. Normal distribution probability plot of reduction of area data for 8620 normalized and tempered cast steel.

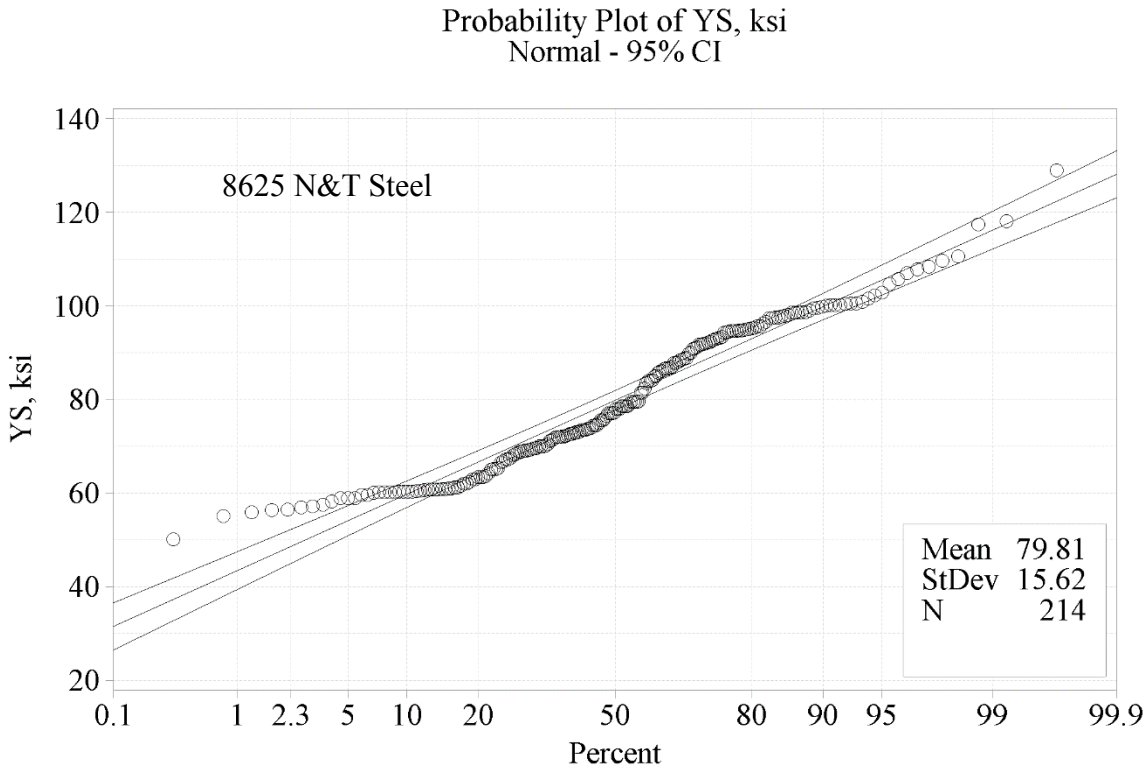

Figure B21. Normal distribution probability plot of yield strength data for 8625 normalized and tempered cast steel.

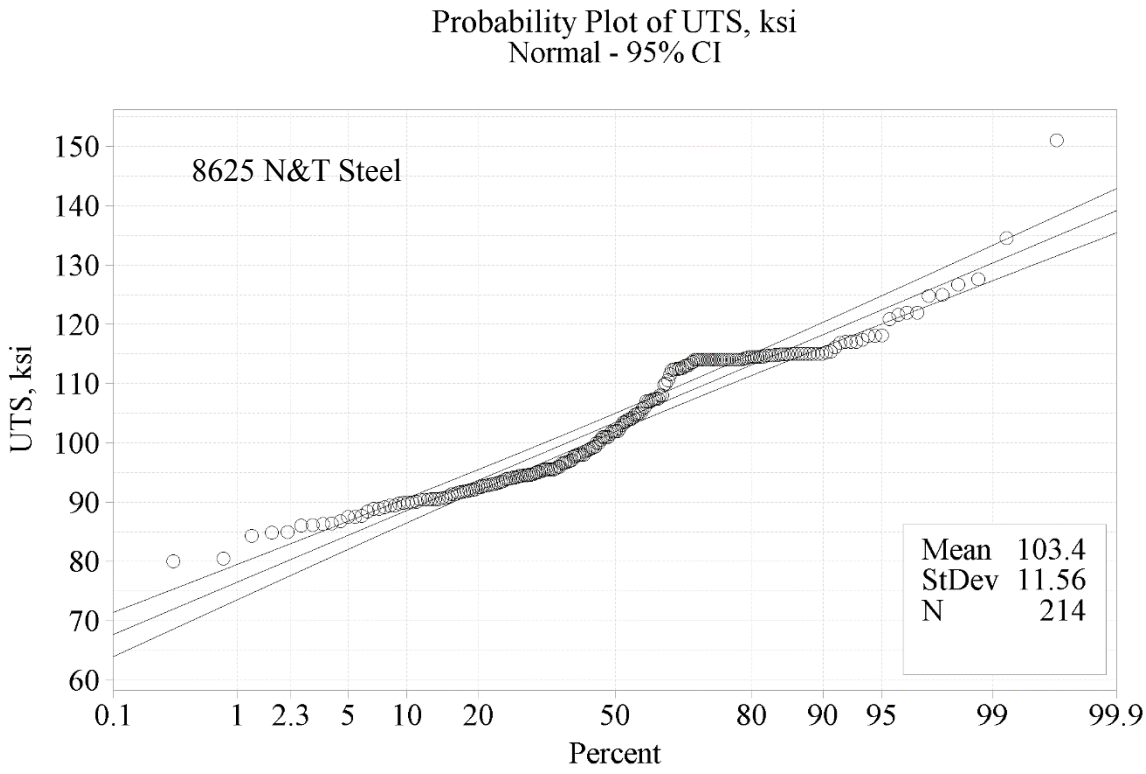

Figure B22. Normal distribution probability plot of ultimate strength data for 8625 normalized and tempered cast steel.

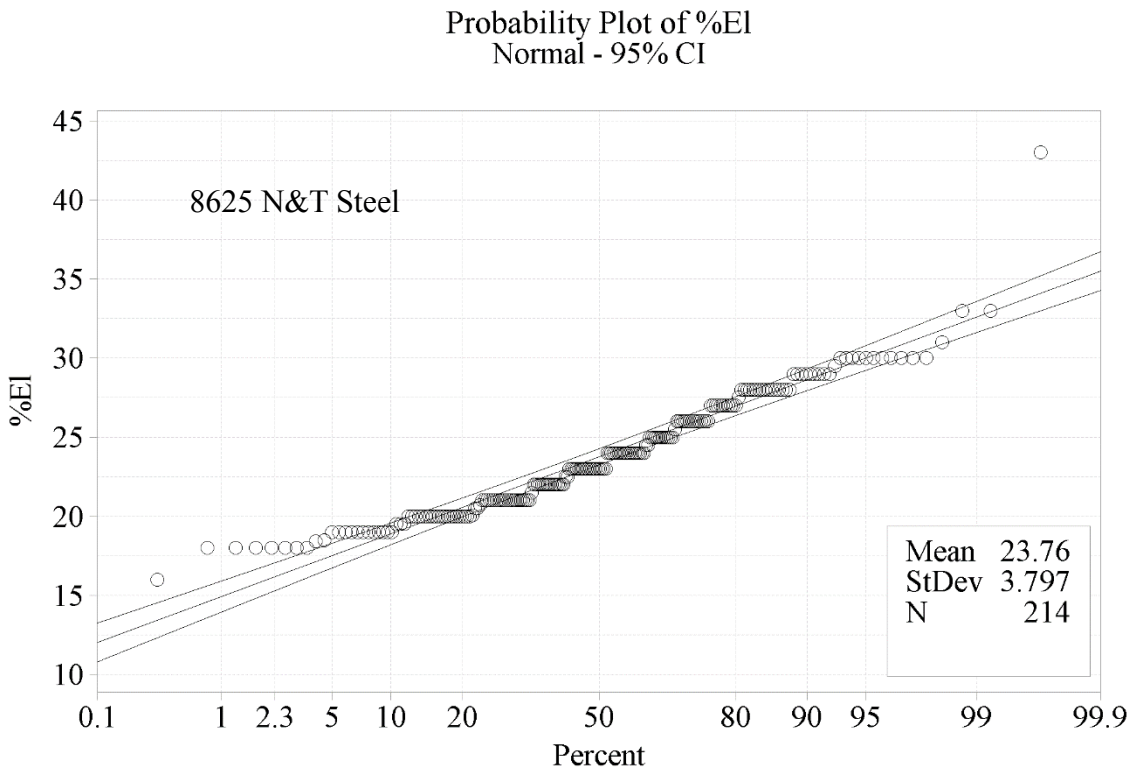

Figure B23. Normal distribution probability plot of elongation data for 8625 normalized and tempered cast steel.

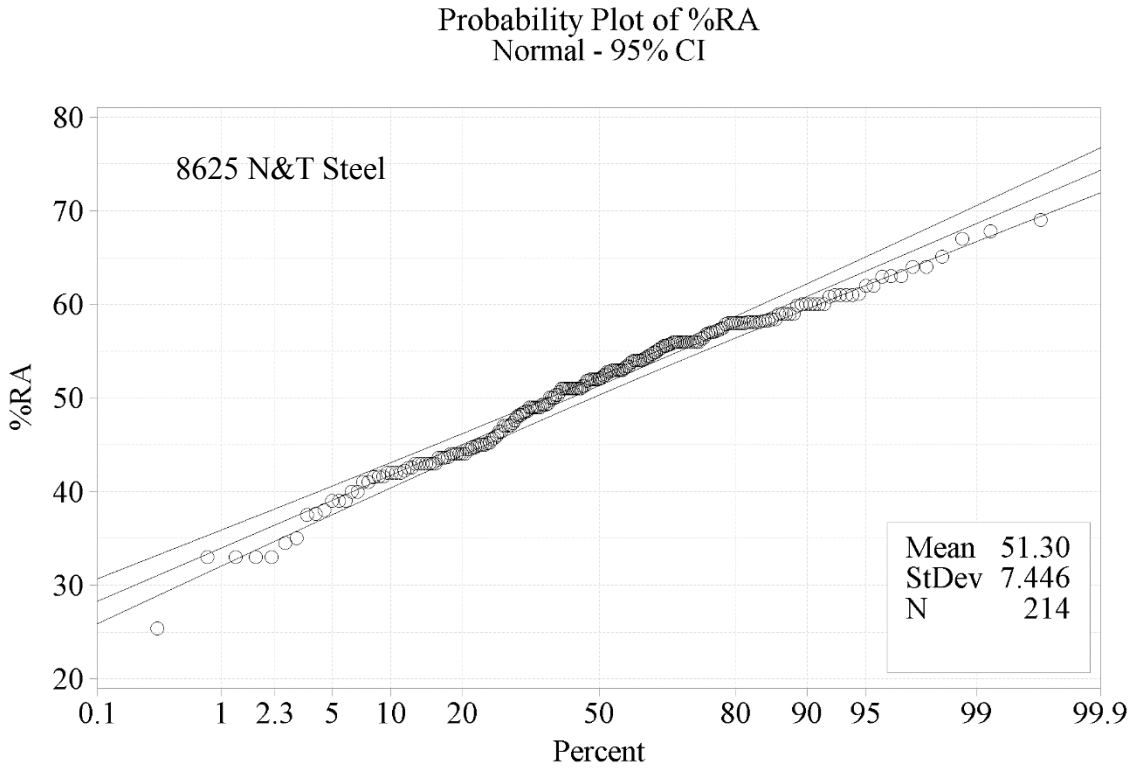

Figure B24. Normal distribution probability plot of reduction of area data for 8625 normalized and tempered cast steel.

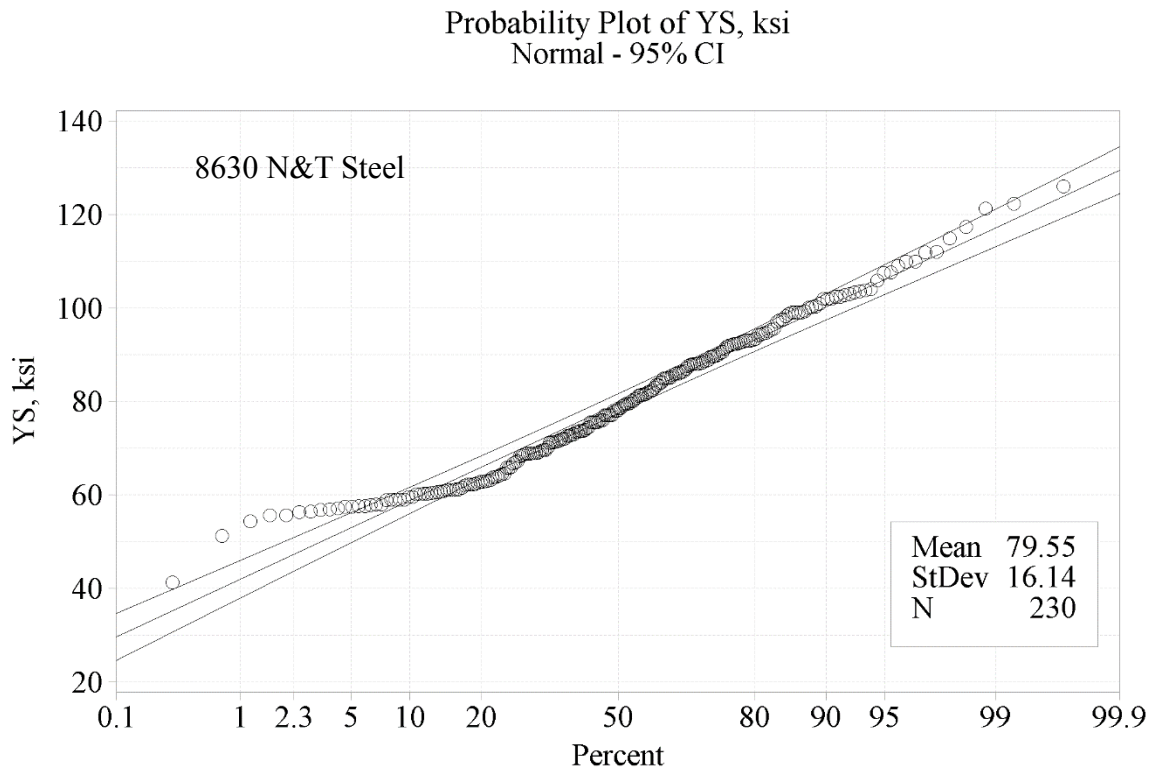

Figure B25. Normal distribution probability plot of yield strength data for 8630 normalized and tempered cast steel.

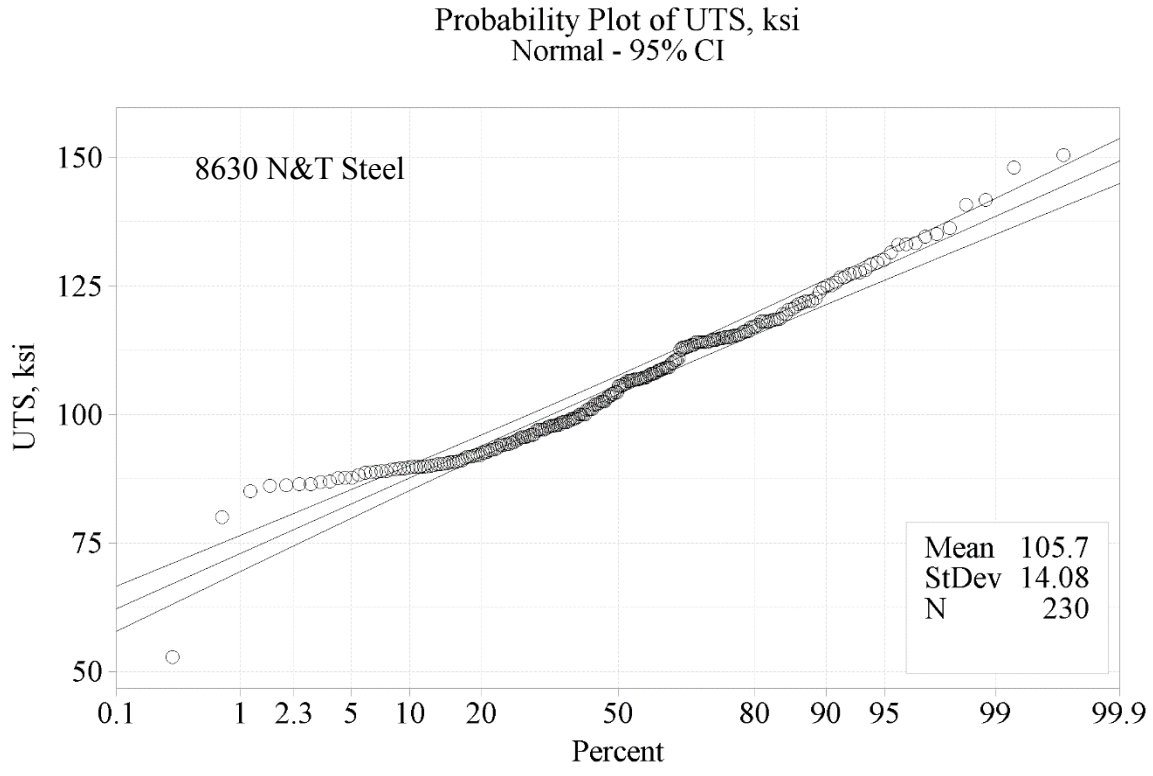

Figure B26. Normal distribution probability plot of ultimate strength data for 8630 normalized and tempered cast steel.

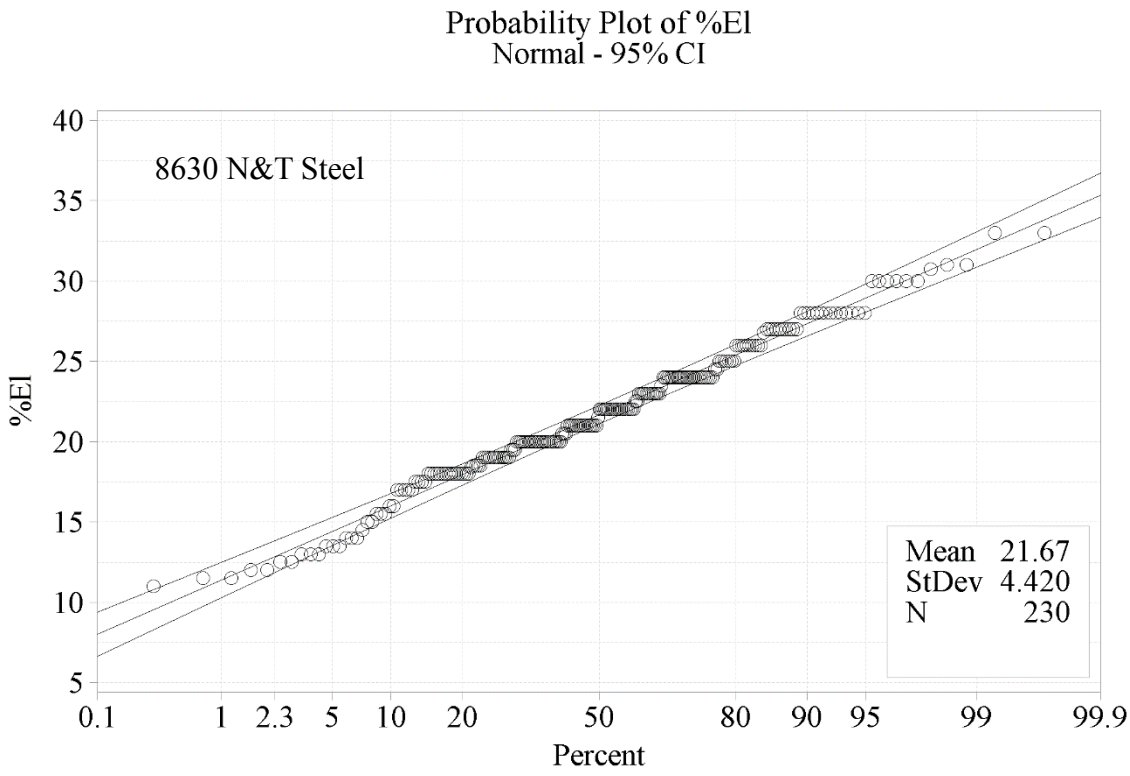

Figure B27. Normal distribution probability plot of elongation data for 8630 normalized and tempered cast steel.

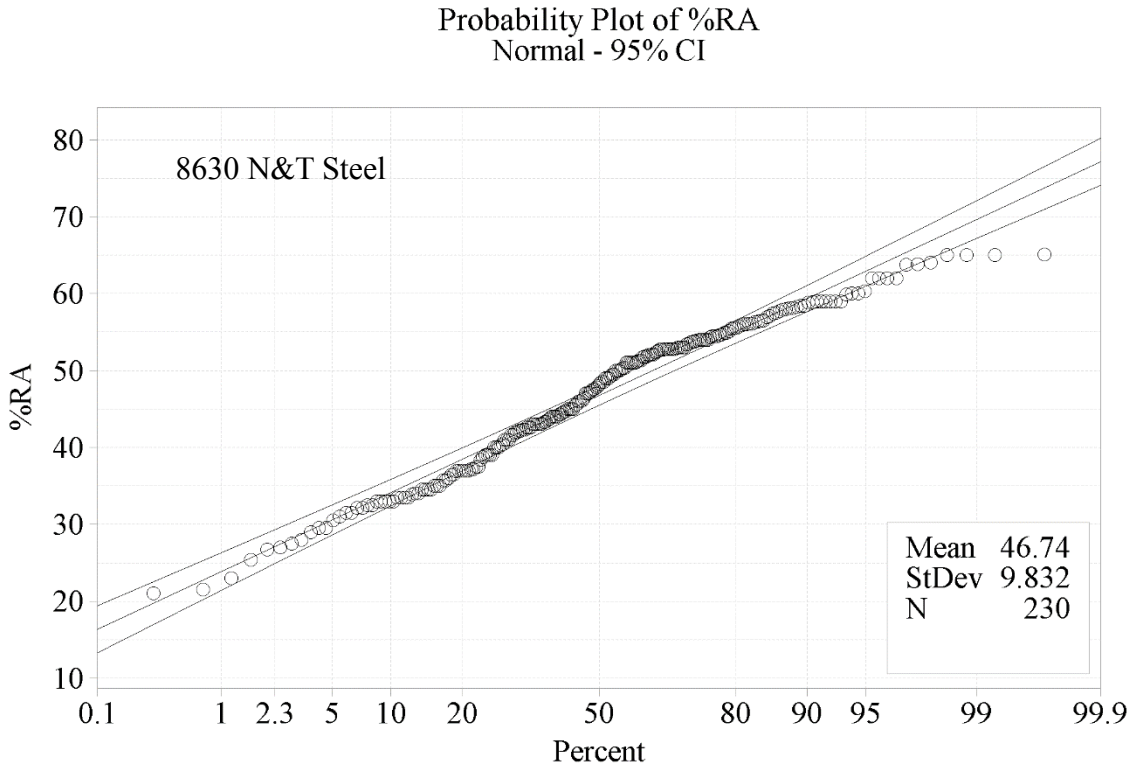

Figure B28. Normal distribution probability plot of reduction of area data for 8630 normalized and tempered cast steel.

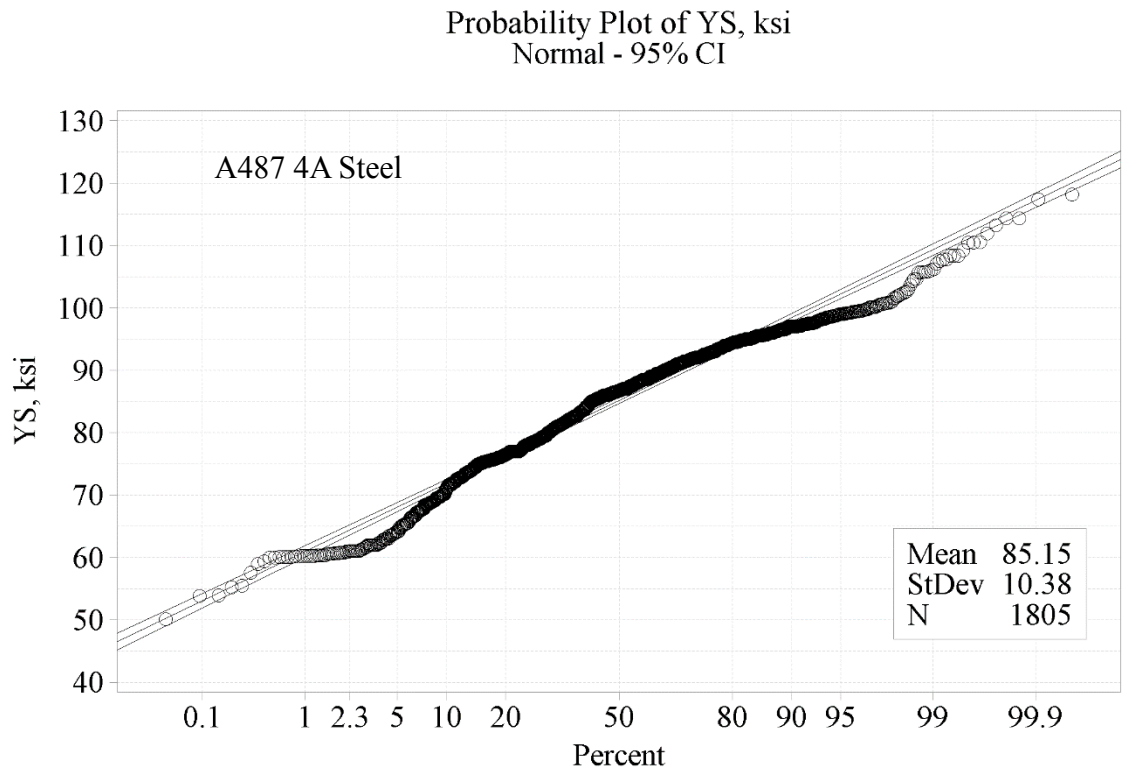

Figure B29. Normal distribution probability plot of yield strength data for A487 4A steel.

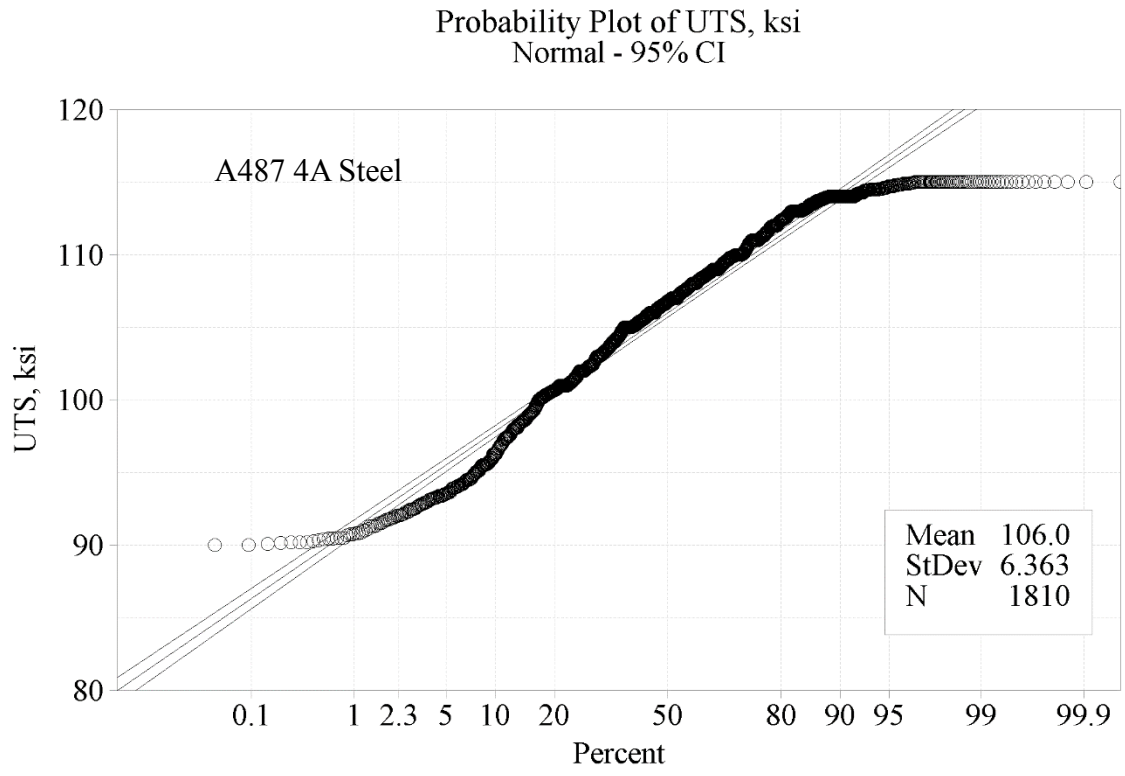

Figure B30. Normal distribution probability plot of ultimate strength data A487 4A steel.

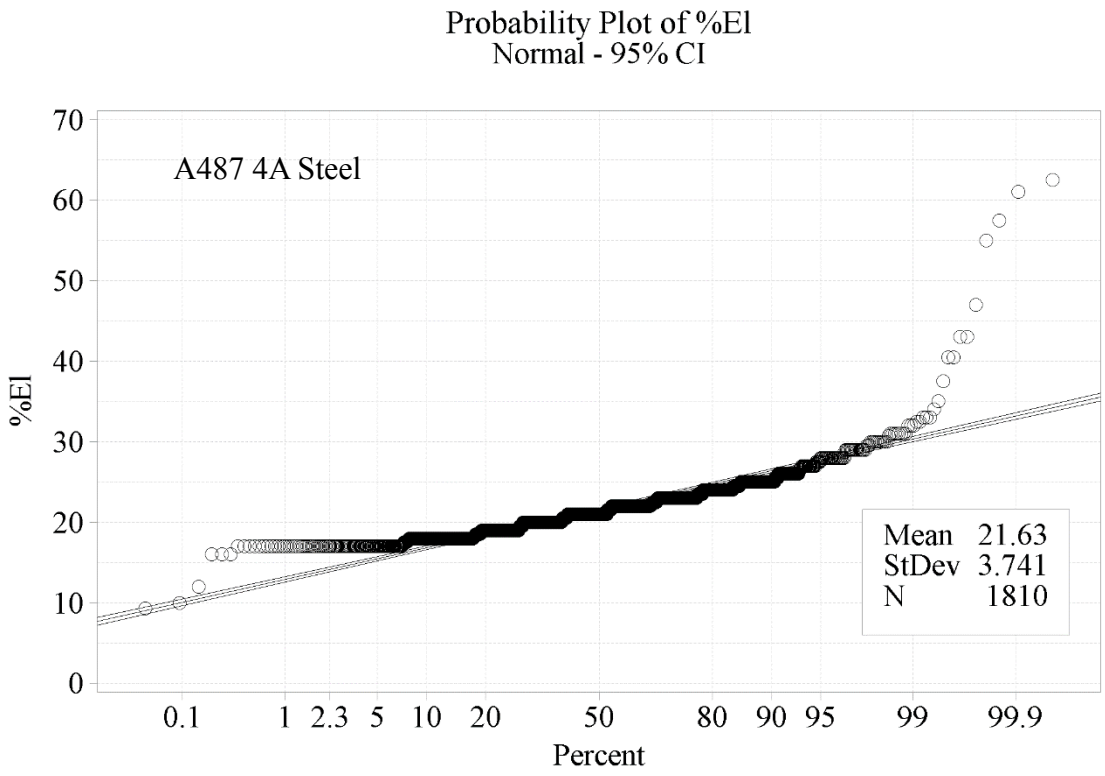

Figure B31. Normal distribution probability plot of elongation data A487 4A steel.

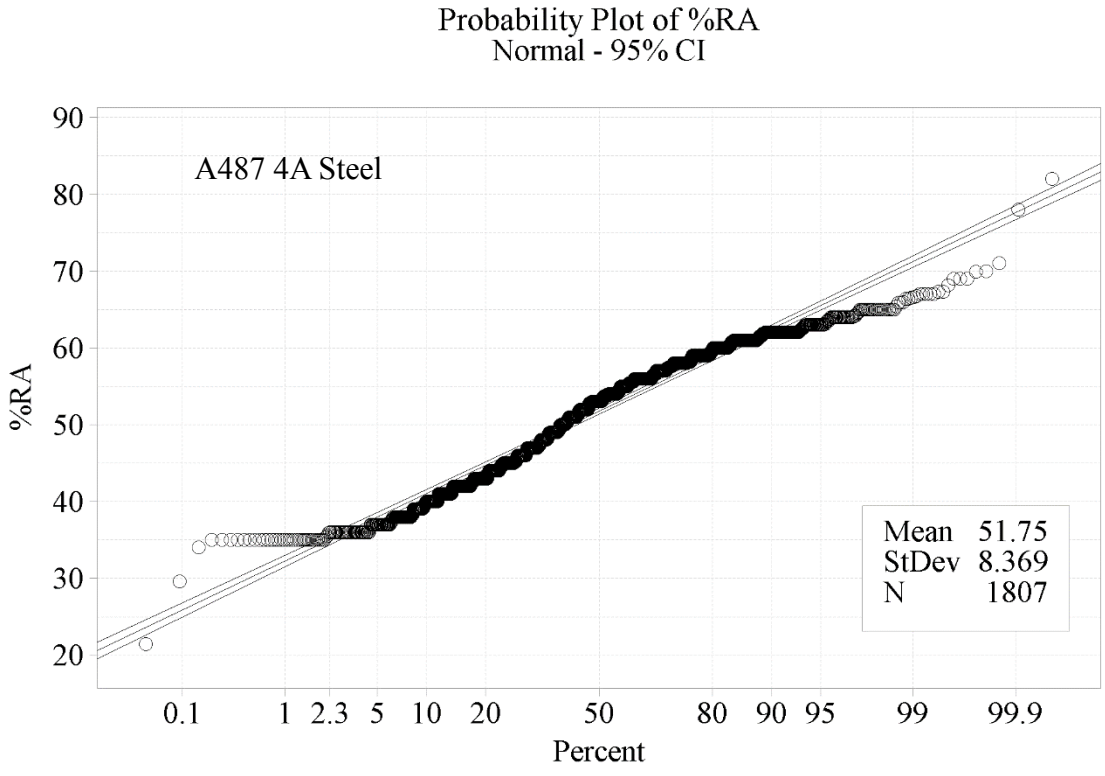

Figure B32. Normal distribution probability plot of reduction of area data for A487 4A steel.

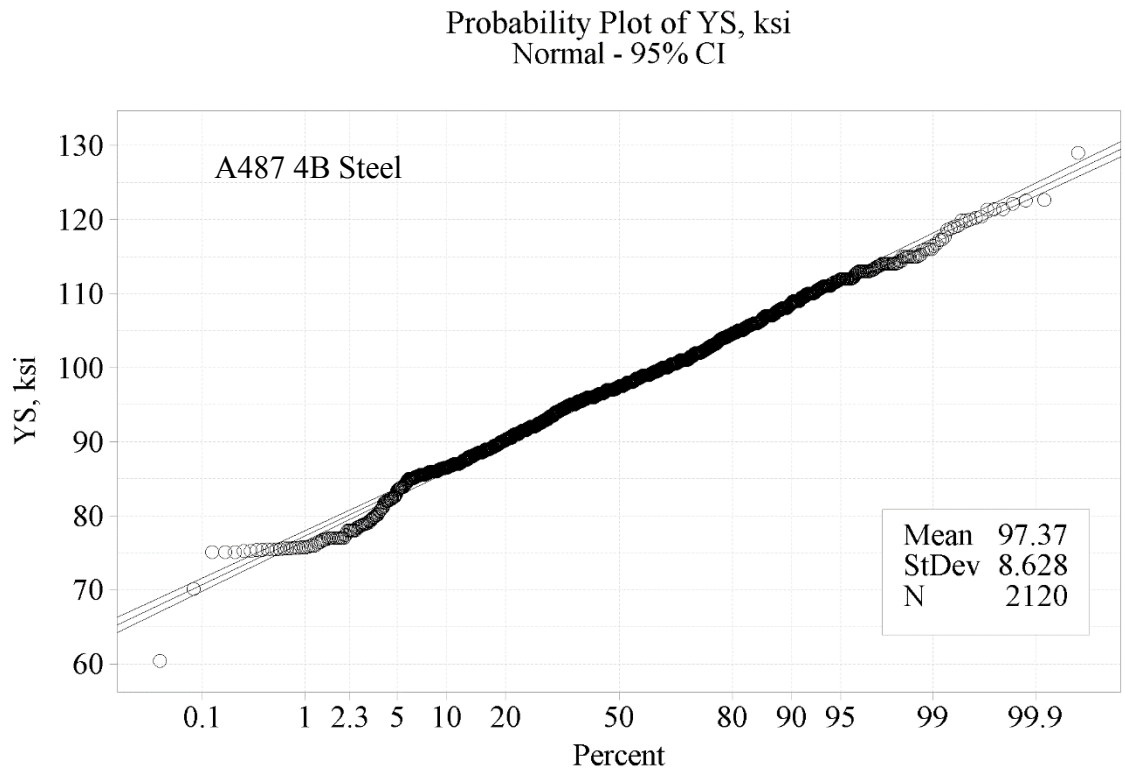

Figure B33. Normal distribution probability plot of yield strength data for A487 4B steel.

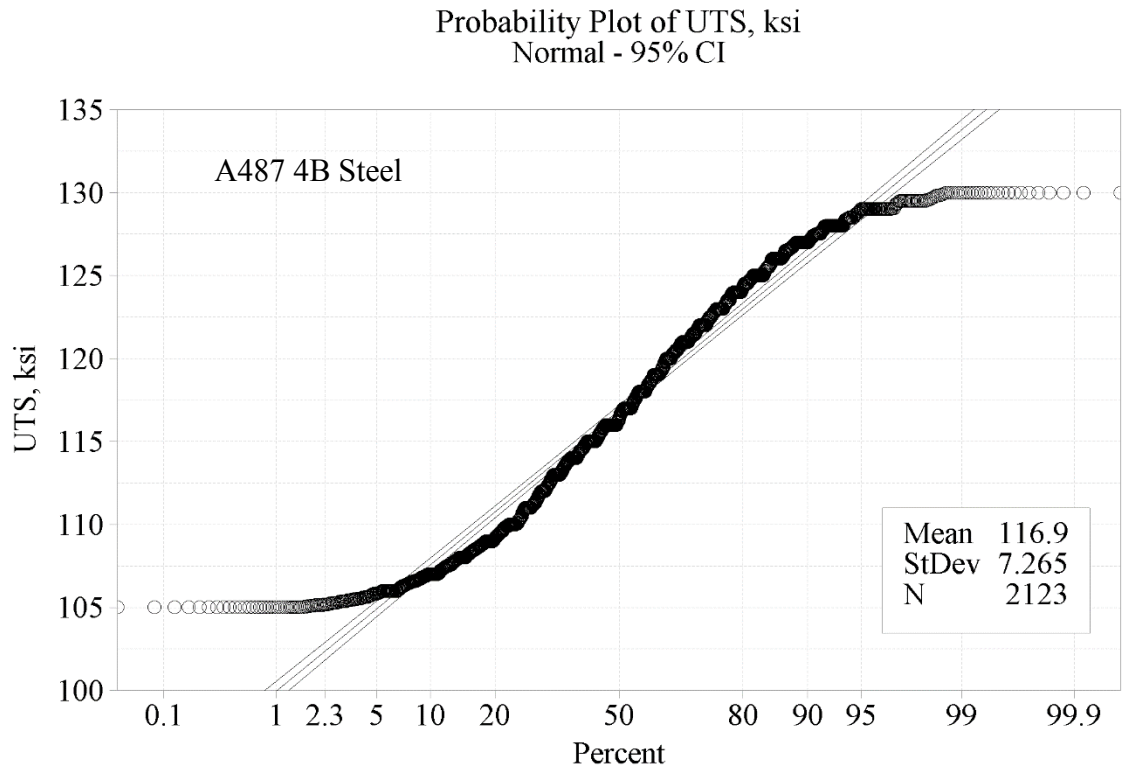

Figure B34. Normal distribution probability plot of ultimate strength data for A487 4B steel.

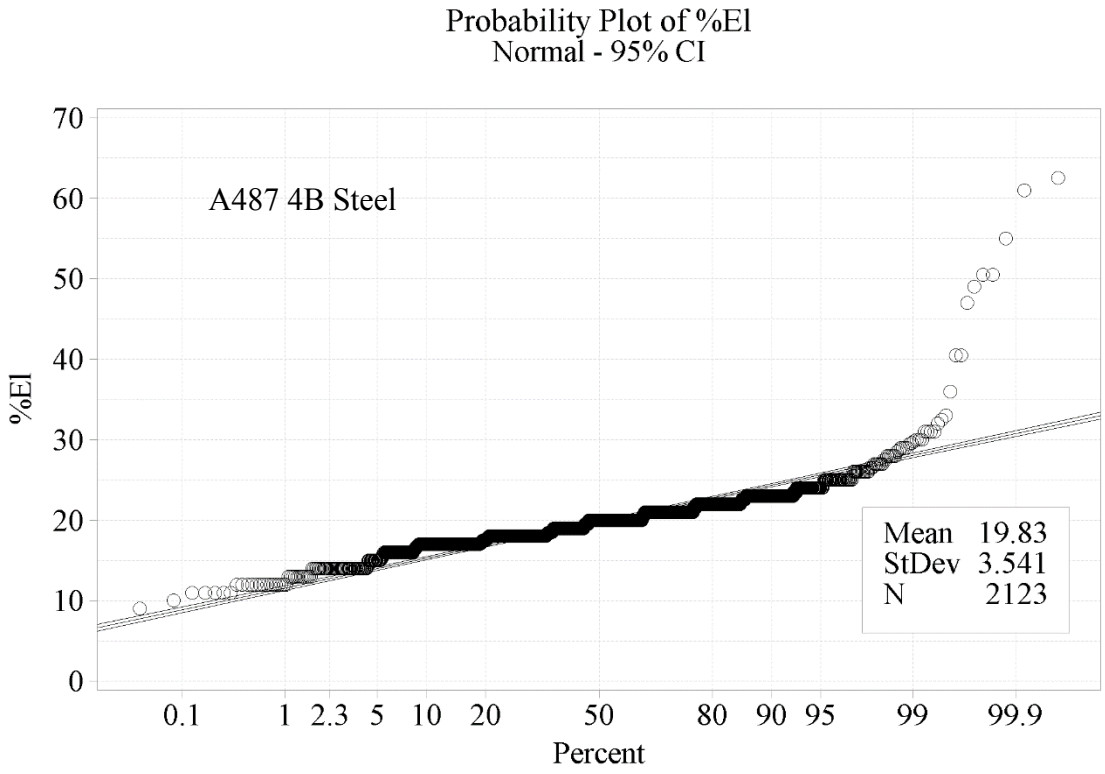

Figure B35. Normal distribution probability plot of elongation data for A487 4B steel.

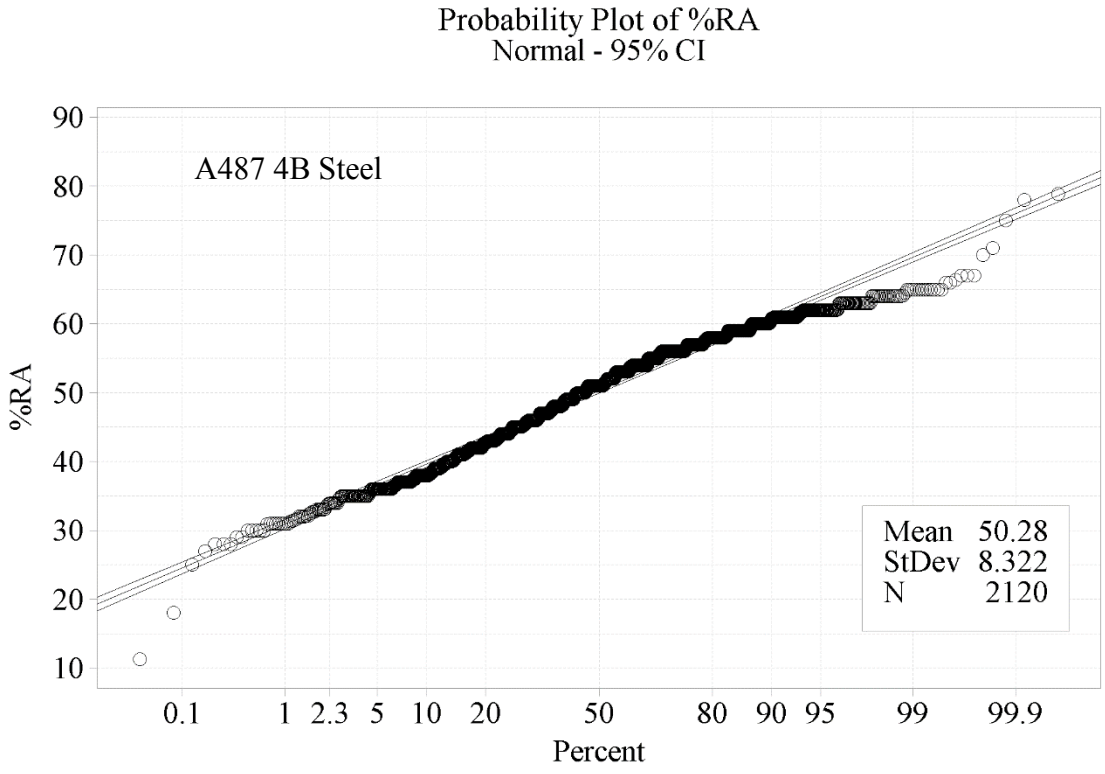

Figure B36. Normal distribution probability plot of reduction of area data for A487 4B steel.

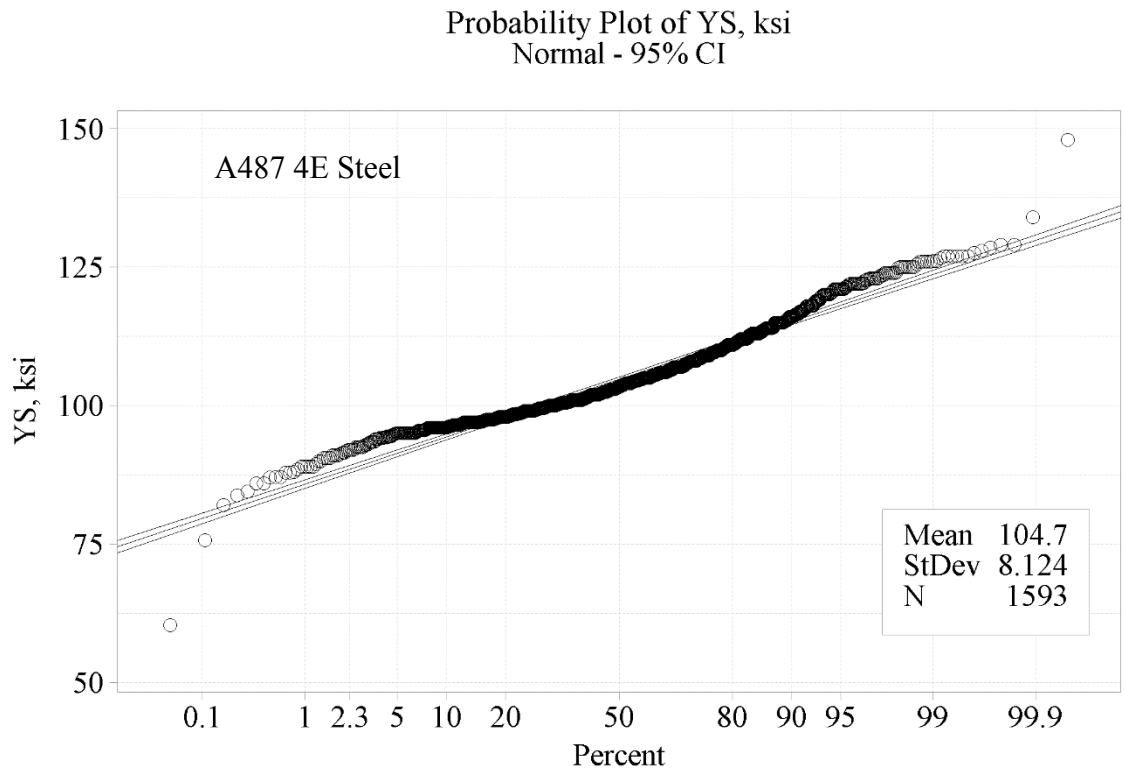

Figure B37. Normal distribution probability plot of yield strength data for A487 4E steel.

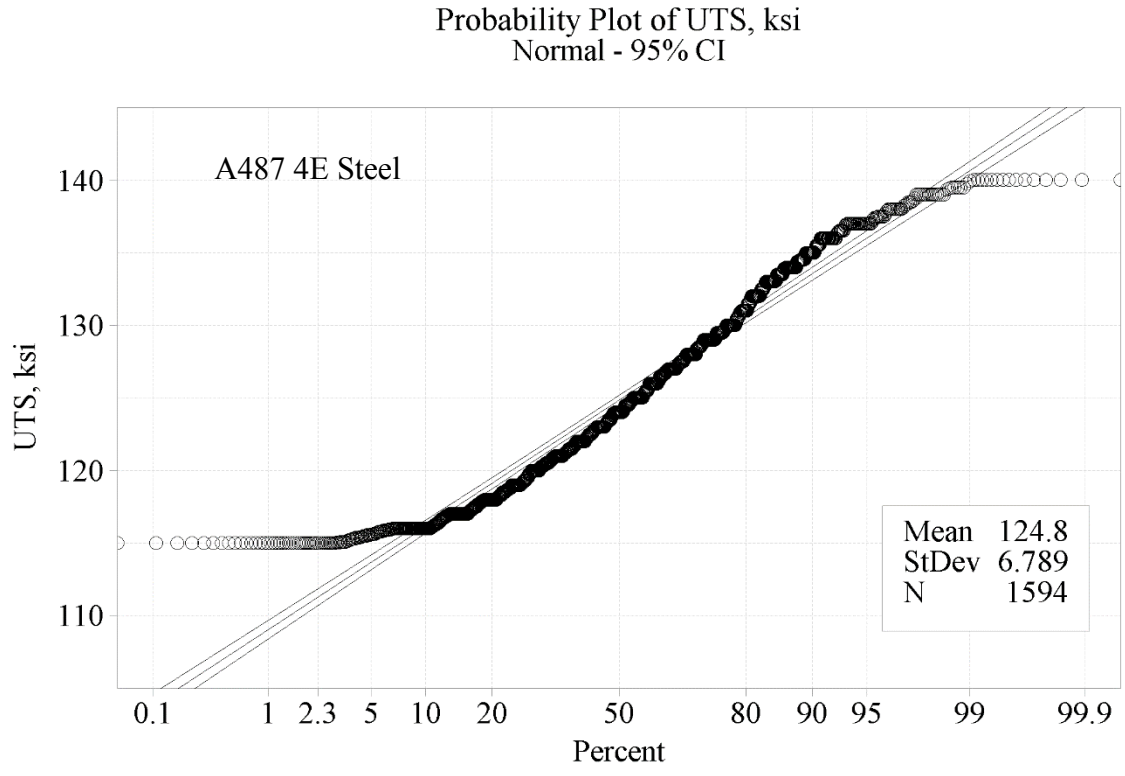

Figure B38. Normal distribution probability plot of ultimate strength data for A487 4E steel.

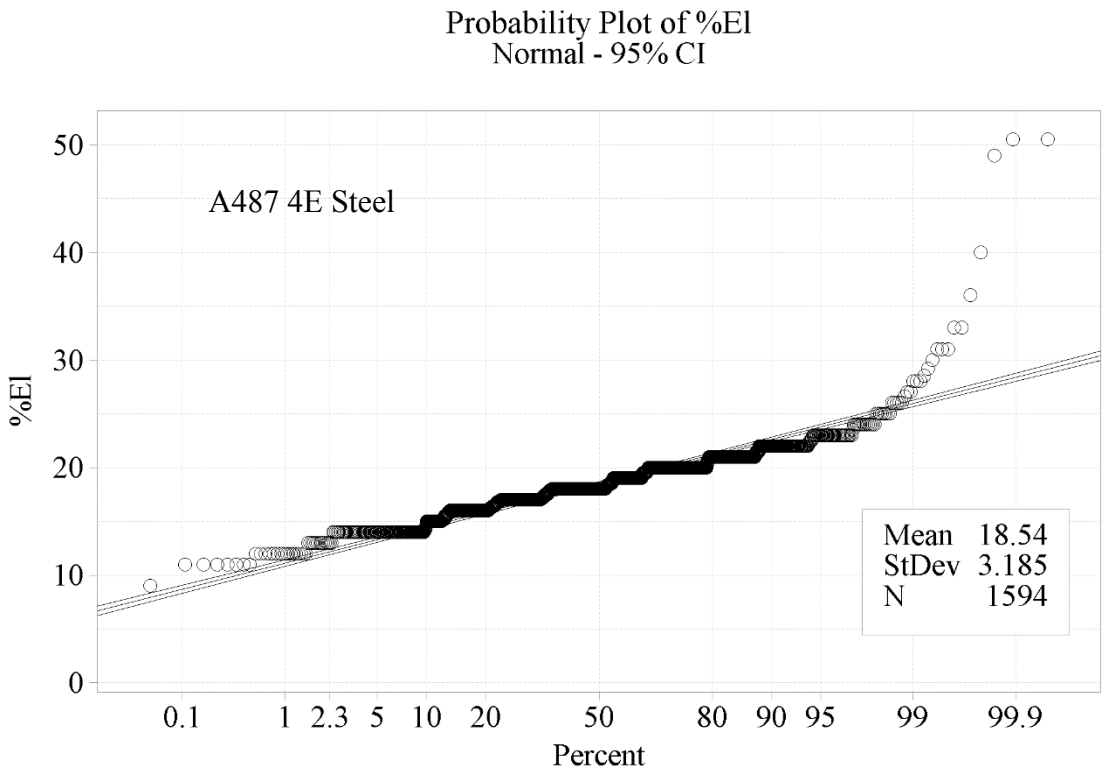

Figure B39. Normal distribution probability plot of elongation data for A487 4E steel.

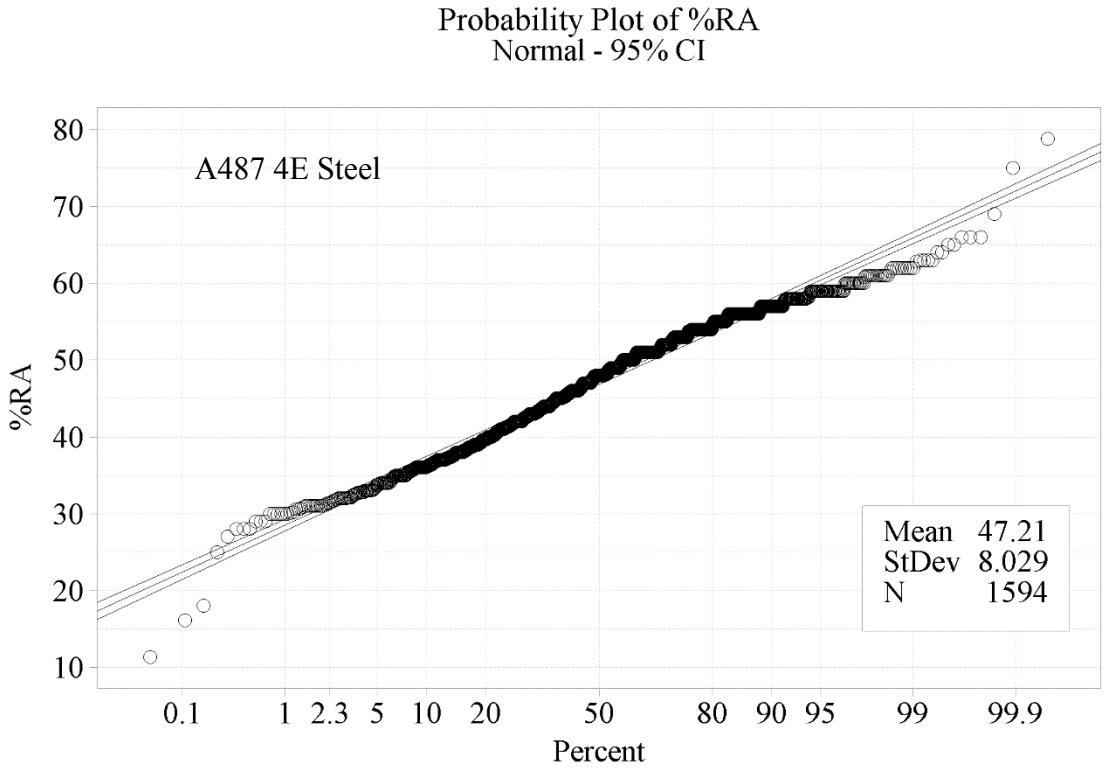

Figure B40. Normal distribution probability plot of reduction of area data for A487 4E steel.